PERFORMANCE INVESTIGATIONS OF VECTOR CONTROLLED INDUCTION MOTOR DRIVE

A DISSERTATION

Submitted in partial fulfillment of the requirements for the award of the degree of

MASTER OF TECHNOLOGY

in

ELECTRICAL ENGINEERING

(With Specialization in Power Apparatus and Electric Drives)

By

KOTHANA VENKATA NARESH

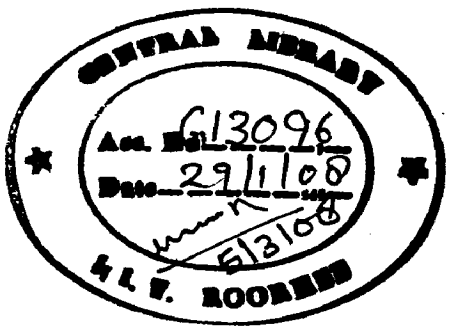

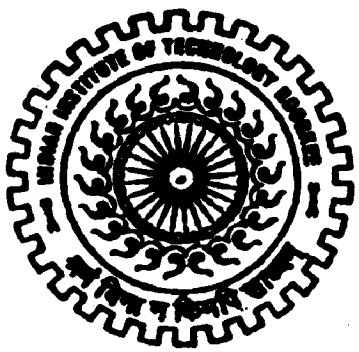

DEPARTMENT OF ELECTRICAL ENGINEERING
INDIAN INSTITUTE OF TECHNOLOGY ROORKEE
ROORKEE-247 667 (INDIA)

JUNE, 2007

I.D. No.-M.T. 385/2007-18/PA-SGC

CANDIDATE'S DECLARATION

I hereby declare that the work, which is presented in this dissertation report, entitled **"PERFORMANCE INVESTIGATIONS OF VECTOR CONTROLLED INDUCTION MOTOR DRIVE"**, being submitted in partial fulfillment of the requirements for the award of the degree of **MASTER OF TECHNOLOGY** with specialization in **POWER APPARATUS AND ELECTRIC DRIVES,** in the Department of Electrical Engineering, Indian Institute of Technology, Roorkee, is an authentic record of my own work carried out from July 2006 to June 2007, under the guidance and supervision of Dr. Pramod Agarwal, Professor and Dr. S. Ghatak Choudhuri, Lecturer, Department of Electrical Engineering, Indian Institute of Technology, Roorkee.

The results embodied in this dissertation have not submitted for the award of any other Degree or Diploma.

Date: 24-06-07

Place: Roorkee

K.V. Naresh

KOTHANA VENKATA NARESH

CERTIFICATE

This is to certify that the statement made by the candidate is correct to the best of my knowledge and belief.

DR. PRAMOD AGARWAL
Professor
Department of Electrical Engineering
Indian Institute of Technology Roorkee
Roorkee – 247667, (INDIA)

DR. S. GHATAK CHOUDHURI
Lecturer 24.06.2007
Department of Electrical Engineering
Indian Institute of Technology Roorkee
Roorkee – 247667, (INDIA)

ACKNOWLEDGEMENTS

First and foremost, I would like to express my sincere appreciation to my supervisor, Dr. Pramod Agarwal, for the patience and guidance throughout the entire duration of my thesis. Continuous monitoring and time management was an inspiring force for me to complete the work. Without his supervision, this thesis would never have been a success. Working under his guidance has been a great experience which has given me a deep insight in the area of technical research.

I would also like to express my sincere gratitude to my co-guide, Dr. S. Ghatak Choudhuri, for his continuous support and evaluating my progress from time to time in completion of this work.

I am also thankful to my Head of the Department, Dr. S. P. Gupta for providing all facilities in completion of this work.

I would like to take this opportunity to express my deep sense of gratitude to my family for their support and encouragement they have provided me over the years.

Last, but not the least, I would also like to thank my friends and Drives lab assistants who have offered me their unrelenting assistance throughout the course.

Date: 25th June, 2007 KOTHANA VENKATA NARESH

Place: Roorkee.

ABSTRACT

The principle of vector control of AC machine enables the dynamic control of AC motors, and induction motors in particular to a performance level comparable to that of a DC machine. Various control methods of induction motor drive like voltage control, frequency control, voltage and frequency control, current control, etc, provide steady-state performance, but their dynamic response is poor. The vector control technique, which is also known as field-oriented control (FOC), allows a squirrel-cage induction motor to be driven with high dynamic performance that is comparable to the characteristics of DC motor.

The vector control technique decouples the two components of stator current: one providing the air-gap flux and the other producing the torque. It provides independent control of flux and torque, and the control characteristic is linearized. In this technique, the stator currents are converted to a fictitious synchronously rotating reference frame with the flux vector and are transformed back to the stator frame before feeding back to the machine. The two components are d-axis component, i_{ds} analogous to armature current and q-axis component, i_{qs} analogous to the field current of a separately excited DC motor. Thus, the vector control must ensure the correct orientation of the space vectors and generate the control input signals. Therefore, with a vector control, an induction motor can operate as a separately excited DC motor.

In this work, a comprehensive mathematical modeling of vector controlled induction motor drive (VCIMD) system has been carried out to investigate the performance of drive system. The dynamic response of VCIMD under various operating conditions such as starting, speed reversal, speed re-reversal and load perturbation is simulated and examined in MATLAB 6.5 environment using simulink and power system block set toolboxes. Further, the dynamic response of the VCIMD depends on the type of the speed controller used in the closed loop operation. The speed controllers used in this work are Proportional Integral (PI) speed controller, Fuzzy Logic (FL) speed controller, hybrid of PI and FL speed controllers and Fuzzy Pre-compensated PI (FPPI) speed controller. A comparative study of the response of VCIMD is made with different speed controllers using MATLAB-simulink software. PWM signals for a three phase Voltage Source Inverter (VSI) are generated using MATLAB Embedded Controller I-8438.

CONTENTS

LIST OF FIGURES

LIST OF TABLES

CHAPTER I

INTRODUCTION

Faraday discovered electro-magnetic induction in 1831. After this discovery, it took about fifty years for the development of the first induction machine by Nikola Tesla in 1888. The development of this electrical machine that do not require brushes for its operation marked a revolution in electrical engineering and gave a scope for the wide spread use of poly-phase generation and distribution systems. The choice of present mains frequency (60 Hz in the USA and 50 Hz in Europe and Asia) was established in the late 19^{th} century because Tesla found it suitable for his induction motors. 60 Hz was found to produce no flickering when used for lightening applications.

Now-a-days, more than 60% of all the electrical energy generated in the world is used by cage induction motors. Induction machines have been mostly used at fixed speed for more than a century. On the other hand, DC machines have been used for variable speed applications using a Ward-Leonard configuration. This however requires three machines (2 DC machines and an induction motor) and is therefore bulky, expensive and requires careful maintenance.

In DC machines armature mmf axis is established at 90° electrical to the main field axis. The electromagnetic torque is proportional to the product of field flux and armature current. Field flux is directly proportional to the field current and is unaffected by the armature current because of orthogonal orientation between armature mmf and field mmf. Therefore in a separately excited DC machine, with a constant value of field flux, torque is directly proportional to armature current. Hence direct control of armature current gives direct control of motor torque and fast response, because motor torque can be altered as rapidly as armature current can be altered. Hence dc motors are simple in control and offer better dynamic response inherently. Numerous economical reasons, for instance high initial cost, high maintenance cost for commutators, brushes and brush holders of dc motors call for a substitute which is capable of eliminating the persisting problems in dc motors and has all the advantages present in dc motors. Freedom from regular maintenance and a brushless robust structure of the three phase squirrel cage induction motor are among the prime reasons, which brings the motor forward as a good substitute.

The ac induction motors are the most common motors used in industrial motion control systems, as well as in main powered home appliances. Simple and rugged design, low-cost, low

maintenance and direct connection to an ac power source are the main advantages of ac induction motors. Various types of ac induction motors are available in the market. Different motors are suitable for different applications. Although ac induction motors are easier to design than dc motors, the speed and the torque control in various types of ac induction motors require a greater understanding of the design and the characteristics of these motors.

1.1 CONTROL TECHNIQUES OF INDUCTION MOTOR

Various speed control techniques implemented by modern-age VFD [1-2] are discussed in this section. In scalar control, the motor is fed with variable frequency supply generated by an inverter controlled by Pulse Width Modulation (PWM) techniques. Here, the V/f ratio is maintained constant in order to get constant torque through out the operating range of the motor. Since only magnitudes of the input variables – frequency and voltage – are controlled, this is known as "scalar control".

In general, the drives with this type of control are without any feedback devices i.e. open loop control. Hence, a control of this type offers low cost, easy to implement and also a very little knowledge of the motor is required for frequency control. Thus, this type of control is widely used. But there are certain disadvantages with this type of control which includes, the torque developed is load dependent and is not controlled directly. Also, the transient response of such a control is not fast due to the predefined switching pattern of the inverter. Now variable speed applications by induction motors came into existence with the arrival of solid-state power electronic devices like thyristors, IGBTS and MOSFETS, etc. These provide high performance torque, speed and flux control. Although induction machines using V/f control can maintain a constant flux, their torque and flux dynamic performance is extremely poor. The advantages of induction machines are clear in terms robustness and price; however it was not until the development and implementation of Vector Control (VC) or Field Oriented Control (FOC) that induction machines were able to compete with DC machines in high performance applications.

The principle behind FOC is that the machine flux and torque are controlled independently, in a similar fashion to a separately excited DC machine. Instantaneous stator currents are "transformed" to a reference frame rotating at synchronous speed aligned with the rotor, stator or air-gap flux vectors, to produce a d-axis component current(flux producing) and a q-axis component of current(torque producing). Such a rotating frame of reference is referred as the synchronously rotating reference frame (SRRF). In this work, SRRF is aligned with rotor mmf space vector. In the

SRRF, the stator current is split into two decoupled components, one controls flux and other controls torque respectively.

An induction motor is said to be in vector control mode, if the decoupled components of the stator current space vector and the reference decoupled components defined by the vector controller in the SRRF match each other respectively. Alternately, instead of matching the two-phase currents (reference and actual) in the SRRF, the close match can also be made in three phase currents (reference and actual) in the stationary reference frame. Hence in spite of induction machine's nonlinear and highly interacting multivariable control structure, its control has become easy with the help of FOC. Therefore in the FOC method the induction motor can be operated like a separately excited DC motor for high performance applications.

The transformation from the stationary reference frame to the rotating reference frame is done and controlled with reference to a specific flux linkage space vector (stator flux linkage, rotor flux linkage or magnetizing flux linkage). In general, there exists three possibilities for such selection and hence, three different vector controls. They are Stator flux oriented control, Rotor flux oriented control and Magnetizing flux oriented control.

As the torque producing component in this type of control is controlled only after transformation is done and is not the main input reference, such control is known as "indirect torque control". The most challenging and ultimately, the limiting feature of the field orientation, is the method whereby the flux angle is measured or estimated. Depending on the method of measurement, the vector control is divided into two subcategories: direct and indirect vector control. In direct vector control, the flux measurement is done by using the flux sensing coils or the Hall devices. This adds to additional hardware cost and in addition, measurement is not highly accurate. Therefore, this method is not a very good control technique. The more common method is indirect vector control. In this method, the flux angle is not measured directly, but is estimated from the equivalent circuit model and from measurements of the rotor speed, the stator current and the voltage.

1.2 APPLICATIONS OF VCIMD

Because of the efficient, smooth and maintenance free operation of VCIMDs, such drives are finding increasing applications in many drive applications such as air-conditioning refrigerators, fans, flowers, pumps, waste water treatment plants, elevators, lifts, traction, electric vehicles etc.

1.3 LITERATURE REVIEW

Induction motors have been intensively investigated and described in the engineering literature for several decades. BLASCHKE [10] has reported the pioneer concept to initiate the work based on the concept of vector control.

Vector control is a technique, which is capable of introducing decoupled control between flux and torque in an induction motor to control it similar to a separately excited DC motor [3-4]. As a result, the method of vector control also named as FOC has now become a very popular control strategy for 3-ϕ IM. It has transformed the IM from a non linear control structure to a linear decoupled control structure.

Most basic text books [7] develop the induction motor theory using equivalent approach. The commonly used equivalent circuit is convenient only for steady state operating conditions, that is, when the motor is fed from a fixed frequency sinusoidal supply and is rotating at a constant speed. The very purpose of using vector control is to achieve high motor performance under dynamic conditions. Therefore, an approach which is completely based on motor equivalent circuit is not very useful in presenting the concepts of vector control. There forth Joseph Vithayathil[11] presented a paper on field oriented control (vector control) of 3 phase induction motor which explains the basic concepts of vector control, as applied to a 3 phase squirrel cage induction motor and also explained in detail and in exact manner, the variables used in the related mathematical theory. The concept of space vectors, which perhaps the simplest means of presenting the concepts of vector control, is also explained in detail.

. B.K.Bose [7] has explained the principle of Sinusoidal PWM with instantaneous current control and SVM in detail. Space Vector Modulation (SVM) is an advanced and computational intensive technique for control of AC drives. It is the best among all the PWM techniques [21-26]. SVM can be implemented by the representation of voltages in the α-β plane [29]. The authors have given a step by step procedure of generating the PWM pulse pattern for a voltage source inverter in detail.

Various software packages for simulation have been proposed in the recent years, for electronic circuits, like SPICE and SABER, power networks like EMTP and EUROSTAG or specialized simulation of power electronic systems like SIMPLORER, POSTMAC, SIMSEN, ANSIM and PSCAD. Such software packages offer a more or less user friendly environment, but not using the concept of visual design. More recently, a lot of attention have been given to libraries

of models for the various components of a power electronic system and electrical machines, developed in the MATLAB/simulink environment, in order to explore the computational power and flexibility and integrate the visual design facilities[41].

Artificial Intelligence (AI) techniques, such as expert system (ES), fuzzy logic (FL), artificial neural network (ANN), and genetic algorithm (GA) have recently expanded the frontier of power electronics and motor drives which are already complex and interdisciplinary areas. Fuzzy logic and neural network constitute the most important elements of AI and are often defined as "soft computing" or approximate computation compared to hard or precise computation. According to George Boole, who published the article "Investigation of the Laws of Thoughts" in 1854, human beings think and take decisions on the basis of logical "yes/no" or "true/false" reasoning. This gave birth to Boolean algebra and gradually became the basis of our modern digital computers. Lofti Zadeh [28] argued that human thinking is often fuzzy or uncertain in nature and does not always follow crisp "yes/no" logic. He organized the "fuzzy logic" theory in 1965 and created a storm of controversy in the intellectual community. Now fuzzy logic is often applied in the robust control of a feedback system with parameter variation problem and the load torque disturbance.

1.4 CONCLUSION

From the above discussion it can be concluded that the control of induction motor is very necessary as it is the common motor used in industrial motion control systems, as well as in main powered home appliances. Hence a well established induction motor drive which is simple, rugged, low cost and low maintenance can serve the required purpose. Many authors have published several research papers on the control techniques of induction motor. At the same time it is also necessary to control the output voltage of the inverter used in the drive. These control techniques are also explained in the second chapter of this thesis. The modeling and MATLAB implementation of the Vector Controlled Induction Motor Drive (VCIMD) is also explained in detail in the third chapter. The implementation of PWM strategies in MATLAB Embedded Controller, I-8000 and the details of the same controller is explained in the fourth chapter. Fifth chapter gives the results obtained in the simulation of VCIMD in MATLAB environment and also the experimental results. Finally sixth chapter gives the conclusions carried out in this work.

CHAPTER II

CONTROL STRATEGIES OF VSI

2.1 INTRODUCTION

A significant improvement in converter behavior has been achieved by means of closed loop control techniques. A number of control strategies have been applied to three phase AC-to-DC converters some of which include sinusoidal pulse width modulation (SPWM), hysteresis current control (HCC), indirect current control (IDC), SPWM with instantaneous current control, space vector modulation (SVM). All these control strategies achieve the same steady-state characteristics, but with different implementations, dynamic response, PWM patterns and harmonic contents. This new breed of converters has been made possible mainly because of the use of modern solid-state, self-commutating power semi-conducting devices such as Power MOSFETs, IGBTs, GTOs, etc. Because of the advances in solid state power devices and microprocessors, switching power converters are used in more and more modern motor drives to convert and deliver the required energy to the motor.

Pulse Width Modulating (PWM) signals applied to the gates of the power transistors controls the energy that a switching power converter delivers to a motor. PWM signals are pulse trains with fixed frequency and magnitude and variable pulse width. There is one pulse of fixed magnitude in every PWM period. However, the width of the pulse changes from pulse to pulse according to a modulating signal.

When a PWM signal is applied to the gate of a power transistor, it causes the turn on and turn off intervals of the to change from one PWM period to another PWM period according to the same modulating signal. The frequency of a PWM signal must be much higher than that of the modulating signal, the fundamental frequency, such that the energy delivered to the motor and its load depends mostly on the modulating signal.

In many industrial applications, control of the output voltage of the inverters is often necessary:

1. to cope with the variations of the dc input voltage.
2. to regulate voltage of the inverters and
3. to satisfy the constant volts and frequency control requirement.

2.2 ADVANTAGES OF PWM TECHNIQUES

The major advantages of PWM based switching power converter over linear power amplifier are:

- Easy to implement and control.
- No temperature variations and aging-caused drifting or degradation in linearity.
- Compatible with today's digital micro-processors and
- Lower power dissipation.

2.3 VARIOUS VOLTAGE CONTROL TECHNIQUES OF THREE PHASE VSI:

A three phase inverter shown in fig.2.2 may be considered as three single phase inverters and the output of each single-phase inverter is shifted by 120°. The voltage control techniques mentioned above are appreciable to three phase inverters. However, the following techniques are most commonly used for three-phase inverters[9].

1. Sinusoidal PWM
2. Third-harmonic PWM
3. 60° PWM
4. Space Vector Modulation

In this report, the main focus is on SPWM and SVM techniques.

2.3.1 Sinusoidal PWM

The SPWM technique is very popular for industrial converters. The basic principle of the PWM technique involves the comparison of triangular carrier wave frequency with the fundamental frequency sinusoidal modulating wave. In this technique, there are three sinusoidal references waves or modulating waves (v_{mA}, v_{mB}, and v_{mC}) each shifted by 120° as shown in fig2.1.

The three phase reference waves v_{mA}, v_{mB}, and v_{mC} are represented as:

$$v_{mA}(\omega t) = f(m, \omega t)$$
$$v_{mB}(\omega t) = f(m, \omega t-(2/3)\prod)$$
$$v_{mC}(\omega t) = f(m, \omega t+(2/3)\prod) \quad (2.1)$$

where $f(m, \omega t)$ denotes the modulating function employed .

The sinusoidal modulating function f (m, ωt) = m sin (m, ωt). This modulating function can be replaced with any other modulating function, such as third harmonic.

A carrier (triangular) wave is compared with the reference signal corresponding to a phase to generate the gating signals for that phase. Comparing the carrier signal v_{cr} (or v_{tri}) with the reference phases v_{mA}, v_{mB}, and v_{mC} produces g_1, g3 and g_5 respectively as shown in fig. Then the instantaneous line-to-line output voltage is $V_{AB}= V_s(g_1-g_3)$. The output voltage as shown in fig2.2 is generated by eliminating the condition that two switching devices in the same arm cannot conduct at the same time.

The fundamental frequency component in the inverter output voltage can be controlled by amplitude modulation index,

$$m_a = \hat{V}_m / \hat{V}_{cr} \qquad (2.2)$$

Where $\hat{V}_m$ and $\hat{V}_{cr}$ are the peak values of the modulating and carrier waves respectively. The amplitude modulation index m_a is usually adjusted by varying $\hat{V}_m$ while keeping $\hat{V}_{cr}$ fixed. The frequency modulation index is defined by,

$$m_f = f_{cr} / f_m \qquad (2.3)$$

Where f_m and f_{cr} are the frequencies of the modulating and carrier waves respectively.

The waveform of the fundamental frequency component, V_{LL1} of inverter line-to-line voltage, V_{AB} is also shown in fig 2.2 .The magnitude and frequency of V_{LL1} can be independently controlled by m_a and f_m respectively.

The operation of the switches S_1 to S_6 is determined by comparing the modulating waves with the carrier wave. When $v_{ma} \geq v_{cr}$, the upper switch S_1 in inverter leg A is turned on. The lower switch S_4 operates in a complementary manner and thus is switched off. The resultant inverter terminal voltage V_{AN}, which is the voltage of the phase A terminal with respect to the negative dc bus, is equal to the dc bus voltage V_d. When $v_{mA}<v_{cr}$, S_4 is on and S_1 is off, leading to $V_{AN}=0$ as shown in fig2.1. Since the waveform of V_{AN} has only two levels, V_d and 0, the inverter is known as **two-level inverter.**

The normalized carrier frequency m_f should be odd multiple of three. Thus, all phase-voltages (V_{AN},V_{BN} and V_{CN}) are identical, but 120° out of phase without even harmonics; moreover, harmonics at frequencies multiple of three are identical in amplitude and phase in all phases. Thus, the ac output line voltages $V_{AB}= V_{AN} - V_{CN}$ does not contain the ninth harmonic. Therefore, for odd multiples of three times the normalized carrier frequency m_f, the harmonics in the ac output voltage appear at normalized frequencies f_h centered around m_f and its multiples.

Because the maximum amplitude of the fundamental phase voltage in the linear region ($M \leq 1$) is $V_s/2$, the maximum amplitude of the fundamental ac output line voltage is $V_{AB1(max)} = \sqrt{3}\, V_s/2$. Therefore one can write the fundamental peak amplitude as

$$V_{AB1(max)} = M\sqrt{3}\, V_s/2 \qquad \text{for } 0 < M \leq 1 \tag{2.4}$$

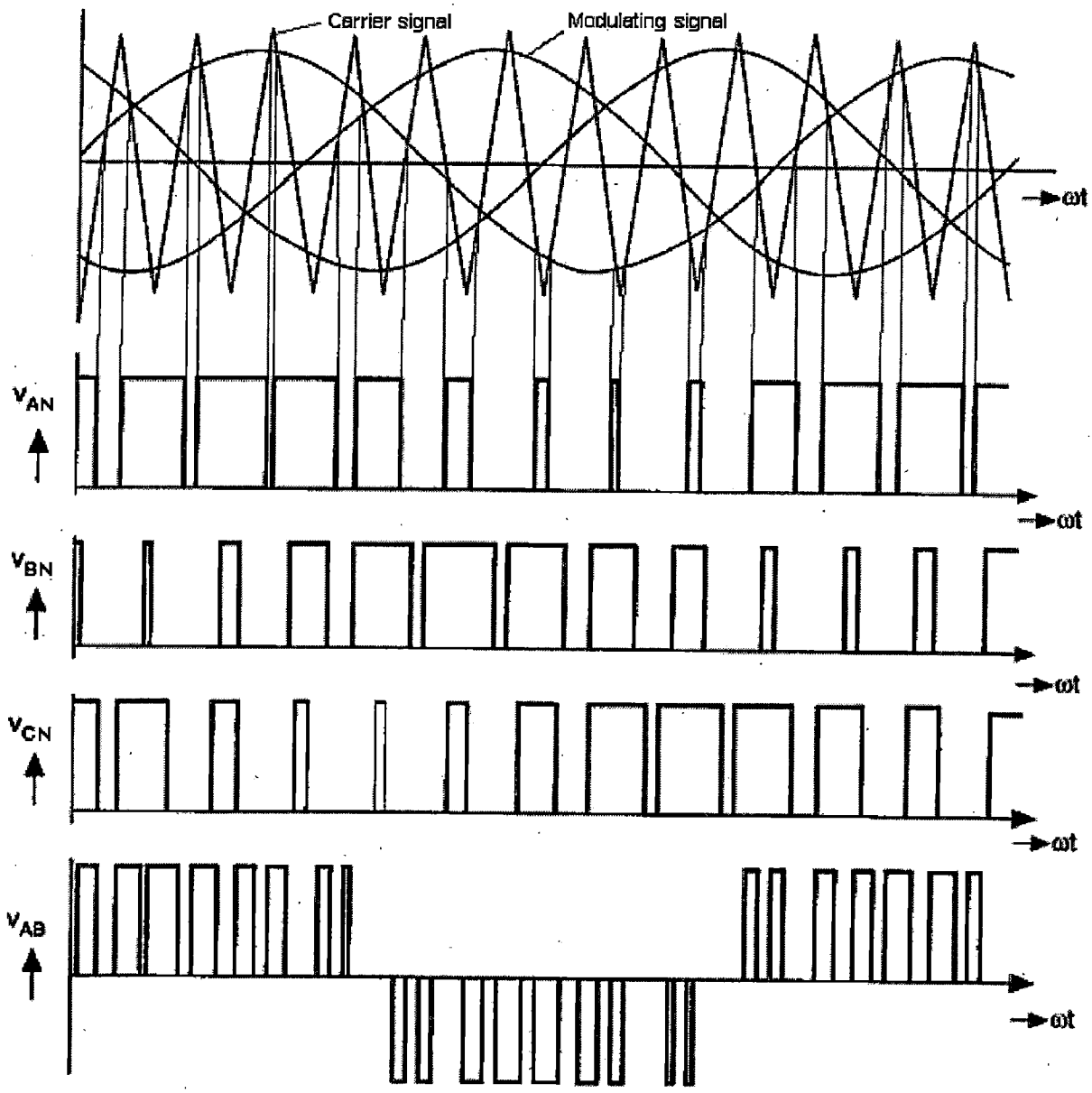

Figure 2.1. Three phase sinusoidal PWM waveforms

Overmodulation: To further increase the amplitude of the load voltage, the amplitude of the modulating signal V_{tri} can be made higher than the amplitude of the carrier signal V_{cr}, which leads to over- modulation. The relationship between the amplitude of the fundamental ac output line

voltage and the dc link voltage becomes nonlinear. Thus, in the overmodulation region, the line voltage region in, $\sqrt{3}\frac{V_s}{2} < \hat{V}_{ab1} = \hat{V}_{bc1} = \hat{V}_{ca1} < \frac{4}{\pi}\sqrt{3}\frac{V_s}{2}$ (2.5)

2.3.2 60-Degree PWM

The idea behind 60° PWM is to "flat top" the waveform from 60° to 120° and 240° to 300°. The power devices are held ON for one-third of the cycle (when at full voltages) and have reduced switching losses. All triple harmonics (3^{rd}, 9^{th}, 15^{th}, 21^{st}, 27^{th}, etc.) are absent in the three-phase voltages. The 60° PWM creates a larger fundamental ($2/\sqrt{3}$) and utilizes more of the available dc voltage (phased voltage $V_p = 0.57735V_s$ and line voltage $V_L=V_s$) than does sinusoidal PWM[14]. The output waveform can be approximated by the fundamental and the first few terms as shown in fig.2.2

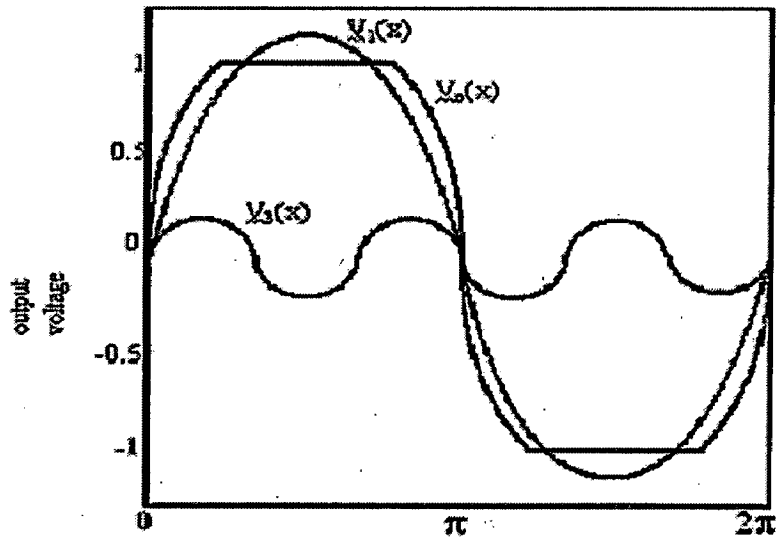

Where, $V_0(x)$ ------ 60° PWM output

$V_1(x)$ ------ fundamental

$V_3(x)$ ------ third harmonic

Figure 2.2. Output waveform for 60° PWM

2.3.3 Third-Harmonic PWM

This technique is implemented in the same manner as sinusoidal PWM. The difference is that the reference ac waveform is not sinusoidal but consists of both a fundamental component and a third-harmonic component as shown in fig 2.3 As a result, the peak-to-peak amplitude of the resulting reference function does not exceed the DC supply voltage V_s, but the fundamental component is higher than the available supply V_s.

The presence of exactly the same third-harmonic component in each phase results in an effective cancellation of the third harmonic component in the neutral terminal, and the line-to-line phase voltages(V_{AN}, V_{BN} and V_{CN}) are all sinusoidal with peak amplitude of $V_p = V_s/\sqrt{3} = 0.57735V_s$. The fundamental component is the same peak amplitude $V_{p1} = 0.57735V_s$ and the peak line voltage is $V_L = \sqrt{3}\, V_p = \sqrt{3} * 0.57735V_s = V_s$. This is approximately 15.5% higher in amplitude than that achieved by the sinusoidal PWM. Therefore, the third-harmonic PWM provides better utilization of the dc supply voltage than the sinusoidal PWM does.

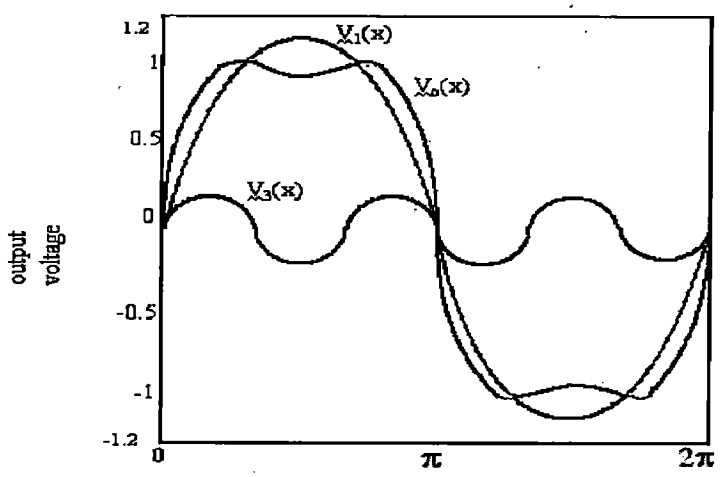

Where, $V_0(x)$ ------ Third-Harmonic injection
$V_1(x)$ ------ fundamental
$V_3(x)$ ------ third harmonic

Figure 2.3. Output waveform of third-harmonic PWM

2.3.4 Space Vector Modulation

Space Vector modulation (SVM) technique was originally developed as a vector approach to pulse-width modulation (PWM) for three-phase inverters. It is a more sophisticated technique for generating sine wave that provides a higher voltage to the motor with lower total harmonic distortion. It confines space vectors to be applied according to the region where the output voltage vector is located. A different approach to PWM modulation is based on the space vector representation of voltage in the α-β plane. The Space vector modulation technique is an advanced, computation intensive PWM technique and is possibly the best among all the PWM techniques for drives applications. Because of its superior performance characteristics, it is been finding wide spread application in recent years.

One of the most preferred pulse width modulation (PWM) strategies today is space-vector modulation (SVPWM). This kind of scheme in voltage source inverter (VSI) drives offers improved bus voltage utilization and less commutation losses. Three-phase inverter voltage control by space vector modulation includes switching between the two active and zero voltage vectors so that the time interval times the voltages in the chosen sectors equals the command voltage times the time period within each switching cycle. During the switching cycle the reference voltage is assumed to be constant as the time period would be very low. By simple digital calculation of the switching time one can easily implement the SVPWM scheme. However, the switching sequence may not be unique.

The three-phase full-bridge circuit with six semiconductor power switches is shown in fig.2.4. V_d and V_q are the d-q voltage components of the output voltage vector v(t) which is generated by d-q current controllers.

2.4 SPACE VECTOR MODULATION(SVM)

2.4.1 Definition

Space Vector Modulation(SVM) is a digitally modulating technique where the objective is to generate PWM load line voltages that are in average equal to a given (or reference) load line voltages. SVM is quite different from the other PWM methods. With PWMs, the inverter can be thought of as three separate push-pull driver stages, which create each phase waveform

independently. SVM, however, treats the inverter as a single unit; specifically, the inverter can be driven into eight unique states. Modulation is accomplished by switching the state of the inverter. The control strategies are implemented in digital systems.

SVM was originally developed as a vector approach to PWM for three phase inverters. It is a more sophisticated technique for generating sine wave that provides a higher voltage to the motor with lower total harmonic distortion. It confines space vectors to be applied according to the region where the output voltage vector is located.

2.4.2 Features of Space Vector PWM

The main aim of any modulation technique is to obtain variable output (voltage) having a maximum fundamental component with minimum harmonics.

During the past years many PWM techniques have been developed for allowing the inverters to posses various desired output characteristics to achieve:

- Wide linear modulation range
- Less switching losses
- Lower total harmonic distortion(THD)

The SVM technique is more popular than conventional PWM technique because of the following excellent features:

- It achieves the wide linear modulation range associated with PWM third harmonic injection automatically.
- It has lower base band harmonics than regular PWM or other sine based modulation methods or otherwise optimizes harmonics[30].
- 15% more output voltage than conventional modulation, that is better DC link utilization.
- More efficient use of DC supply voltage
- SVM increases the output capability of SPWM without distorting line-line output voltage wave form.
- Advanced and computation intensive PWM technique.
- Higher efficiency.
- Prevent unnecessary switching and hence less commutation losses[21].
- A different approach to PWM modulation based on space vector representation of the voltages in the α-β plane.

2.4.3 Space Vector(SV) concept:

The concept of SV is derived from the rotating field of AC machine which is used for modulating the inverter output voltage[21-26].

In this modulation technique, the three phase quantities can be transformed to their equivalent two phase quantity either in synchronously rotating frame or stationary frame. From this two phase component, the reference vector magnitude can be found and used for modulating the inverter output. The process of obtaining the rotating space vector is explained below, considering the stationary reference frame.

Let the three phase sinusoidal voltage components be,

$$V_a = V_m \sin(\omega t)$$
$$V_b = V_m \sin(\omega t - 2\pi/3)$$
$$V_c = V_m \sin(\omega t - 4\pi/3) \qquad (2.6)$$

When this three phase voltage is applied to the AC machine, it produces a rotating flux in the air gap of the AC machine. This rotating flux component can be represented as a single rotating voltage vector.

The magnitude and angle of the rotating vector can be found by means of Clark's Transformation as explained below in the stationary reference frame.

The representation of rotating vector in complex plane is shown in fig.2.1.

Space vector representation of the three phase quantity:

$$\overline{V^*} = V_\alpha + jV_\beta = 2/3(V_a + aV_b + a^2V_c) \qquad (2.7)$$

where $a = e^{j2\pi/3}$

$$\left|\overline{V^*}\right| = \sqrt{V_\alpha^{\,2} + V_\beta^{\,2}} \qquad \text{And} \qquad \alpha = \tan^{-1}(V_\beta / V_\alpha)$$

$$\overline{V^*} = V_\alpha + jV_\beta = 2/3(V_a + e^{j2\pi/3}V_b + e^{-j2\pi/3}V_c)$$
$$= 2/3(V_a + \cos(2\pi/3)V_b + \cos(2\pi/3)V_c) +$$
$$j\,2/3(\sin(2\pi/3)V_b - \sin(2\pi/3)V_c) \qquad (2.8)$$

Equating real and imaginary parts:

$$V_\alpha = 2/3(V_a+\cos(2\pi/3)V_b+\cos(2\pi/3)V_c) \quad (2.9)$$

$$V_\beta = 2/3(0V_a+\sin(2\pi/3)V_b-\sin(2\pi/3)V_c) \quad (2.10)$$

$$\begin{bmatrix} V_\alpha \\ V_\beta \end{bmatrix} = 2/3 \begin{bmatrix} 1 & \cos(2\pi/3) & \cos(2\pi/3) \\ 0 & \sin(2\pi/3) & -\sin(2\pi/3) \end{bmatrix} \begin{bmatrix} V_a \\ V_b \\ V_c \end{bmatrix}$$

$$= 2/3 \begin{bmatrix} 1 & -1/2 & -1/2 \\ 0 & \sqrt{3}/2 & -\sqrt{3}/2 \end{bmatrix} \begin{bmatrix} V_a \\ V_b \\ V_c \end{bmatrix} \quad (2.11)$$

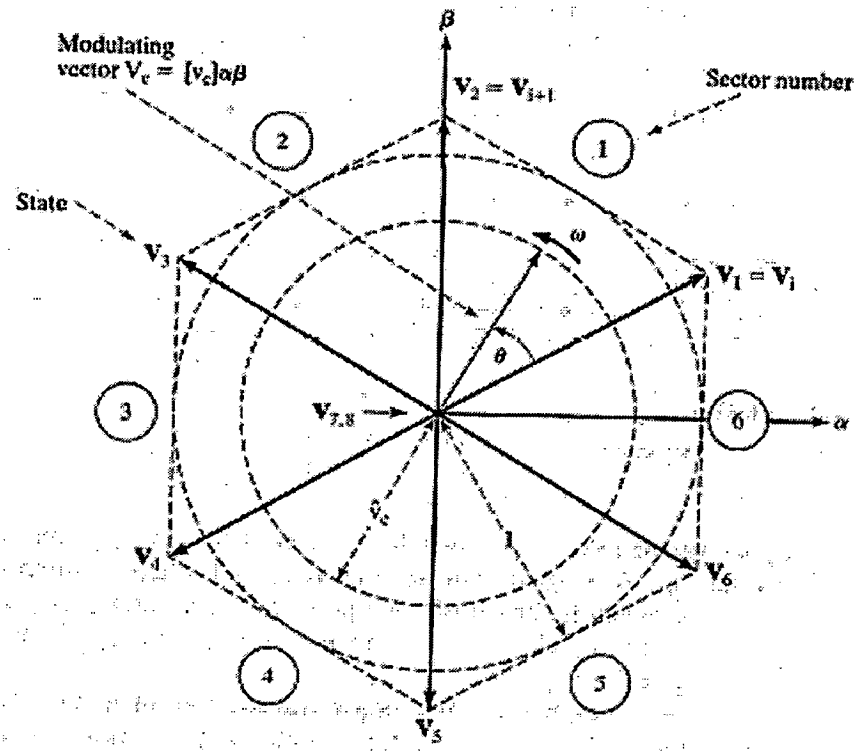

V_7 and V_8 are zero vectors

Figure 2.4. Representation of rotating vector in complex plane

2.4.4 Generalization of the SVM:

Five steps can be identified to implement the SVM for VSI [33]:

1. Definition of the possible switching vectors in the output voltage space: In this step, it is possible to include a co-ordinate transformation in the output voltage space, to simplify its representation.
2. Identification of the separation planes between the sectors in the output voltage space: The separation planes are required in an algorithm that determines the sector where the desired output voltage vector is located.
3. Identification of the boundary planes in the output voltage space: The boundary planes define whether a given voltage vector can be implemented by the inverter. If it is possible to implement this voltage vector, go to 4^{th} step.
4. Obtaining the decomposition matrices: The decomposition matrices allow computing the time duration that each switching vector should be applied in a sampling period.
5. Definition of the switching sequence: Finally, the switching sequences are selected to minimize an additional quantity, which can include.

- Commutation losses
- THD, in some inverters
- The unbalance of the DC bus neutral point

In the following sections methodology is applied to three phase three wire inverters.

2.4.5 Three-phase three-wire VSI: Modeling of SVM

Here the concepts of SVM are applied to three phase three wire inverter as shown in fig2.5. It is assumed that S_1 and S_4, S_3 and S_6 as well as S_5 and S_2 are switched in complementary way. Thus there are 8 possible switching vectors presented in table 2.1.

It can be verified that the output voltage space of the inverter shown in fig.2.4 is two dimensional, because if two voltages are known, for instance V_{ab} and V_{bc}, the third V_{ca}, is implicitly defined. In order to simplify the practical implementation, it is useful to transform the coupled three phase system in a decoupled two-phase system by using one orthogonal linear transformation, called $\alpha\beta$ transformation, given by,

$$T_{\alpha\beta} = 2/3\begin{bmatrix} 1 & -1/2 & -1/2 \\ 0 & \sqrt{3}/2 & -\sqrt{3}/2 \end{bmatrix} \quad (2.12)$$

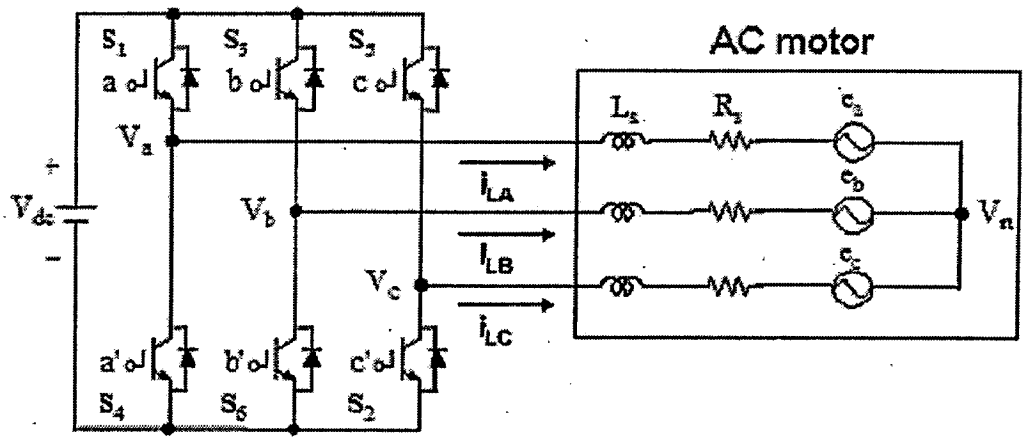

where a,b and c are switching variable vectors

Figure 2.5.Three phase three wire VSI

Then the output voltage space can be constructed by projecting the leg-voltage space onto a two-dimensional plane orthogonal to the $[1\ 1\ 1]^T$ vector in abc co-ordinates. This can be accomplished by applying equation 2.7 to the eight switching vectors in table 2.1.

2.4.5.1 Switching pattern and switching vectors

In the new co-ordinate system (αβ), there are 6 non-zero vectors (whose extremes are the vertices of a regular hexagon), which have a phase angle of 60° among them, with amplitude equal to 2/3. In addition there are two vectors with amplitude equal to zero, as shown in fig.2.4.

a = 1; top switch in leg 'a' is ON.
a = 0; lower switch in leg 'a' is ON.

b = 1; top switch in leg 'b' is ON.
b = 0; lower switch in leg 'b' is ON.

c = 1; top switch in leg 'c' is ON.

c = 0; lower switch in leg 'c' is ON.

Where a, b and c are switching variable vectors.

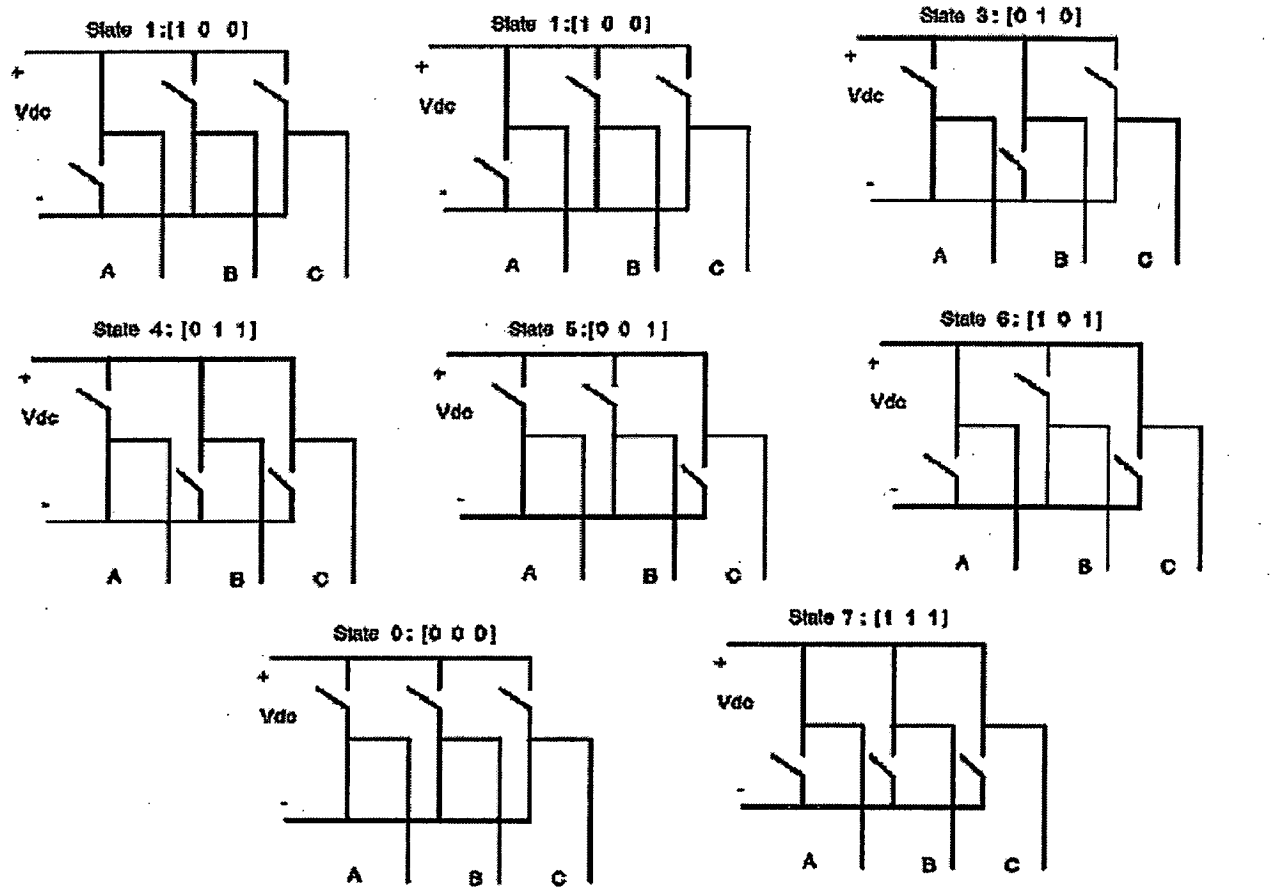

Figure 2.6. Possible switching pattern of the inverter

2.4.5.2 Separation and boundary planes

From fig.2.4, it is possible to identify 6 sectors between two adjacent vectors to the command vector $\overline{V}$. The separation planes of these sectors can be defined by the following equations:

PS_1: $V_\beta + \sqrt{3}V_\alpha = 0$

PS_2: $V_\beta - \sqrt{3}V_\alpha = 0$

PS_3: $V_\beta = 0$ (2.13)

On the other hand the boundary planes of each sector are presented in table 2.2.

Voltage Vectors	Switching Vectors			Line to neutral voltage			Line to line voltage		
	a	b	c	V_{an}	V_{bn}	V_{cn}	V_{ab}	V_{bc}	V_{ca}
V_0	0	0	0	0	0	0	0	0	0
V_1	1	0	0	2/3	-1/3	-1/3	1	0	-1
V_2	1	1	0	1/3	1/3	-2/3	0	1	-1
V_3	0	1	0	-1/3	2/3	-1/3	-1	1	0
V_4	0	1	1	-2/3	1/3	1/3	-1	0	1
V_5	0	0	1	-1/3	-1/3	2/3	0	-1	1
V_6	1	0	1	1/3	-2/3	1/3	1	-1	0
V_7	1	1	1	0	0	0	0	0	0

(Note that the respective voltage should be multiplied by V_{dc})

Table 2.1. Possible switching vectors of three-phase three-wire VSI.

Sector	Plane
S_1	$PL_1: V_\beta + \sqrt{3}V_\alpha - \sqrt{2} = 0$
S_2	$PL_2: V_\beta - \sqrt{2}/2 = 0$
S_3	$PL_1: V_\beta - \sqrt{3}V_\alpha - \sqrt{2} = 0$
S_4	$PL_1: V_\beta + \sqrt{3}V_\alpha + \sqrt{2} = 0$
S_5	$PL_1: V_\beta + \sqrt{2}/2 = 0$
S_6	$PL_1: V_\beta - \sqrt{3}V_\alpha + \sqrt{2} = 0$

Table 2.2. Boundary planes of the three-phase three-wire VSI.

2.4.5.3 Decomposition matrices

It is assumed that the command vector $\overline{V}$ is into the sector 1 and the implemented switching sequence is V_0, V_1, V_2, V_7, V_2, V_1,V_0 . That is switching vectors utilized are V_1, V_2 and V_7/V_0 , and the duration times associated to each vector are T_1, T_2 and T_0 respectively.

Therefore the average output voltage vector of the inverter in a sampling period is equal to $\overline{V}$ if the following equation is satisfied.

$$V_1 . T_1 + V_2 . T_2 + V_0 . T_0 = \overline{V} . T_s \tag{2.14}$$

Where $T_1+T_2+T_0 = T_s$ (or T_z), sampling period

Rewriting equation (2.9) in the matrix form,

$$\begin{bmatrix} V_1 & V_2 & V_0 \\ 1 & 1 & 1 \end{bmatrix} \begin{bmatrix} T_1 \\ T_2 \\ T_0 \end{bmatrix} = \begin{bmatrix} \overline{V} \\ 1 \end{bmatrix} T_s \tag{2.15}$$

It is important to observe that the last row added to the matrix of switching vectors makes this matrix non-singular. This is desirable because the computation of the duration times can be carried out in a unique way,

$$\text{i.e.} \begin{bmatrix} T_1 \\ T_2 \\ T_0 \end{bmatrix} = M_1 \begin{bmatrix} V_\alpha \\ V_\beta \\ 1 \end{bmatrix} T_s \tag{2.16}$$

$$\text{Where } M_1 = \begin{bmatrix} V_1 & V_2 & V_0 \\ 1 & 1 & 1 \end{bmatrix}^{-1}$$

Where V_α and V_β are the components of the command vector $\overline{V}$ and M_1 is the decomposition matrix associated with sector 1.

2.4.5.3.1 Duration times of sector 1:

The duration times T_1, T_2 and T_0 of sector 1 are determined as follows[9][38]:

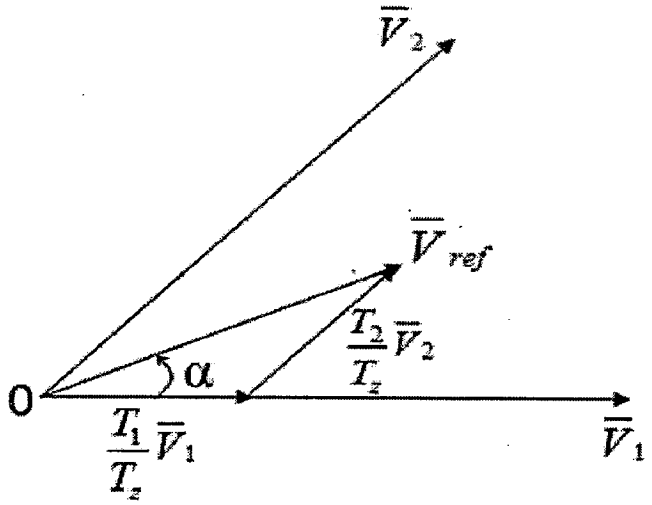

Figure 2.7. Reference vector as a combination of adjacent vectors at sector 1.

$$\int_0^{T_z} \overline{V}_{ref}\,dt = \int_0^{T_1} \overline{V}_1 dt + \int_{T_1}^{T_1+T_2} \overline{V}_2 dt + \int_{T_1+T_2}^{T_z} \overline{V}_0 dt \qquad (2.17)$$

$$\Rightarrow T_z \,.\, \overline{V}_{ref} = T_1 \,.\, \overline{V}_1 + T_2 \,.\, \overline{V}_2 \qquad (2.18)$$

$$\Rightarrow T_z \,.\, \left|\overline{V}_{ref}\right| \begin{bmatrix}\cos\alpha \\ \sin\alpha\end{bmatrix} = T_1\,(2/3)\,V_{dc} \begin{bmatrix}1 \\ 0\end{bmatrix} + T_2\,(2/3)\,V_{dc} \begin{bmatrix}\cos(\pi/3) \\ \sin(\pi/3)\end{bmatrix} \qquad (2.19)$$

(Where $0 \le \alpha \le 60^o$)

Equating two rows and simplifying, we get,

$$\therefore \quad T_1 = T_z \,.\, a \,.\, \frac{\sin(\frac{\pi}{3} - \alpha)}{\sin(\frac{\pi}{3})} \qquad (2.20)$$

and $$T_2 = T_z \,.\, a \,.\, \frac{\sin(\alpha)}{\sin(\frac{\pi}{3})} \qquad (2.21)$$

$$\therefore \quad T_0 = T_z - (T_1 + T_2), \qquad (2.22)$$

$$[\text{ where } T_z = 1/f_s \text{ and } a = \frac{\left|\overline{V}_{ref}\right|}{\frac{2}{3}V_{dc}}]$$

Where T_1 , T_2 and T_0 represent the time widths for vectors V_1, V_2 and V_0 respectively. T_0 is the period in a sampling period for null vectors should be filled.

As each switching period (half of sampling period) T_z starts and ends with zero vectors, that is there will be two vectors T_z or four null vectors per T_s, duration of each null vector is $T_0/4$.

2.4.5.3.2 Switching time duration at any sector:

$$T_1 = \frac{\sqrt{3}.T_z.\left|\overline{V}_{ref}\right|}{V_{dc}}.\left[\sin\left(\frac{\pi}{3}-\alpha+\frac{n-1}{3}\pi\right)\right] \tag{2.23}$$

$$= \frac{\sqrt{3}.T_z.\left|\overline{V}_{ref}\right|}{V_{dc}}.\left[\sin\left(n\frac{\pi}{3}-\alpha\right)\right]$$

$$= \frac{\sqrt{3}.T_z.\left|\overline{V}_{ref}\right|}{V_{dc}}.\left[\sin\frac{n}{3}\pi.\cos\alpha-\cos\frac{n}{3}\pi.\sin\alpha\right] \tag{2.24}$$

$$T_2 = \frac{\sqrt{3}.T_z.\left|\overline{V}_{ref}\right|}{V_{dc}}.\left[\sin\left(\alpha-\frac{n-1}{3}\pi\right)\right] \tag{2.25}$$

$$= \frac{\sqrt{3}.T_z.\left|\overline{V}_{ref}\right|}{V_{dc}}.\left[-\sin\frac{n-1}{3}\pi.\cos\alpha+\cos\frac{n-1}{3}\pi.\sin\alpha\right] \tag{2.26}$$

$$\therefore \quad T_0 = T_z - T_1 - T_2 \tag{2.27}$$

where $n = 1$ through 6 (i.e. sector 1 to 6) and $0 \le \alpha \le 60°$)

Note: The null time has been conveniently distributed between the V_0 and V_7 vectors to describe the symmetric pulse width. Studies have shown that a symmetric pulse pattern gives minimal output harmonics.

Fig.2.8 gives the switching patterns of each thyristor in each sector and table 2.3 gives the switching time table of each thyristor at each sector.

2.4.5.3.3 Determining switching time for each thyristor:

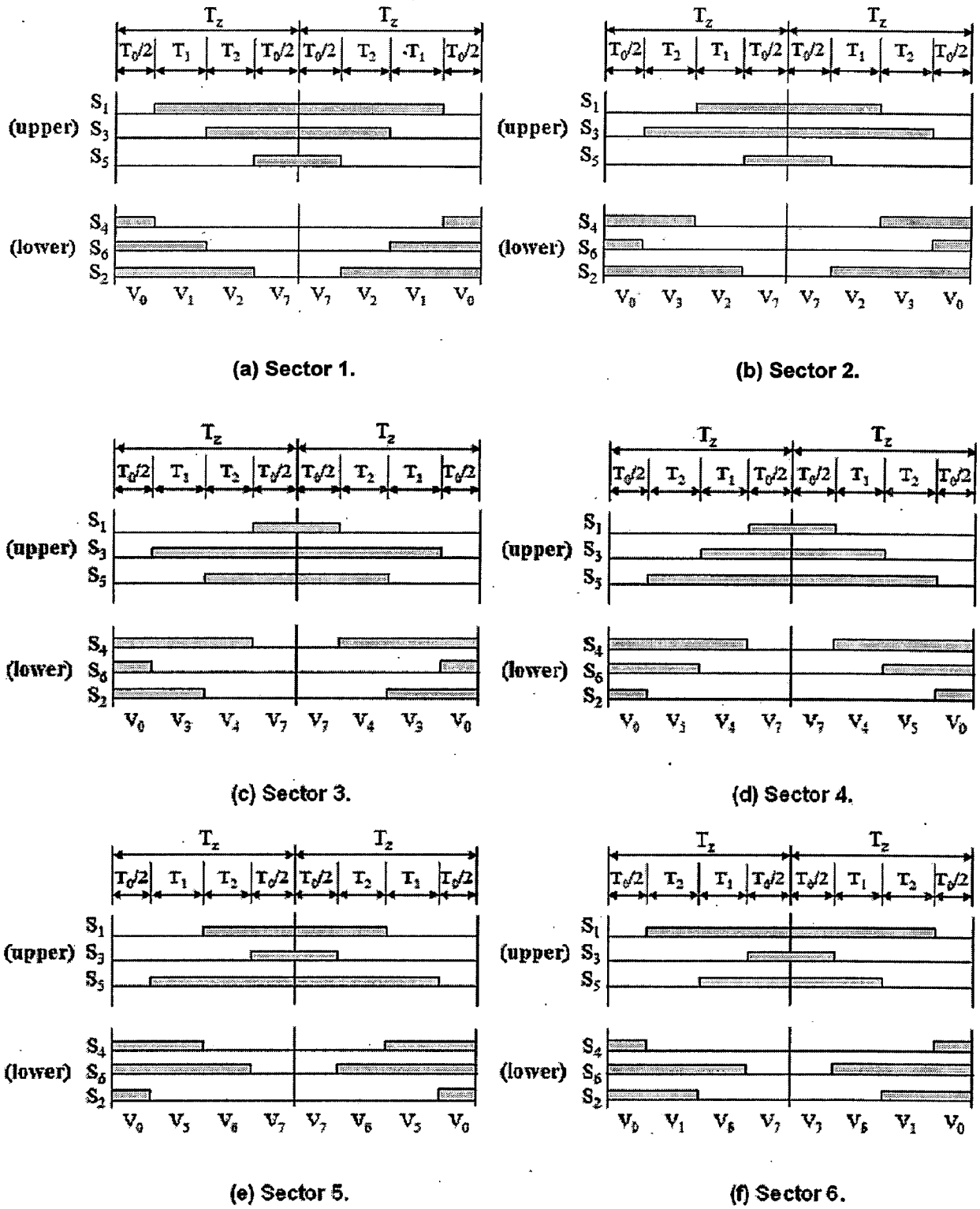

Figure 2.8. Space vector PWM switching patterns at each sector

Sector	Upper Switches (S_1, S_3, S_5)	Lower Switches (S_4, S_6, S_2)
1	$S_1 = T_1 + T_2 + T_0/2$ $S_3 = T_2 + T_0/2$ $S_5 = T_0/2$	$S_4 = T_0/2$ $S_6 = T_1 + T_0/2$ $S_2 = T_1 + T_2 + T_0/2$
2	$S_1 = T_1 + T_0/2$ $S_3 = T_1 + T_2 + T_0/2$ $S_5 = T_0/2$	$S_4 = T_2 + T_0/2$ $S_6 = T_0/2$ $S_2 = T_1 + T_2 + T_0/2$
3	$S_1 = T_0/2$ $S_3 = T_1 + T_2 + T_0/2$ $S_5 = T_2 + T_0/2$	$S_4 = T_1 + T_2 + T_0/2$ $S_6 = T_0/2$ $S_2 = T_1 + T_0/2$
4	$S_1 = T_0/2$ $S_3 = T_1 + T_0/2$ $S_5 = T_1 + T_2 + T_0/2$	$S_4 = T_1 + T_2 + T_0/2$ $S_6 = T_2 + T_0/2$ $S_2 = T_0/2$
5	$S_1 = T_2 + T_0/2$ $S_3 = T_0/2$ $S_5 = T_1 + T_2 + T_0/2$	$S_4 = T_1 + T_0/2$ $S_6 = T_1 + T_2 + T_0/2$ $S_2 = T_0/2$
6	$S_1 = T_1 + T_2 + T_0/2$ $S_3 = T_0/2$ $S_5 = T_1 + T_0/2$	$S_4 = T_0/2$ $S_6 = T_1 + T_2 + T_0/2$ $S_2 = T_2 + T_0/2$

Table 2.3. Switching time table at each sector

2.4.5.4 Switching sequence

The SV sequence should assure that the load line voltages have the quarter-wave symmetry to reduce even harmonics in their spectra. To reduce the switching frequency, it is also necessary to arrange the switching sequence in such a way that the transition from one to the next is performed by switching only one inverter leg at a time. Although there is no systematic approach to generate an SV sequence, these conditions are met by the sequence $\mathbf{V_z}$, $\mathbf{V_n}$, $\mathbf{V_{n+1}}$, $\mathbf{V_z}$ (where $\mathbf{V_z}$ is alternatively chosen between $\mathbf{V_0}$ and $\mathbf{V_7}$). The switching pattern in each sector can be seen in fig.2.8.

Using the same concepts explained in the previous section, table IV presents a symmetric switching sequence, where the 3 legs of the inverter switch at high frequency, resulting in an output voltage with low THD. Another switching sequence is also shown in table.2.4, which reduces the commutation losses due to the fact that in each sector one leg commutates at 60 Hz.

Sector	Symmetric-sequence	One leg at 60 Hz
S_1	V_0-V_1-V_2-V_7-V_2-V_1-V_0	V_1-V_2-V_7-V_2-V_1
S_2	V_0-V_3-V_2-V_7-V_2-V_3-V_0	V_2-V_3-V_0-V_3-V_2
S_3	V_0-V_3-V_4-V_7-V_4-V_3-V_0	V_3-V_4-V_7-V_4-V_3
S_4	V_0-V_5-V_4-V_7-V_4-V_5-V_0	V_4-V_5-V_0-V_5-V_4
S_5	V_0-V_5-V_6-V_7-V_6-V_5-V_0	V_5-V_6-V_7-V_6-V_5
S_6	V_0-V_1-V_6-V_7-V_6-V_1-V_0	V_6-V_1-V_0-V_1-V_6

Table 2.4. Switching sequences for the three-phase three-wire VSI

2.4.6 Output waveforms of space vector modulation:

The instantaneous phase voltages can be found by time averaging of the SVs during one switching period for sector 1 as given by[9],

$$V_{aN} = \frac{V_s}{2T_s}\left(\frac{-T_z}{2} + T_1 + T_2 + \frac{T_z}{2}\right) = \frac{V_s}{2}\sin\left(\frac{\pi}{3} + \theta\right) \tag{2.28}$$

$$V_{bN} = \frac{V_s}{2T_s}\left(\frac{-T_z}{2} - T_1 + T_2 + \frac{T_z}{2}\right) = V_s\frac{\sqrt{3}}{2}\sin\left(\theta - \frac{\pi}{6}\right) \tag{2.29}$$

$$V_{cN} = \frac{V_s}{2T_s}\left(\frac{-T_z}{2} - T_1 - T_2 + \frac{T_z}{2}\right) = -V_{aN} \tag{2.30}$$

To minimize characteristic harmonics in SV modulation, the normalized sampling frequency f_{sn} should be an integer multiple of 6; that is,

$$T \geq 6nT_s \quad \text{for } n = 1,2,3....$$

This is due to the fact that all the six sectors should be equally used in one period for producing symmetric line output voltages. As an example, fig.2.10 shows typical waveforms of an SV modulation for f_{sn} = 18 and M=0.8.

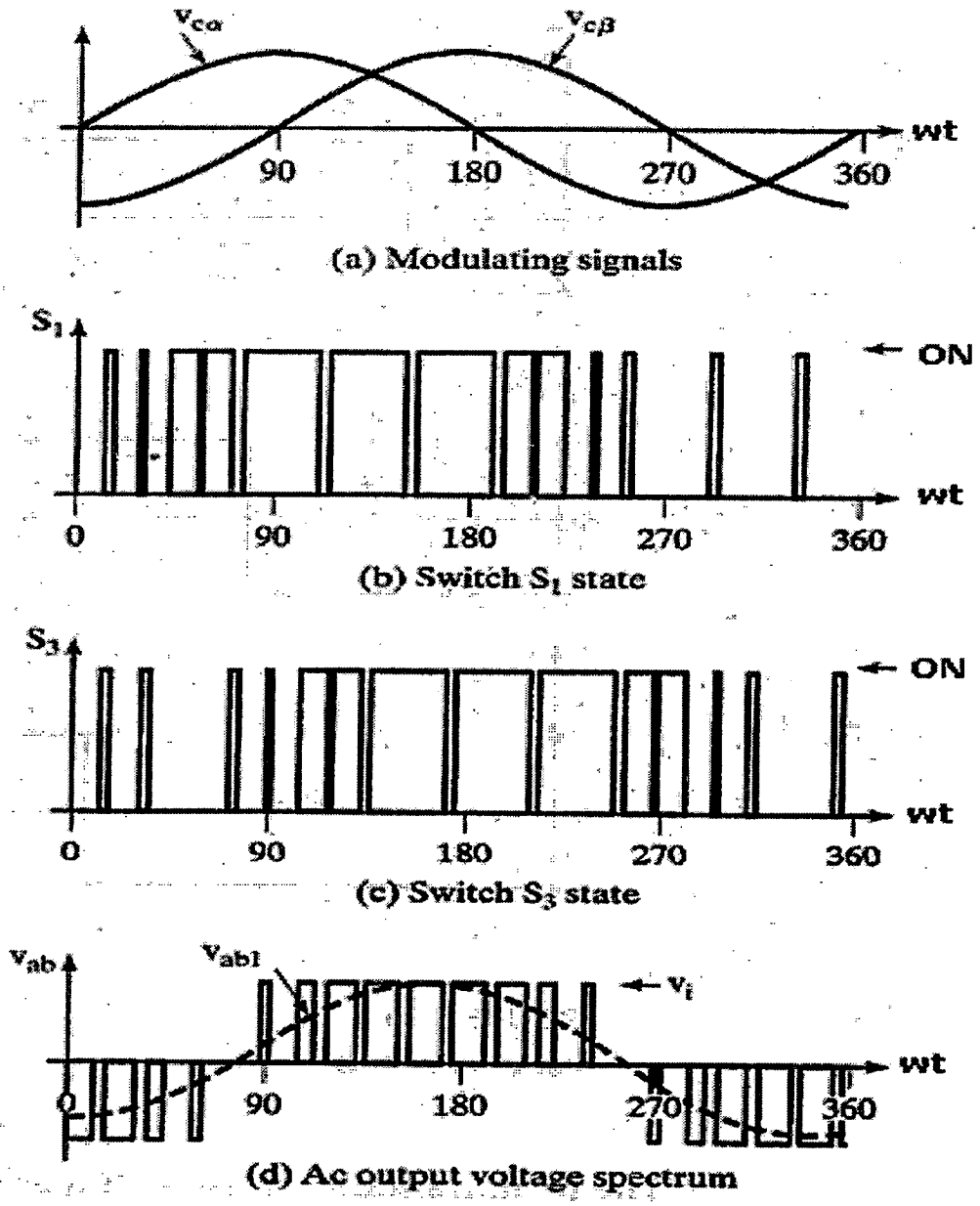

Figure 2.10. Three phase waveforms for space vector modulation (M=0.8, f_{sn}=18)[9]

2.5 CONCLUSION

From the above discussions, it can be concluded that SVM technique is superior PWM technique for three phase inverters drives compared to the traditional PWM techniques. The significant advantages of SVM are the ease of microprocessor implementation and the fact that the waveforms produced are very nearly loss mininised. But sinusoidal PWM technique is easy for implementation.

CHAPTER III

MODELING AND IMPLEMENTATION OF VECTOR CONTROLLED INDUCTION MOTOR DRIVE (VCIMD) IN MATLAB ENVIRONMENT

3.1 INTRODUCTION

There are various issues attached to the driving of the motor apart from the nonlinear characteristics of the induction motor. Now these issues are discussed briefly. Earlier motors tended to be over designed to drive a specific load over its entire range which resulted in a highly inefficient drive, as a significant part of the input power was not doing any useful work. Most of the time, the generated motor torque was more than the required load torque.

Moreover, the steady state motoring region for an induction motor is restricted from 80% of the rated speed to 100% of the rated speed due to the fixed supply frequency and the number of poles. Further, a very high inrush current is drawn by induction motor during starting due to absence of back EMF at starting. This results in high power losses in the transmission line and also in the rotor, which will eventually heat up and may fail due to insulation failure. This high inrush current may also cause a voltage dip in the supply line, which will affect the performance of other utility equipment connected on the same supply line.

When the motor is operated at a minimum load (i.e. open shaft), the current drawn by the motor is primarily the magnetizing current and is almost purely inductive. As a result, the PF is very low, typically as low as 0.1. The magnetizing current remains almost constant ove r the entire operating range, from no load to full load. Hence, with the increase in the load, the working current begins to increase, the PF will also improve.

When the motor operates at a PF less than unity, the current drawn by the motor is not sinusoidal in nature. This condition degrades the power quality of the supply line and may affect the performance of the other equipment connected to the same supply line. The most important thing to consider while operating the motor is, it is often necessary to stop the motor quickly and also to reverse it. In many applications like cranes or hoists, the torque of the drive motor may have to be controlled so that the load does not have any undesirable acceleration. The speed and accuracy of stopping or reversing operations improve the productivity of the system and the quality of the product.

In the applications such as fan, blower, pump, etc., the input power is a function of the speed. In these type of loads, the torque is proportional to the square of the speed and the power is proportional to the cube of the speed. Hence, variable speed, depending upon the load requirement, provides significant energy saving. A reduction os 20% in the operating speed of the motor from its rated speed will result in an almost 50% reduction in the input power to the motor. This is not possible in a system where the motor is directly connected to the supply line.

When the supply line is delivering the power at a PF less than unity, the motor draws current rich in harmonics. This result in higher rotor loss affecting the motor life. The torque generated by the motor will be pulsating in nature due to harmonics. At high speeds, the pulsating torque frequency is large enough to be filtered out by the motor impedance. But at low speeds, the pulsating torque results in the motor speed pulsation. This results in jerky motion on motor and affects the bearings' life.

Hence, all the above mentioned problems are faced by both consumers and the industry. Thus, it is strongly recommended for an intelligent motor control. Thus, as mentioned in chapter 1, with the advancement of solid state device technology (BJT, MOSFET, IGBT, SCR, etc.) and IC fabrication technology, which gave rise to high-speed microcontrollers and microprocessors capable of executing real-time complex algorithm to give excellent dynamic performance of the AC induction motor.

3.2 CONCEPT OF VECTOR CONTROL

As explained earlier, with vector control, it is possible to achieve high dynamic performance equivalent to that of a separately excited DC motor, in variable speed AC drives. Therefore a vector controlled induction motor drive(VCIMD) can be used in the place of a dc motor as the induction motor is smaller, mechanically more rigid, less expensive, maintenance and sparking free as it does not have commutator and brushes.

3.2.1 Controlled quantities in vector control

Like in a dc motor, torque is produced in the induction motor by the electromagnetic interaction of current in the rotor conductor and the magnetic flux density in the air gap to which the rotor is subjected. But in three phase induction motor of squirrel cage type, all the electrical inputs

are given to stator only. It is neither convenient nor practical to sense the rotor currents as there is no electrical connection to the rotor.

The currents flowing on the stator coils are primarily responsible for two things:

1. inducing currents in the rotor
2. creating magnetic field in the airgap

The technique of vector control is based on a method of separating out these basic two functions of the stator current. In a VCIM, the current flowing in the stator phase is the sum of two components at every instant – one component known as **field component** responsible for producing the magnetic field in the airgap and the other component known as **torque component** responsible for inducing the torque by inducing the corresponding current in the rotor conductors.

The necessary computation for determining the torque component and the field component of each stator phase current is done online by suitably programmed computing blocks (MATLAB – Simulink blocks are used in this work). Then a closed loop controller compares the torque component against the demanded torque. The demanded torque is the reference input provided by an outer speed control loop. This loop determines the necessary change to make he torque component equal to the demanded torque. In a similar way there is a control loop for field control. This loop compares the computed value of the field component against the field reference. The field reference has a constant value at all speeds below the base speed as in the case of a DC motor. To implement field weakening above the base speed, the reference input to the field controller is reduced. In either case, the field control loop compares the computed value of the actual field component against the field reference. This loop determines the change, if any, necessary to make the actual field component equal to the commanded value.

In this manner, the torque control loop determines the required change in the torque component and the field control loop determines the change required in the field component. These two individual values of the required changes are added to get the total change required in the output current of the inverter. The inverter switching times are appropriately modified to implement the required total change.

3.2.2 Mathematical analysis and simulation of vector control :

The proposed field oriented control scheme shown in fig.3.1 uses three control loops namely, the flux control loop, torque control loop and current control loop. It utilizes the rotor speed to

derive the field coordinates (i_{ds}^* and i_{qs}^*, i.e. the flux producing component and the torque producing component) of the stator current vector. The reference torque T^* is computed in torque control loop. For the same error signal $\omega_{e(n)}$ obtained from the rotor speed ω_r and its reference counterpart ω_r^* is used. T^* is used to compute the reference value of torque producing component (i_{qs}^*) of the stator current vector i_s.

Each and every subsystem of the block diagram shown fig. 3.1 is modeled individually by using a definite set of equations and then all the subsystems are integrated to obtain the desired vector control for an induction motor. The description and modeling of the different subsystems is given in the following sections.

3.2.2.1 Mathematical Model of Induction Machine:

The squirrel cage induction motor is modeled using d-q theory in the stationary reference frame so that we get less number of equations and the analysis becomes easy. The voltage-current relationship in the stationary reference frame of the induction motor in terms of the d-q variable is expressed as [1]:

$$[v]=[R][i]+[L]p[i]+\omega[G][i] \tag{3.1}$$

Therefore by simplifying equation (3.2), the current derivative vector can be expressed as follows:

$$p[i]=[L]^{-1}\{[v]-[R][i]-\omega[G][i]\} \tag{3.2}$$

where 'p' is the differential operator (d/dt) and 'ω' is the rotor speed in electrical 'rad/sec'.

Current and Voltage vectors are given as follows:

$$[i]=\begin{bmatrix} i_{qss} & i_{dss} & i_{qrs} & i_{drs} \end{bmatrix}^T \tag{3.3}$$

$$[v]=\begin{bmatrix} v_{qss} & v_{dss} & v_{qrs} & v_{drs} \end{bmatrix}^T \tag{3.4}$$

where v_{qss} and v_{dss} are the q- and d-axis voltages applied across the stator windings referred to the stator and v_{qrs} and v_{drs} are the q- and d-axis voltages across the rotor windings referred to the stator. As the rotor bars are short circuited in a squirrel cage induction motor, the voltages v_{qrs} and v_{drs} are zero. Similarly the currents are also defined. [L] is the inductance vector, [R] is the resistance vector and [G] is the rotational inductance matrix and have the usual meaning. All the voltages and currents are expressed in the stationary reference frame.

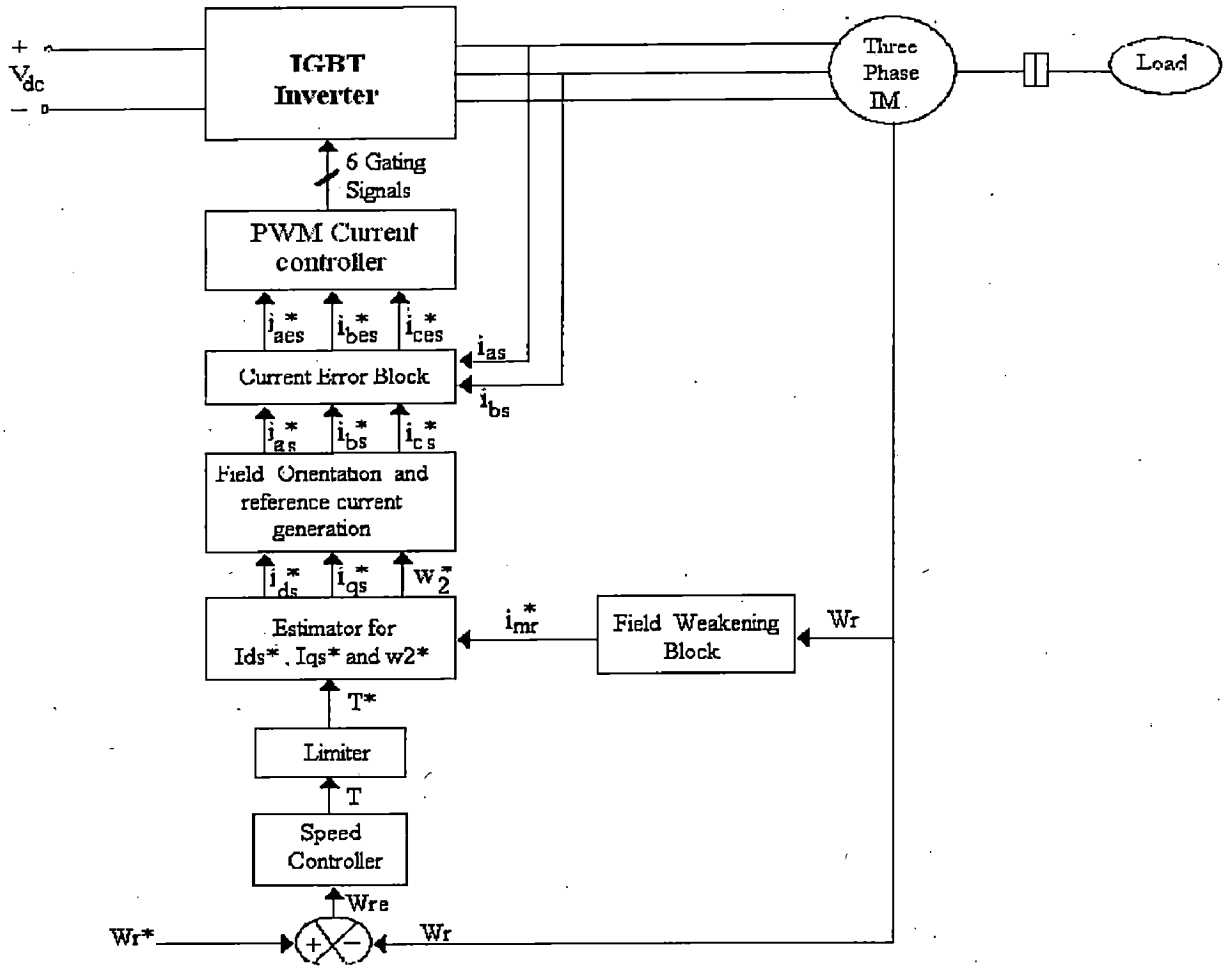

Figure 3.1. Basic block diagram of Vector Controlled Induction Motor Drive

3.2.2.2 Speed Controllers:

In this work, four different speed controllers have been used. Each speed controller has been modeled separately as given below. Each speed controlled is followed by a limiter. Generally the speed error, which is the difference of reference speed and actual speed, is given as input to these controllers. These speed controllers process the speed error and give torque value as an output. Then the toque value is fed to the limiter which gives the final limited reference torque. The speed error at any nth instant of time is given as:

$$\omega_{r\,e(n)} = \omega_{r(n)}^{*} - \omega_{r(n)} \tag{3.5}$$

where $\omega_{r(n)}^{*}$ is the reference speed of the motor

$\omega_{r(n)}$ is the actual speed of the motor

Various speed controllers used in this work are explained in the below sections.

3.2.2.2.1 Proportional Integral (PI) speed controller

The PI speed controller is the simplest speed controller compare to any other speed controller. The general block diagram of the PI speed controller is shown in fig 3.2. The output of the speed controller at nth instant is expressed as follows:

$$T_{(n)} = T_{(n-1)} + K_p\{\omega_{re(n)} - \omega_{re(n-1)}\} + K_i\omega_{re(n)} \tag{3.6}$$

where $T_{(n)}$ is the torque output of the speed controller at the n^{th} instant.

K_p and K_i are proportional and integral gain constants

$\omega_{re(n-1)}$ is the speed error at (n-1)th instant

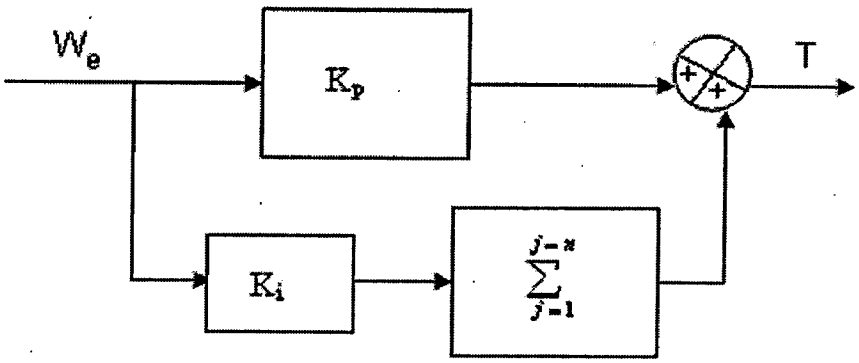

Figure 3.2 Block diagram of PI speed controller

The PI speed controller gain parameters shown in the block diagram and the equation (3.4) are selected by trial and error basis by observing their effects on the response of the drive. The numerical values of these controller gains depend on the ratings of the motor and they are presented in the Appendix-B for the motor drive system used in this work.

The MATLAB/simulink model diagram of the PI controller in discrete time is shown in fig.3.3. As seen in figure, using the proportional and integral gain parameters namely, k_p and k_i respectively along with the limiter, the reference torque is calculated in accordance to the motor rating used.

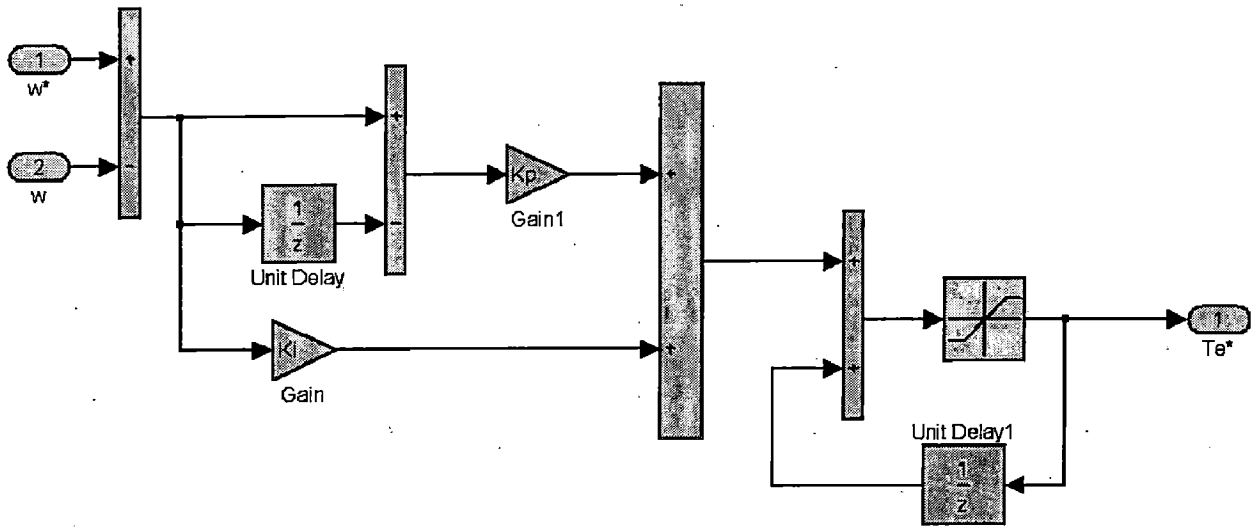

Figure 3.3 MATLAB model for Proportional Integral (PI) Controller

3.2.2.2.2 Fuzzy Logic (FL) speed controllers

The conventional speed controllers for vector controlled induction motor drive (VCIMD) suffer from the problem of stability, besides these controllers show either steady state error or sluggish response to the perturbation in reference setting or during load perturbation. The motor control issues are traditionally handled by fixed gain PI and Proportional-integral-derivative (PID) controllers. However, the fixed-gain controllers are very sensitive to parameter variations, load disturbances, etc. Thus, the controller parameters have to be continually adapted. However, it is often difficult to develop an accurate system mathematical model due to unknown load variation, temperature variations, unknown and unavoidable parameter variations due to saturation and system disturbances. In order to overcome the above problems, recently, the fuzzy-logic controller (FLC) is being used for motor control purpose. The mathematical tool for the FLC is the fuzzy set theory introduced by Zadeh [28]. As compared to the conventional PI, PID, and their adaptive versions, the FLC has some advantages such as:

1. It does not need any exact system mathematical model.
2. It can handle nonlinearity of arbitrary complexity.
3. It is based on the linguistic rules with an IF-THEN general structure, which is the basis of human logic.

However, the application of FLC has faced some disadvantages during hardware and software implementation due to its high computational burden.

MODELING OF FUZZY LOGIC BASED SPEED CONTROLLER:

A. Variables of input and output for controller:

The block diagram of speed control system using a fuzzy logic controller (FLC) is shown in fig.3.4 In order to establish the FLC, firstly, variables of the input and the output for the controller must be clearly defined. Though the FLC can have several observed values as inputs, the most significant variables entering the FLC have been selected as the speed error (ω_{re}) and its time derivative i.e. change in error ($\Delta\omega_{re}(n)$). The output of this controller is the torque, T.

At a sampling time n, the input variables are expressed as

$$\omega_{re}(n) = \omega_r^*(n) - \omega_r(n) \tag{3.7}$$

$$\Delta\omega_{re}(n) = \omega_{re}(n) - \omega_{re}(n-1) \tag{3.8}$$

Where ω_r^* and ω_r are reference speed command and the actual speed of the induction motor.

B. Fuzzy variables and control rules:

In order to obtain better control results, it is necessary to use appropriate number of fuzzy variables and to formulate appropriate control rules. In this study, we use the fundamental seven kinds of fuzzy variables as follows:

NL : Negative Large PL : Positive Large

NM : Negative Medium PM : Positive Medium

NS : Negative Small PS : Positive Small

ZE : Approximately Zero

The next step is to decide the appropriate shape of the membership functions for w_e and w_{ee}. More fuzzy sets in w_e and w_{ee} will lead to higher precision in this input space. Hence seven fuzzy sets are assigned to each of the inputs in their respective universe of discourse. Consequently, if the number of fuzzy sets in a particular universe of discourse is increased to infinity, then all fuzziness will be lost and it will be equivalent to a conventional input domain. To simplify mathematical computations, the shape of the fuzzy sets on the two extreme ends of the respective universe of discourse is taken as trapezoidal whereas all other intermediate fuzzy sets are triangular. This is illustrated in fig.3.5.

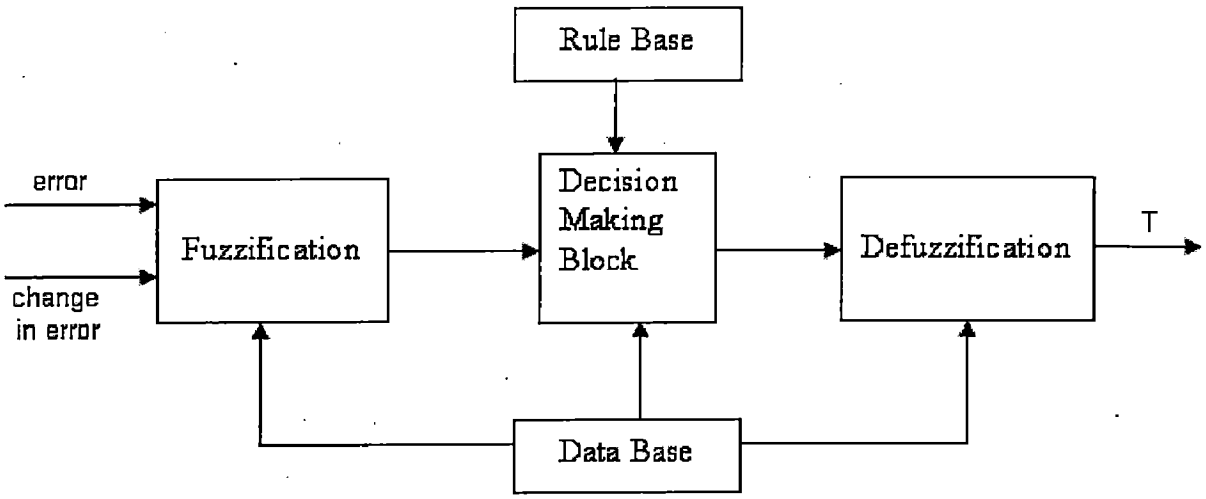

Figure 3.4 Block diagram of Fuzzy Logic Controller (FLC)

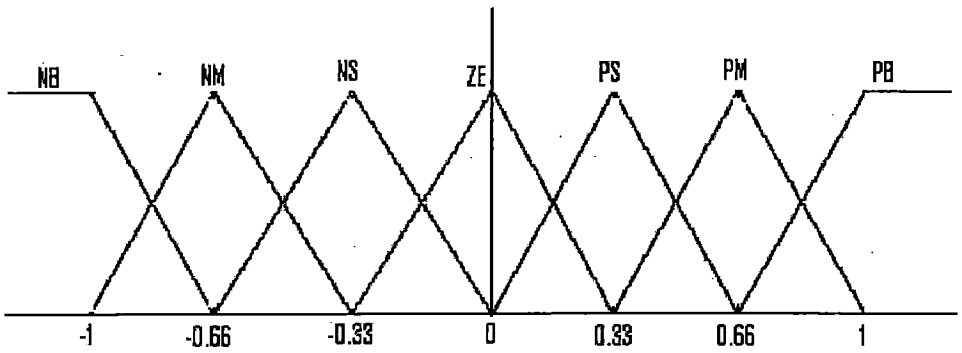

Figure 3.5 Fuzzy sets considered for speed control

The control rules for the FLC can be described by language using the input variables w_e and w_{ee}, and the output variable, T. For example the i-th control rule can be usually written as:

Rule i : if w_e is F_i and w_{ee} is G_i then T is H_i.

Where F_i, G_i and H_i are fuzzy variables.

In general, it is difficult to formulate control rules for an unknown system. However, we already know the system and can predict a step response of the motor speed. Therefore it is comparatively easy to formulate control rules.

The typical step response of the speed from 0 rpm to a set value as shown in fig.3.6

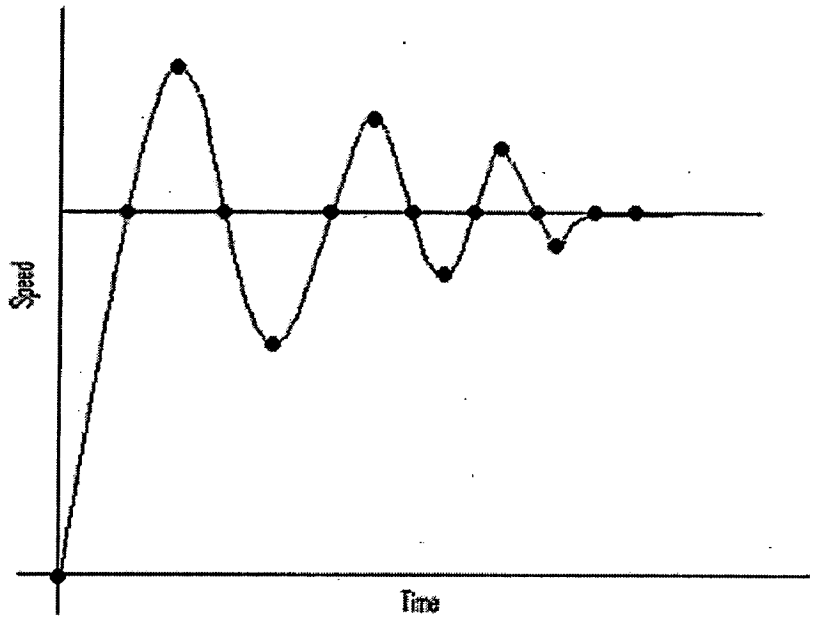

Figure 3.6. Step Response of the speed

The characteristic points are shown with dots in this figure. To formulate control rules, it is necessary to examine the condition at each characteristic point and to consider the relation among E_r, E_r (dot) and ΔT_c, so as to bring the step response close to the set speed value. The fuzzy rule table used in this work is given in table 3.1 [35].

Figure 3.7 shows the simulink model block diagram for the FL speed controller. The two inputs namely speed error and change in speed error are properly scaled and fed to the MATLAB fuzzy logic controller. The defuzzified output of the FL block is scaled by proper scaling factor and after limiting, forms the reference torque for the vector controller.

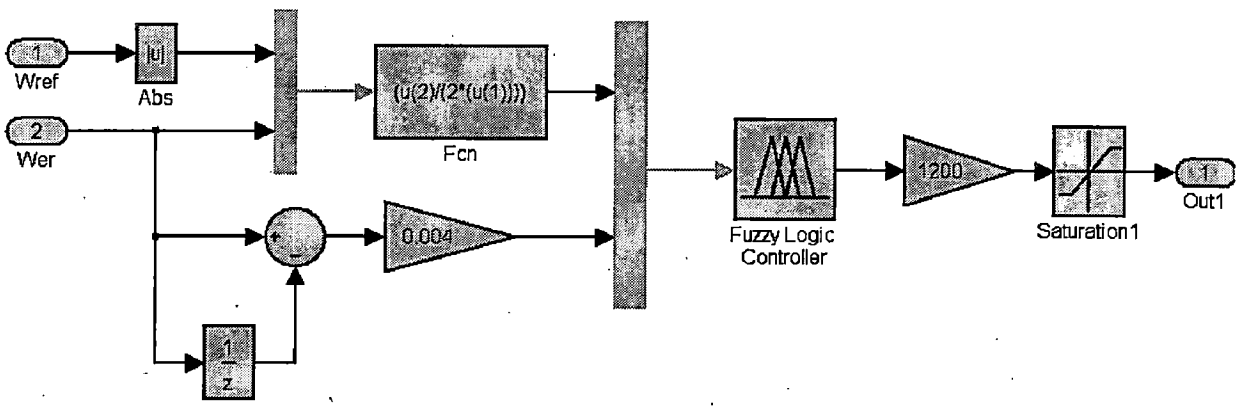

Figure 3.7 MATALB model for Fuzzy Logic (FL) speed controller

ω_{re} / $\Delta\omega_{re}$	NB	NM	NS	ZE	PS	PM	PL
NB				NB	NB		
NM	NB			NB	NB		
NS	NB			NM	NM	NM	PM
ZE	NB	NM	NS	ZE	PS	PM	PB
PS	NM		PS	PS	PM		
PM				PM	PB	PB	
PL			PM	PM	PB		

Table 3.1 Logic rules for Fuzzy Logic (FL) speed controller

3.2.2.2.3 Hybrid speed controller

A hybrid fuzzy controller for a VCIMD is presented in this section. The hybrid fuzzy controller consists of proportional-integral (PI) control at steady state, fuzzy logic (FL) control at transient state and a simple switching mechanism between steady state and transient states, to achieve satisfied performance under steady state and transient conditions[27].

The major disadvantage with FL control is the presence of steady state error on load. Therefore, to eliminate this disadvantage it is necessary to combine this FL controller with another simple suitable controller, such as PI speed controller which is capable of removing the disadvantage of FL controller. A switching mechanism is incorporated between FL and PI controllers such that near the operating point the PI controller takes over action eliminating the disadvantage of FL controller. Similarly, when away from the operating point FL controller dominates and eliminates the errors due to PI such as occurrence of overshoot and undershoot in the drive response.

Hence, a speed controller where the weighted combination of two controller outputs contributes to the net output is called Hybrid Speed Controller.

In this work, the total operating region is divided into four regions namely A, B, C and D in which only FL controller takes over action outside these regions i.e. away from the operating point, only PI controller takes over action near the operating point and both PI and FL acts in the regions

A, B, C and D in a particular ratio. Fig 3.8 shows the pattern of combination of torque outputs of PI and FL speed controllers respectively as a function of speed error scaled with in a suitable range.

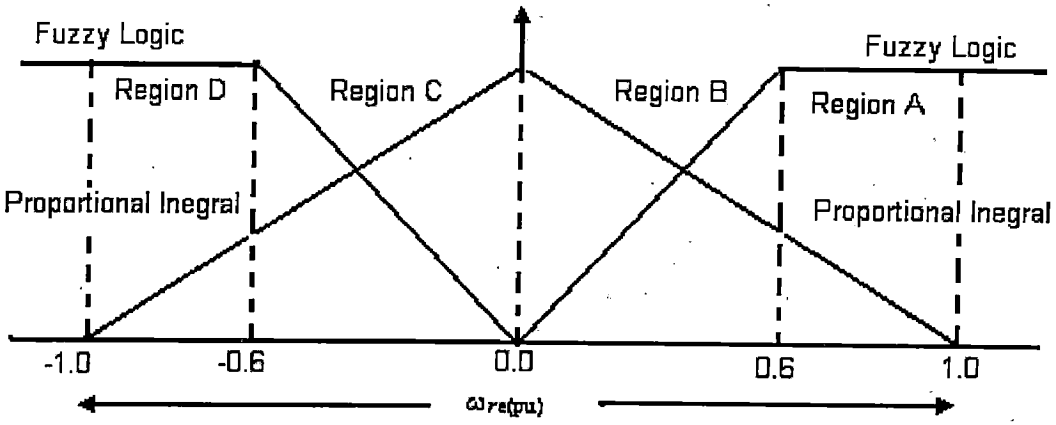

Figure 3.8 Contribution of FL and PI controllers in hybrid controllers

The net torque output of the hybrid speed controller is expressed as:

$$T_k = W_{FLK}\, T^*_{FLk} + W_{PIK}\, T^*_{PIK} \qquad (3.13)$$

where k = A, B, C and D

T^*_{FLk} refers to the torque output of the FL speed controller in the k^{th} region of the combination pattern, T^*_{PIK} refers to the torque output of the PI speed controller in the k^{th} region of combination pattern and T_k refers to the net output torque of the hybrid speed controller from the k^{th} region of combination pattern fed to the limiter.

For ease of the mathematical calculation, four sub regions in the combination pattern are defined as below with respect to fig 3.7.

Region A : Speed error between 0.6 pu and 1 pu

$W_{FL} = 1.0$

$W_{PI} = 1 - \omega_{re(pu}$

Region B: Speed error between 0.0 pu and 0.6 pu

$W_{FL} = (1/0.6)\, \omega_{re(pu}$

$W_{PI} = 1 - \omega_{re(pu}$

Region C : Speed error between -0.6 pu and 0.0 pu

$W_{FL} = -(1/0.6)\, \omega_{re(pu}$

$W_{PI} = 1 + \omega_{r\,e(pu}$

Region D: Speed error between -1pu and -0.6 pu

$W_{FL} = 1.0$

$W_{PI} = 1 + \omega_{r\,e(pu)}$

where W_{FL} refers to the weight of the FL speed controller, W_{PI} refers to the weight of the PI speed controller and $\omega_{r\,e(pu)}$ represents the speed error in pu scale.

Figure 3.9 shows the MATLAB/simulink model for the hybrid speed controller which combines the outputs of FL and PI speed controllers respectively as a weighted sum. T_{fl} represents torque output of FL speed controller and T_{pi} represents the torque output of PI controller. Ta, Tb, Tc and Td represent the hybrid controller output is the regions A, B, C and D respectively.

3.2.2.2.4 Fuzzy Pre-compensated Proportional Integral (FPPI) speed controller

The block diagram for the FPPI speed controller is shown in fig.3.10. Fuzzy pre-compensation means that the reference speed signal (ω_r^*) is altered in advance using fuzzy logic in accordance with the rotor speed (ω_r), so that a new reference speed signal (ω_{r1}^*) is obtained. By using this controller, some specific features such as overshoot and undershoot occurring in the speed response which are obtained with PI controller can be eliminated [35].

As usual, the inputs to the FL are speed error ($\omega_{r\,e}^{*}{}_{(n)}$) and the change in speed error ($\Delta\omega_{e(n)}$) and the output of the FL controller is added to the reference speed to generate a pre-compensated reference speed (δ), which is to be used as a reference speed signal by the PI controller.

The fuzzy pre-compensator cab be mathematically modeled as follows:

$$\omega_{r\,e(n)} = \omega_r^*{}_{(n)} - \omega_{r(n)} \quad (3.9)$$

$$\Delta\omega_{e(n)} = \omega_{e(n)} - \omega_{e(n-1)} \quad (3.10)$$

$$\delta_{(n)} = F\,[\,\omega_{e(n)}, \Delta\omega_{e(n)}] \quad (3.11)$$

$$\omega_{r1}^* = \delta_{(n)} + \omega_{r(n)} \quad (3.12)$$

where F is fuzzy logic mapping

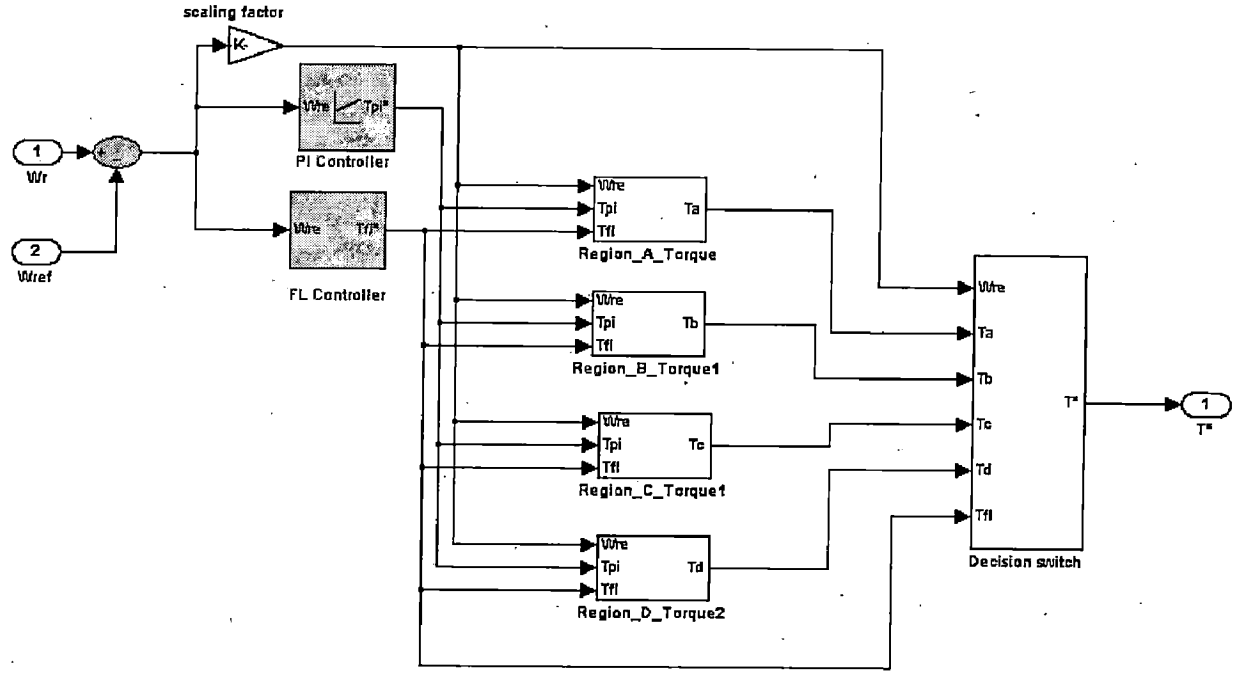

Figure 3.9 MATLAB model for Hybrid speed controller

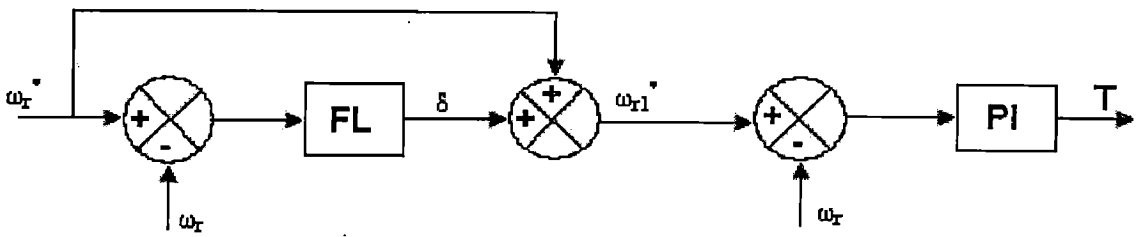

Figure 3.10 Block diagram of fuzzy pre compensated FPPI controller

Figure 3.11 shows the MATLAB model of the FPPI . As shown in figure the FL controller produces the modified reference speed signal by which the speed error is calculated and is fed as a reference signal for the PI controller.

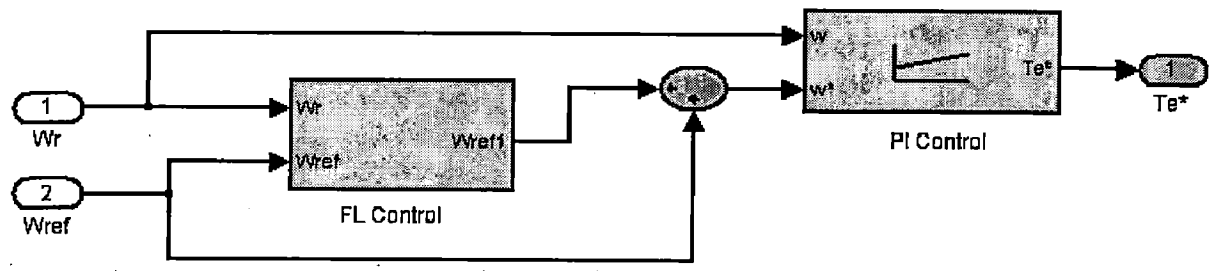

Figure 3.11 MATLAB model for Fuzzy Pre-compensated Proportional Integral (FPPI) speed controller.

3.2.2.3 Field Weakening Controller:

The reference value of the exciting current (i_{mr}^*) is a function of the rotor speed. However, as long as the motor operates below the base speed in either direction, the rated air gap flux is maintained to achieve the desired speed in the constant torque mode. This is analogous to the operation of a separately excited dc motor below rated speed. However, above the base speed, field weakening is allowed and corresponding value of the magnetizing current vector (i_{mr}^*) is obtained from fuction expressed between rotor speed and i_{mr}^*. Mathematically the logic for computation of the exciting current (i_{mr}^*) may be stated as follows:

$$i_{mr}^*(n) = I_m \qquad \text{if } \omega_r(n) < \text{base speed of motor} \tag{3.14}$$

$$i_{mr}^*(n) = K_f I_m / \omega_r(n) \qquad \text{if } \omega_r(n) >= \text{base speed of motor} \tag{3.15}$$

where K_f is flux constant and

I_m is rms value of the magnetizing current

where the value of the magnetizing current, I_m is calculated from the equivalent circuit of the motor.

Figure 3.12 shows the MATLAB model for the field weakening controller in which the above mention operation takes place.

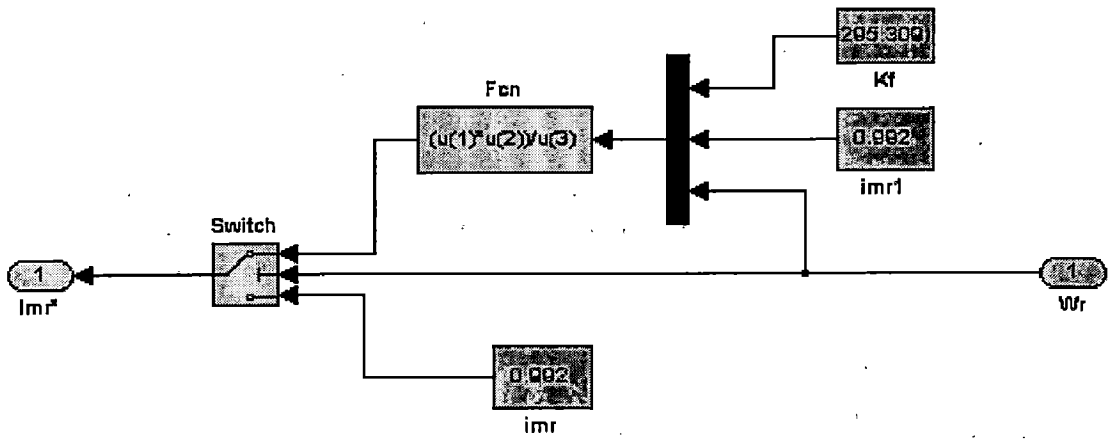

Figure 3.12 MATLAB model for the field weakening controller

3.2.2.4 Vector Controller: [Estimator for i_{ds}^*, i_{qs}^* and ω_2^*]

The modeling of vector controller block is the heart of the entire modeling of the vector controlled induction motor drive. This section calculates the direct and the quadrature axis stator

current components (i_{ds}^* and i_{qs}^*) in the synchronously rotating reference frame (SRRF) aligned with rotor inclined at flux angle (ψ) with respect to stationary reference frame (SRF).

Mathematically, the equations for calculating these two components of the current in the discretised form are stated as follows[1-3][40]:

$$i_{ds}^*(n) = i_{mr}(n) + \tau_r \frac{di_{mr}^*}{dt} \tag{3.16}$$

$$i_{qs}^*(n) = \frac{T^*(n)}{k\, i_{mr}^*(n)} \tag{3.17}$$

$$\omega_2^*(n) = \frac{i_{qs}^*(n)}{\tau_r i_{mr}^*(n)} \tag{3.18}$$

where τ_r is the rotor time constant defined as

$$\tau_r = L_r / R_r$$

$$k = \left(\frac{3}{2}\right)\left(\frac{P}{2}\right)\left(\frac{M}{1+\sigma_r}\right)$$

P is the number of poles, $i_{ds}^*(n)$ and $i_{qs}^*(n)$ refer to flux and torque components of stator current at n^{th} instant, $\omega_2^*(n)$ refer to n^{th} instant reference slip speed of rotor, M is the mutual inductance, σ_r is the rotor leakage factor and L_r is the rotor self inductance and is defined as below

$$L_r = L_{lr} + L_m \quad \text{or} \quad L_r = (1+\sigma_r)M$$

$$\sigma_r = \frac{L_r}{R_r} = \frac{L_{lr} + L_m}{R_r}$$

R_r is the rotor resistance and L_m is the magnetizing inductance.

The MATLAB model for the estimation of i_{ds}^*, i_{qs}^* and ω_2^* is shown in fig.3.13

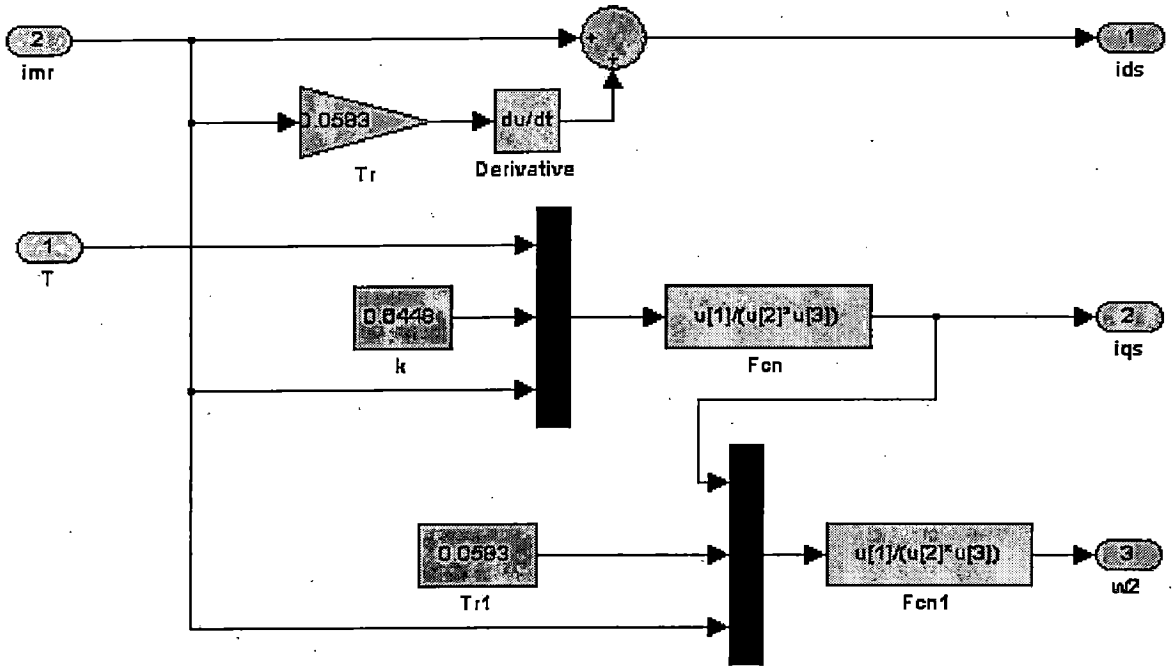

Figure 3.13 MATLAB model for the estimation of i_{ds}^*, i_{qs}^* and ω_2^*

3.2.2.5 Field orientation and Reference current generation:

This block converts the two phase reference currents(i_{ds}^* and i_{qs}^*) in rotating frame into three phase reference currents (i_{as}^*, i_{bs}^* and i_{cs}^*) in stationary frame. In this section, the flux angle (ψ) at which the SRRF is to be inclined is also calculated as given below. First the reference slip frequency of the rotor ($\omega_{2(n)}^*$) is added to the sensed rotor speed ($\omega_{r(n)}$) and then a discrete integration is carried out to calculate the flux angle at the n^{th} instant.

The flux angle (ψ) is defined at the n^{th} instant as:

$$\Psi_{(n)} = \psi_{(n-1)+} (\omega_{2(n)}^* + \omega_{r(n)}) \Delta T \qquad (3.19)$$

where ΔT is the sampling time

After calculating the flux angle and d-q components of the reference stator current in the SRRF, its time to calculate the required three phase reference current (i_{as}^*,i_{bs}^* and i_{as}^*) in the stationary reference frame (SRF). The required transformation from d-q components to abc components is given as below:

Two-Phase rotating to three phase stationary reference frame converter can be modeled as follows:

$$i_{as}^{*} = -i_{qs}^{*} \text{ Sin } \psi + i_{ds}^{*} \text{ Cos } \psi \quad (3.20)$$

$$i_{bs}^{*} = [(-\text{Cos } \psi + \sqrt{3} \text{ Sin } \psi)\, i_{ds}^{*}(\frac{1}{2})] + [(\text{Sin } \psi + \sqrt{3} \text{ Cos } \psi)\, i_{qs}^{*}(\frac{1}{2})] \quad (3.21)$$

$$i_{cs}^{*} = -(i_{as}^{*} + i_{bs}^{*}) \quad (3.22)$$

where i_{ds}^{*} and i_{qs}^{*} refer to decoupled components of the stator circuit i_s^{*} in two-phase system rotor reference frame and i_{as}^{*}, i_{bs}^{*} and i_{cs}^{*} are three phase currents in stator reference frame.

Figure 3.14 shows the calculation of flux angle in the discrete frame in which the sampling time is taken as 10e-6 sec. Similarly the MATLAB model for calculating the three phase reference currents is shown in fig.3.15.

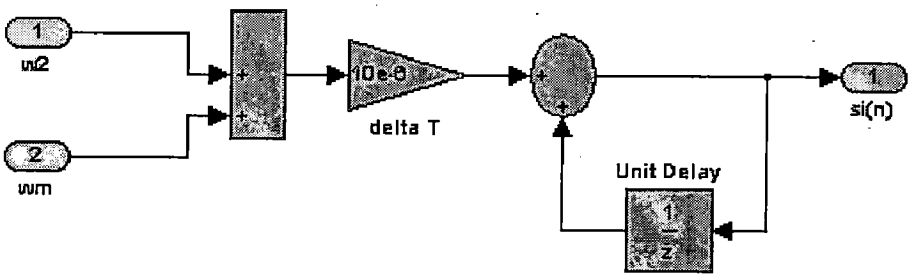

Figure 3.14 MATLAB model for calculating the flux angle

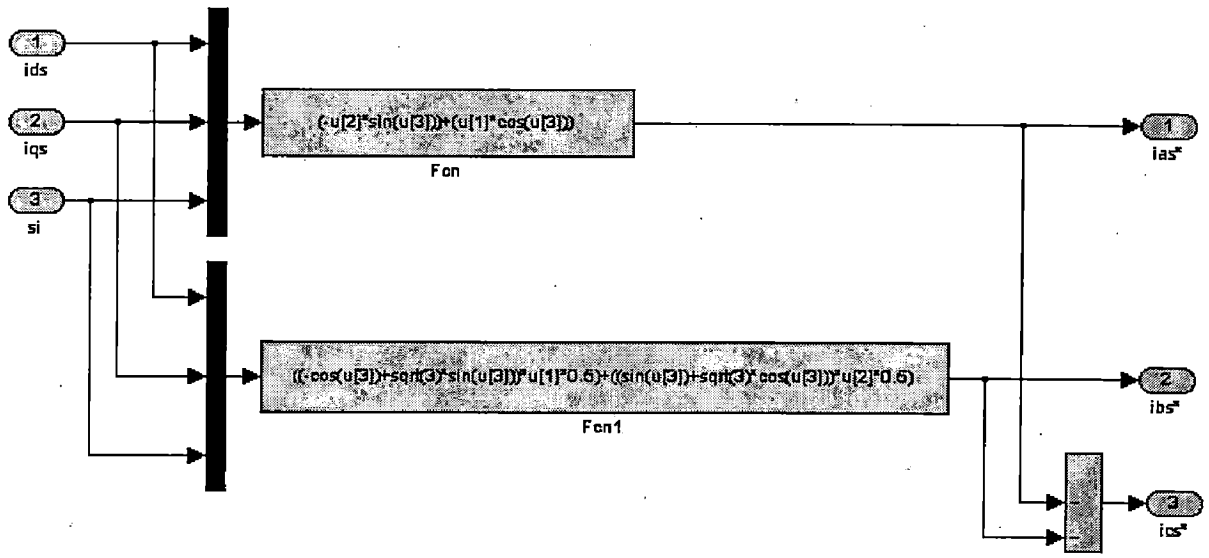

Figure 3.15 MATLAB model for the three phase reference current generation

3.2.2.6 PWM Current Controller

As there are three phases, there will be three current errors. The current error for a particular phase is defined as the difference between the reference current and the sensed (actual) winding current for that phase only. Hence the current errors in the three phases at the n^{th} instant are modeled as below:

$$i_{aes}^{*}(n) = i_{as}^{*}(n) - i_{as(n)} \quad (3.23)$$

$$i_{bes}^{*}(n) = i_{bs}^{*}(n) - i_{bs(n)} \quad (3.24)$$

$$i_{ces}^{*}(n) = i_{cs}^{*}(n) - i_{cs(n)} \quad (3.25)$$

These current errors in each phase are processed through a proportional controller to generate a modulating signal for each phase. This modulating signal is then compared with a triangular carrier waveform to generate a switching signal. The frequency of the modulating signal is the fundamental frequency of the inverter output voltage and the frequency of the carrier wave is the switching frequency of the inverter. The MATLAB model for calculating the current errors required for the PWM current controller is shown in fig3.16.

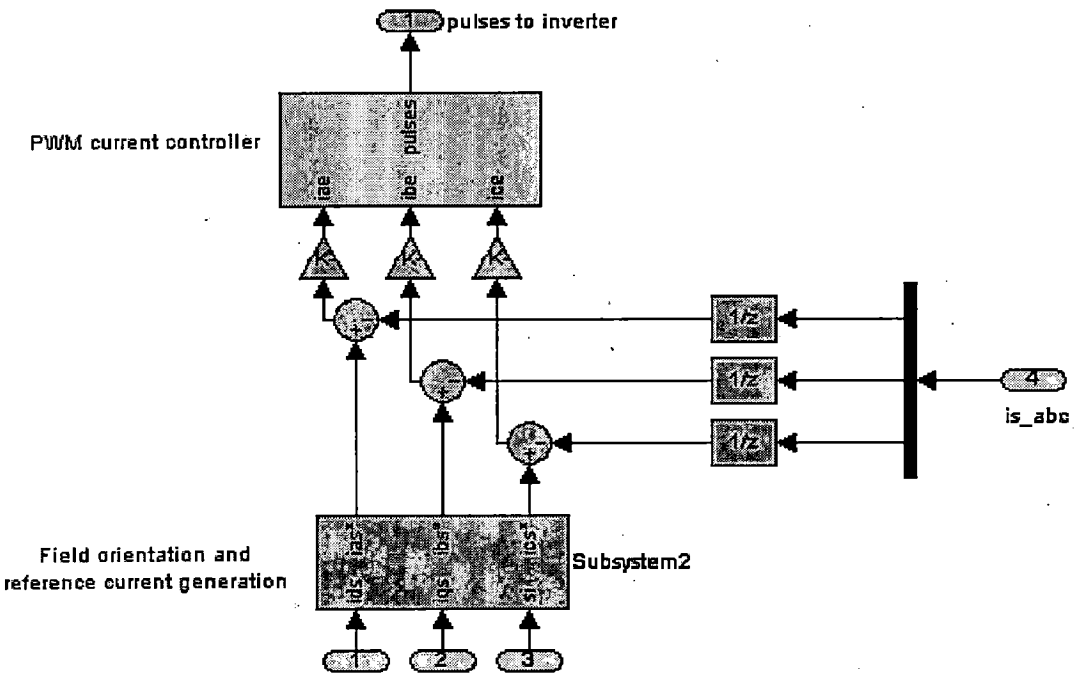

Figure 3.16 MATLAB model for the three phase reference current generation

3.3 SIMULATION OF VCIMD IN MATLAB USING SIMULINK AND POWER SYSTEM BLOCK (PSB) TOOLBOXES

Integrating all the MATLAB models described in the previous sections, vector control can be implemented in MATLAB/Simulink as shown in fig.3.17. This control structure is developed with a controller sampling period of 100μsec. The simulation model have been developed in MATLAB environment along with simulink and power system blockset (PSB) toolbox for simulation response of VCIMD under different operating conditions such as starting, speed reversal and load perturbation.

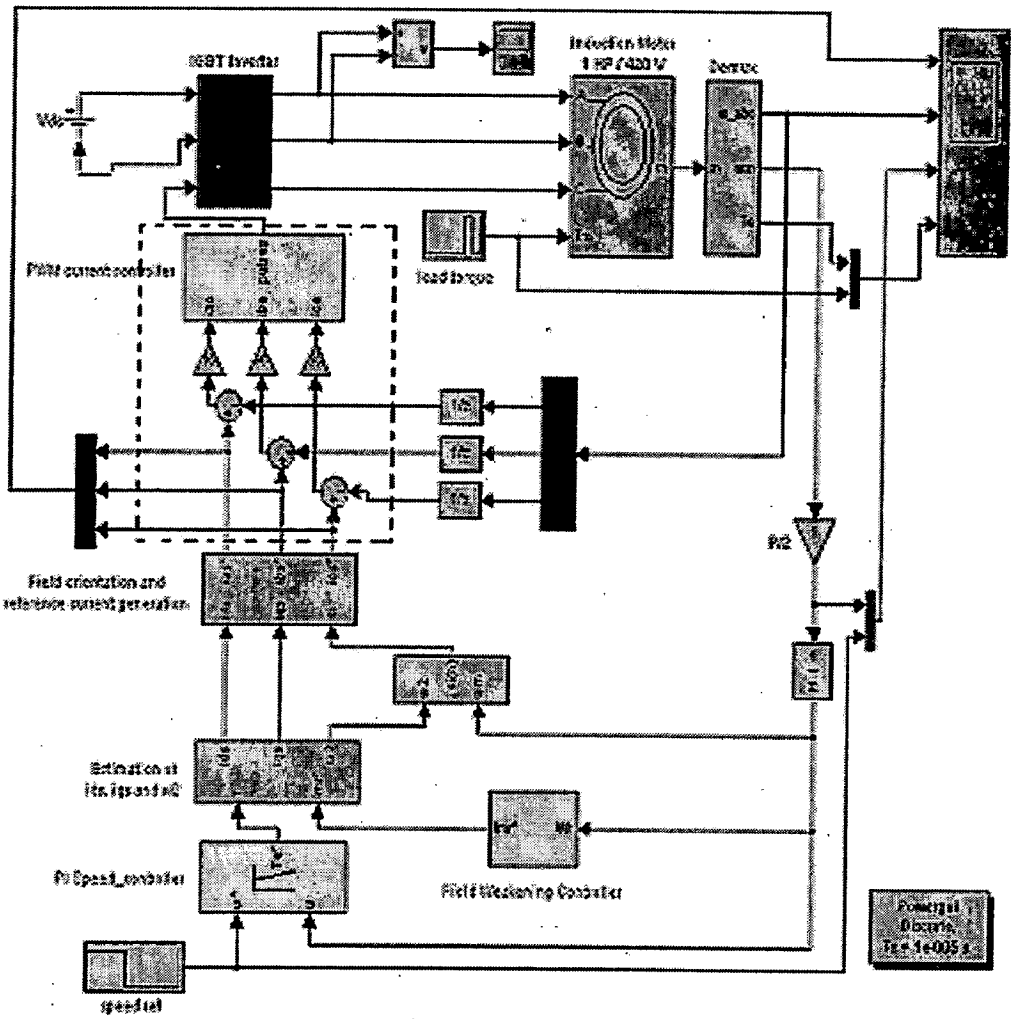

Figure.3.17 Simulation diagram of vector controlled induction motor drive (VCIMD) in MATLAB environment using simulink and Power System Blockset (PSB) toolboxes.

3.4 C0NCLUSION

The technique of vector control is modeled using developed mathematical equations and also simulated in the MATLAB environment. The responses obtained in simulating the VCIMD, shown in fig.3.17, using different speed controllers are shown in fig.3.17. From the above discussions, it can be concluded that developing the MATLAB/Simulink model for VCIMD becomes easy, if the total function of drive is divided into different blocks and than integrating all the individual blocks.

CHAPTER IV

IMPLEMENTATION OF PWM CONTROL STRATEGIES IN MATLAB EMBEDDED CONTROLLER I-8438

4.1 INTRODUCTION

Now a days more and more applications require that the front AC-to-DC converters have both rectifying and regenerating abilities with fast response to improve the dynamic performance of the whole system. A better solution is to use Pulse Width Modulated (PWM) AC-to-DC voltage source converters or current controlled converters which have the merits of nearly sinusoidal input/output current, good power factor and regeneration capability. Various PWM techniques are explained in the third chapter and the implementation of sinusoidal PWM technique in MATLAB Embedded Controller I-8000 is explained in this chapter.

4.2 INVERTERS

Inverters can be classified as voltage source inverters (VSIs) and current source inverters (CSIs). A voltage source inverter is fed by a stiff dc voltage, whereas a current source inverter is fed by a stiff current source. A voltage source can be converted to a current source by connecting a series inductance and then varying the voltage to obtain the desired current.

A VSI can also be operated in current-controlled mode, and similarly a CSI can also be operated in the voltage control mode. The inverters are used in variable frequency ac motor drives, uninterrupted power supplies, induction heating, static VAR compensators, etc. The widely used inverter shown in fig.4.1, known as the three-phase PWM VSI offers many good features such as very low distortion in voltages and currents on the ac side and the dc side, minimum component count, minimum voltage and current stresses in the components, bi-directional power flow capability, power factor correction and dc voltage regulation capabilities, high power density and high efficiency. Hence, a VSI is chosen in this work and the operation of VSI is explained in the below section.

4.2.1 Voltage Source Inverter

A three-phase voltage source inverter configuration is shown in Fig.4.1. The VSIs are controlled either in square-wave mode or in pulsewidth-modulated (PWM) mode. In square-wave mode, the frequency of the output voltage is controlled within the inverter, the devices being used to switch the output circuit between the plus and minus bus. Each device conducts for 180 degrees, and each of the outputs is displaced 120 degrees to generate a six-step waveform, as shown in Fig.4.2. The amplitude of the output voltage is controlled by varying the dc link voltage. This is done by varying the firing angle of the thyristors of the three-phase bridge converter at the input. The square-wave-type VSI is not suitable if the dc source is a battery. The six-step output voltage is rich in harmonics and thus needs heavy filtering.

In PWM inverters, the output voltage and frequency are controlled within the inverter by varying the width of the output pulses. Hence at the front end, instead of a phase-controlled thyristor converter, a diode bridge rectifier can be used. A very popular method of controlling the voltage and frequency is by sinusoidal pulse width modulation.

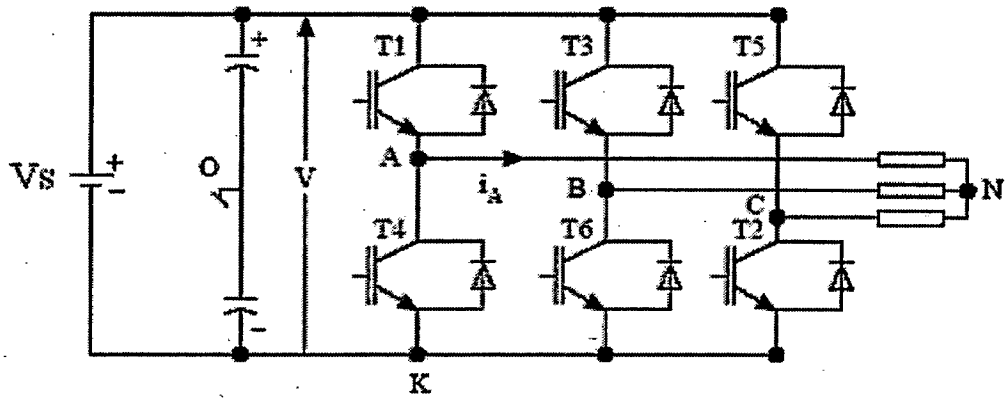

Figure.4.1. Three phase voltage source inverter configuration

The harmonic components in a PWM wave are easily filtered because they are shifted to a higher-frequency region. It is desirable to have a high ratio of carrier frequency to fundamental frequency to reduce the harmonics of lower-frequency components. There are several other PWM techniques mentioned in the literature. The most notable ones are selected harmonic elimination, hysteresis controller, and space vector PWM technique.

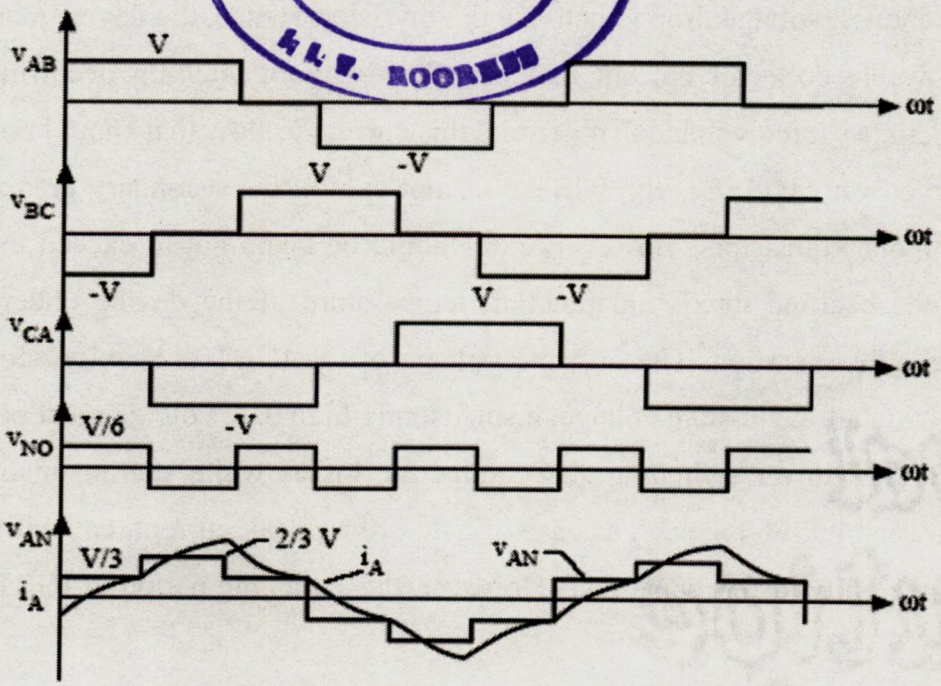

Figure.4.2. Three phase square wave inverter waveforms

In inverters, if SCRs are used as power switching devices, an external forced commutation circuit has to be used to turn off the devices. Now, with the availability of **IGBT**s above 1000-A, 1000-V ratings, they are being used in applications up to 300-kW motor drives. Above this power rating, GTOs are generally used. Power Darlington transistors, which are available up to 800 A, 1200 V, could also be used for inverter applications.

4.2.2 Insulated-Gate Bipolar Transistor (IGBT):

The IGBT has the high input impedance and high-speed characteristics of a MOSFET with the conductivity characteristic (low saturation voltage) of a bipolar transistor. The IGBT is turned on by just applying a positive gate voltage to open the channel for n carriers that is, by applying a positive voltage between the gate and emitter and, as in the MOSFET, it is turned off by removing the gate voltage to close the channel that is, by making the gate signal zero or slightly negative. It requires a very simple driver circuit as shown in fig.4.4. The IGBT's equivalent circuit is shown in fig.4.3.

The IGBT has a much lower voltage drop than a MOSFET of similar ratings. An IGBT is a voltage controlled device similar to a power MOSFET. The structure of an IGBT is more like a thyristor and MOSFET. For a given IGBT, there is a critical value of collector current that will

cause a large enough voltage drop to activate the thyristor. Hence, the device manufacturer specifies the peak allowable collector current that can flow without latch-up occurring. There is also a corresponding gate source voltage that permits this current to flow that should not be exceeded.

Like the power MOSFET, the IGBT does not exhibit the secondary breakdown phenomenon common to bipolar transistors. However, care should be taken not to exceed the maximum power dissipation and specified maximum junction temperature of the device under all conditions for guaranteed reliable operation. The on state voltage of the IGBT is heavily dependent on the gate voltage. To obtain a low on-state voltage, a sufficiently high gate voltage must be applied.

An IGBT has lower switching and conducting losses while sharing many of the appealing features of power MOSFETS, such as ease of gate drive , peak current, capability, and ruggedness. An IGBT is inherently faster than a BJT. However, the switching period of IGBTs is inferior to that of MOSFETs.

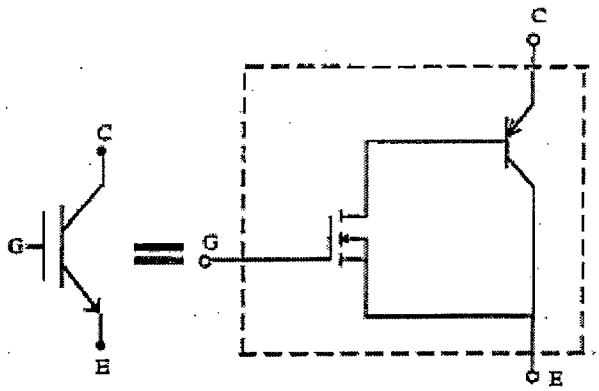

Figure.4.3. Equivalent Circuit of IGBT

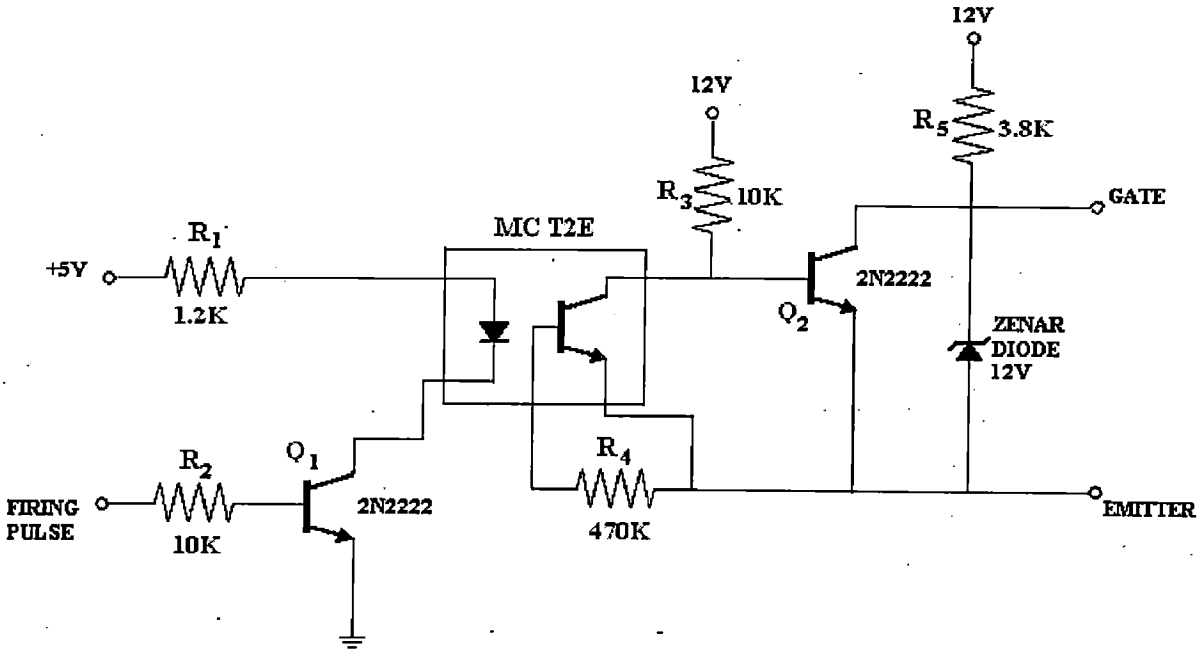

Figure.4.4. Driver circuit of IGBT

The current rating of single IGBT can be up to 1200 V, 400A, and the switching frequency can be up to 20kHz. IGBTs are finding increasing applications in medium-power applications such as dc and ac motor drives, power supplies, solid-state relays, and contractors. As the upper limits of commercially available IGBT ratings are increasing (e.g., as high as 6500 V and 2400 A), IGBTs are finding and replacing applications where BJTs and conventional MOSFETs were predominantly used as switches.

Protection circuits are normally required to keep the operating di/dt and dv/dt protection within the allowable limits of the transistor. A typical IGBT protection circuit is shown in fig.4.5 below.

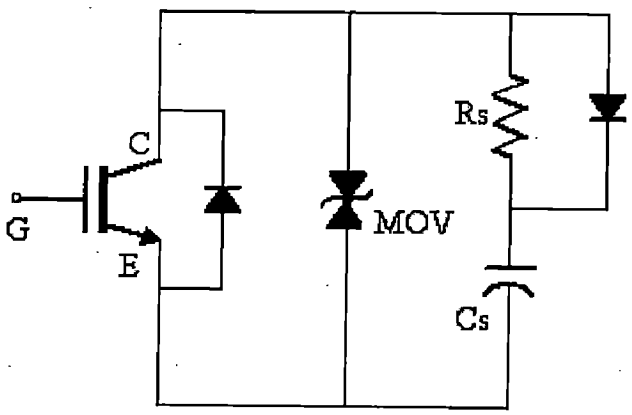

Figure.4.5. Snubber circuit of IGBT

4.3 EMBEDDED CONTROL SYSTEM

4.3.1 Digital implementation:

Any modulation scheme can be used to create the variable-frequency, variable voltage ac waveforms. The ***sinusoidal PWM*** compares a high frequency triangular carrier with three sinusoidal reference signals, known as modulating signals, to generate the gating signals for the inverter switches. This is basically an analog domain technique and is commonly used in power conversion with both analog and ***digital implementation***. In contrast to sinusoidal PWM technique, the ***space vector PWM*** method does not consider each of the modulating voltages as a separate identity. The three voltages are simultaneously taken into account with a two-dimensional reference frame and the complex reference vector is processed as a single unit. The SVM has the advantages of lower harmonics and a higher modulation index in addition to the features of ***complete digital implementation.***

Therefore it is clear from the above discussion, that the two considered control topologies can be implemented using a digital processor. This chapter explains the features, limitation and operation of the considered embedded control system.

What is a *control system?*

- (IEEE): " *A system in which a desired effect is achieved by operating on various inputs to the system until the output, which is a measure of the desired effect, falls within an acceptable range of values.* "

What is an *Embedded system?*

- (IEEE): " *A computer system that is part of a larger system and performs some of the requirements of that system; for example, a computer system used in an aircraft or rapid transit system.* "

Characteristics of embedded control system:

1. Embedding the control system into a product
2. Referring to implementation technology
3. Wide applicability.

4.3.2 8000 SERIES – EMBEDDED CONTROL SYSTEM

4.3.2.1 Introduction:

I-8438/8838 is the MATLAB Embedded Controller solution built in Ethernet and series interface with I/O expansion slot for Matlab development environment. For this application there are over 20 analog and digital I/O modules and also system-level Simulink Blocksets have been developed[10].

Hence by using the Simulink development environment and the Matlab Driver's blocksets, control algorithm can be easily constructed and verified without writing any code. Once the algorithm has been verified, by pressing a build button, we can convert a model to executable code, and download it to controller for test or practical implementation via RS232, Ethernet, RS485 and even Modem.

4.3.2.2 Features of I-8438/8838 series modules:

- The I-8438/8838 series modules software driver for MATLAB development perfectly and easily combines with MATLAB/Simulink/stateflow.
- The sophisticated tasks of creating, analyzing and simulating block diagram models can all be solved conveniently with MATLAB/Simulink/stateflow with the support of library of many extended powerful blocks for the I-8000 series module I/O hardware driver.
- Communication Interfaces: The I-8000 Matlab solution gives us the function needed for our control algorithm to download and upload experimental data through the media of RS232 and Ethernet communication interfaces as shown in fig.4.6 below.
- Easy-to-use: The I-8000 Matlab solution provides GUI (Graphical User Interface) for easy application, which enables us to communicate conveniently with the I-8xx8 target hardware.
- Extensibility of I/O driver blocks: This Matlab solution is tailored for the I-8438/8838 control system, which provides 4 or 8 expansion slots. Therefore I/O capability can be extended if necessary. Currently this software provides over 20 I/O blocks to cooperate with matlab development environment, which includes DI, DO, DIO, AI, AO, Relay and encoder blocks.

4.3.2.3 Limitations:

I. The I-8000 series module software driver for MATLAB only supports *single tasking* and *Fixed-step* modes, due to the limitations of the Real-Time Workshop (RTW) Embedded Coder.

➢ In simulink *single tasking* means In Simulink, *single tasking* means that only one sample rate can be used in the whole control system. That is, every block must have the same sampling rate.

➢ Because the RTW 4.x or 5.0 have not supported variable step time, the *Solver options* on the *Simulation Parameters* dialog box can only be set to *Fixed-step*.

II. Furthermore, the RTW Embedded Coder does not support the following built-in blocks yet.

1. Simulink\Continuous

- No blocks in this library are supported

2. Simulink\Discrete

- First-Order Hold

3. Simulink\Function and Tables

- MATLAB Fcn

4. Simulink\Math

- Algebraic Constraint
- Matrix Gain

5. Simulink\Nonlinear

- Rate Limiter

6. Simulink\Signals & System

- Bus Selector
- IC

7. Simulink\Sinks

- XY Graph
- Display
- To File

8. Simulink\Sources

- Clock

- Chirp Signal
- Pulse Generator
- Ramp
- Repeating Sequence
- Signal Generator

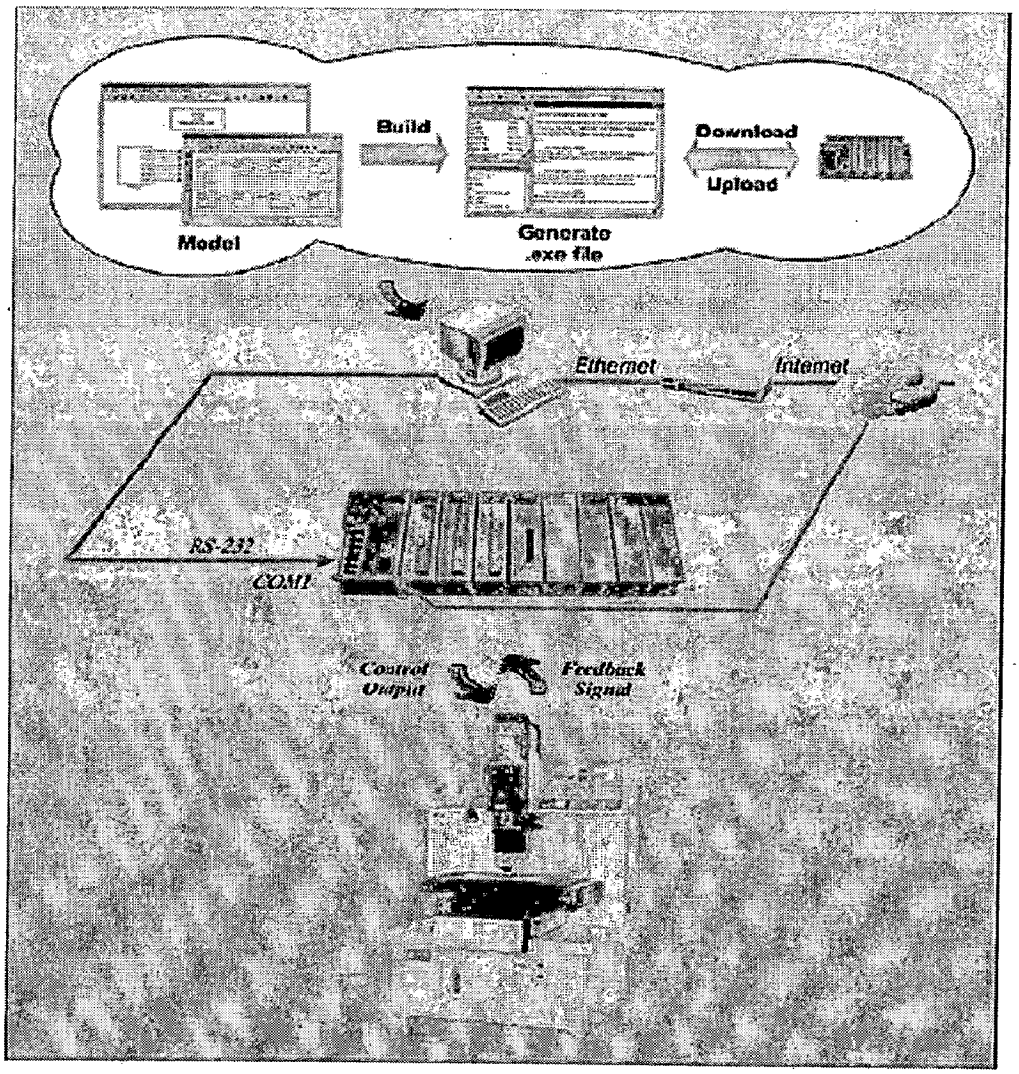

Figure.4.6. I-8000 series MATLAB solution logo [10]

4.3.2.4 Module list supported for Matlab Driver :

The following table is a list of currently supported I-8000 I/O modules by Matlab Driver. They include DI, DO, DIO, AI, AO, relay, and encoder modules.

Type	Description	Module Model
DI	Digital input module	I-8040, I-8051, I-8052, I-8053, I-8058
DO	Digital output module	I-8041, I-8056, I-8057
DIO	Digital input & output module	I-8042, I-8054, I-8055, I-8063
AI	Analog input module	I-8017H
AO	Analog output module	I-8024
Relay	Relay output module	I-8060, I-8064
Encoder	Encoder counter board	I-8090

Table.4.1. I-8000 I/O modules supported by Matlab Driver.

4.3.2.5 Software and Hardware specifications:

The required toolbox of the MATLAB software for I-8000 MATLAB solution is listed as follows:

- MATLAB 6.1 or 6.5 below installed.
- Simulink 4.1 or 5.0 below installed.
- Real-Time Workshop 4.1 or 5.0 installed.
- Real-Time Workshop Embedded Coder 2.0 or 3.0 installed.
- Stateflow and Stateflow Coder 4.1 or 5.0 (not necessary).

The current solution is only tested in the Window system, which is Win98/2000/XP. The hardware specifications of I-8438/8838 are given in appendix A.

4.4 IMPLEMENTATION OF PWM TECHNIQUE IN I-8438

4.4.1 Objective

The main objective in using the Matlab Embedded controller is to generate six gating pulses by using Simulink blocks, which are supported by the RTW Embedded coder. Once, the simulink block is build up successfully, the six gating pulses can be taken out of the controller via DIO module and can be given to the inverter as shown in fig.4.7.

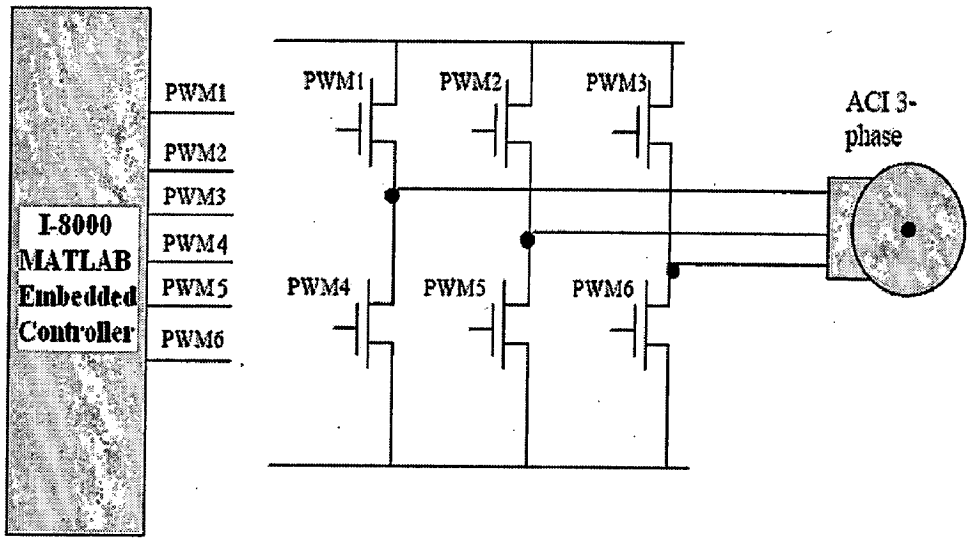

Figure 4.7. Pulses from Embedded controller to the inverter

The MATLAB/Simulink block diagram of the considered PWM control technique is given below. As there are certain limitations of I-8000 mentioned in the previous chapter, a triangular wave, which is required as a carrier wave, cannot be generated using the Repeating sequence in the Simulink/Sources.

Hence a triangular wave is generated in discrete time frame using a discrete time integrator as shown in fig.4.8. The PWM current controller shown in fig. 4.9 generates six PWM signals to the respective gate driver circuits driving IGBTs of the three phase VSI bridge. The inputs to this controller are the modulating signals calculated in the section 3.2.2.6. this modulating signal is compared with the triangular carrier wave to generate the PWM switching signal. Six PWM switching signals are generated, where in two complementary signals are meant for each leg of the bridge inverter.

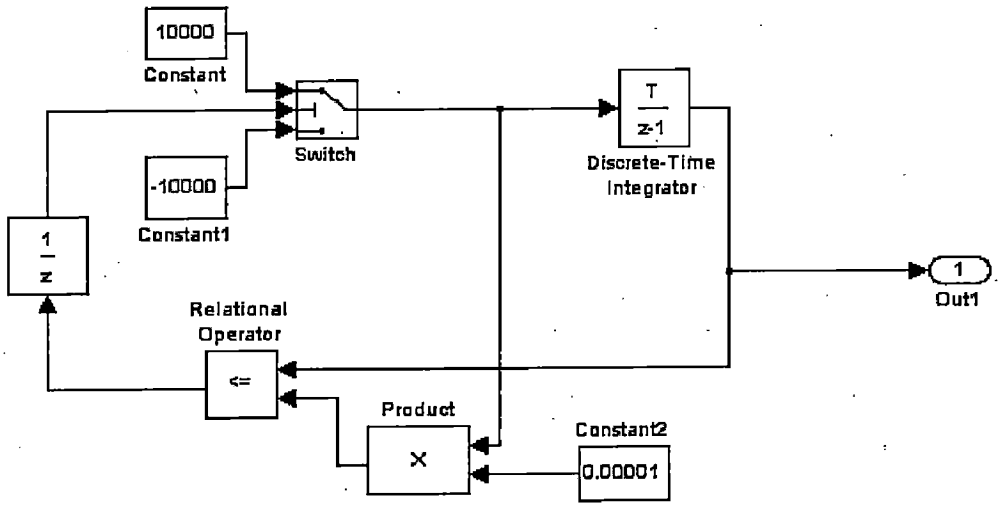

Figure 4.8. MATLAB/Simulink block diagram for triangular wave generation in discrete time frame.

4.4.2 Simulink model with I-8000 driver:

If the simulation output was satisfied, we can replace the built-in Simulink blocks with the I-8000 driver blocks. To add an I-8000 driver block to the model, the following steps are to be followed:

1. A SYS_INIT block is inserted from the system block library.
2. Double click on the SYS_INIT block opens the SYS_INIT dialog box. Then the correct type from the popup menu on the dialog box is selected. Here, we select the type as I-8438.
3. An I-8054 block is copied from the DIO library and the simulation output (6 gate signals) is connected to the DO port of the I-8054 as shown in fig.4.10

After the above steps are done, we can start to build our control model with the I-8000 driver blocks. The simulink block diagram is as shown in fig.4.10 below.

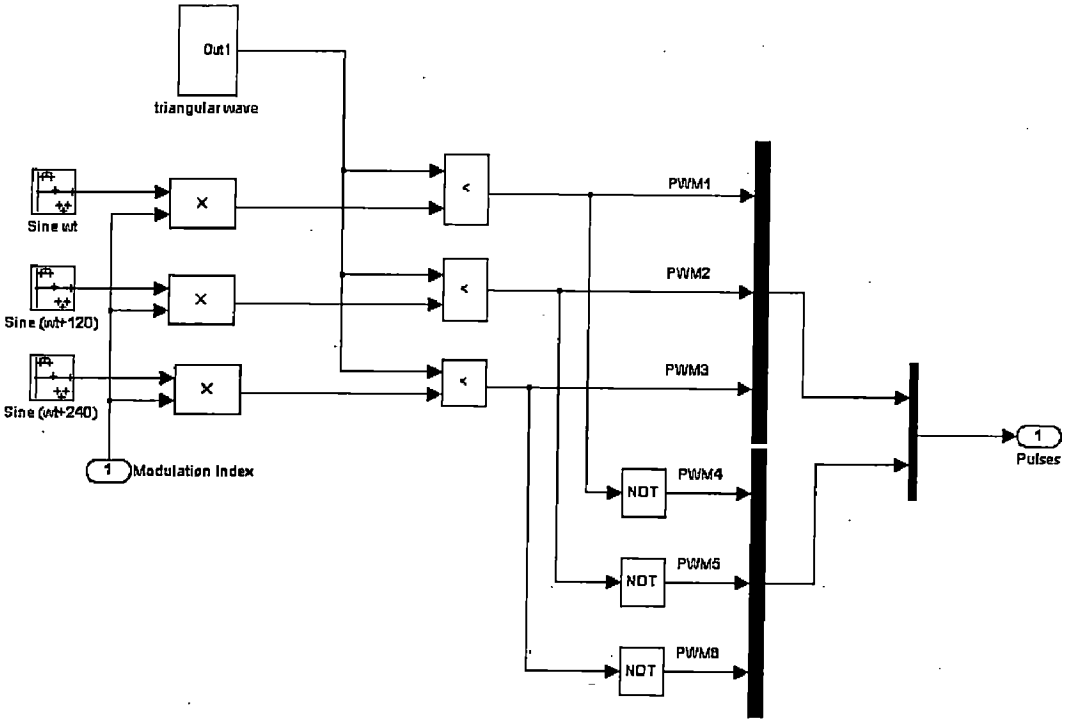

Figure 4.9 Simulink model for PWM current controller

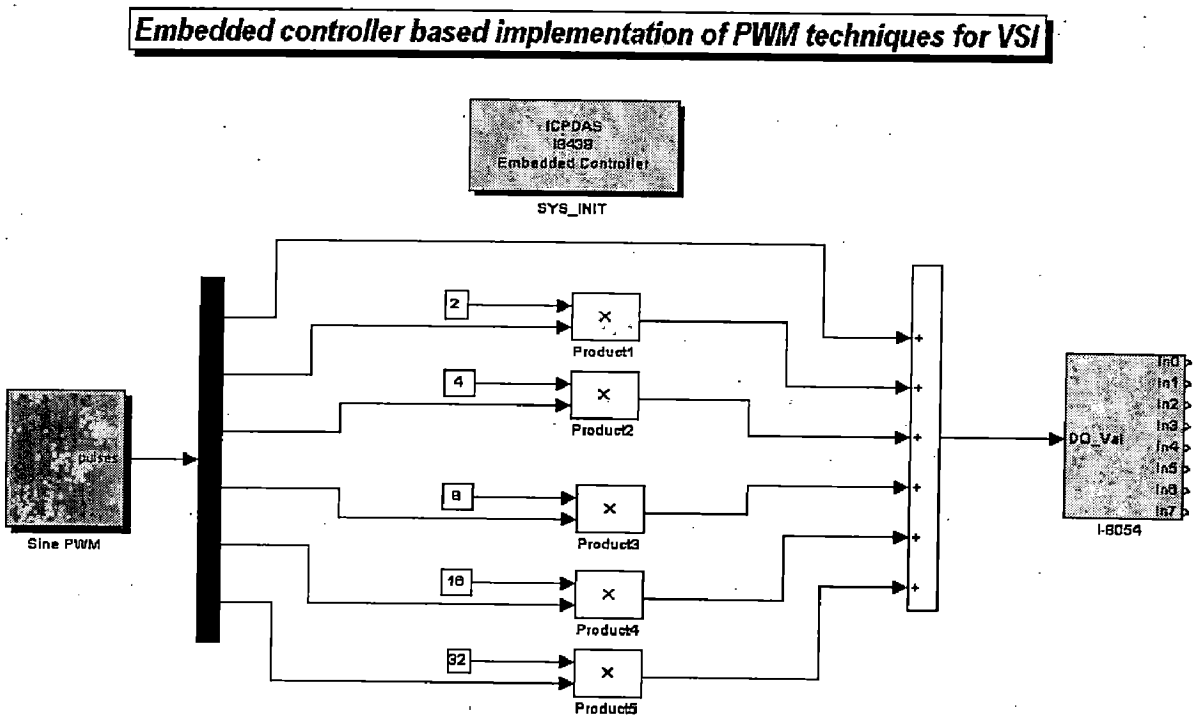

Figure 4.10. Simulink block diagram to generate PWM pulses with I-8000 drivers

4.4.3 Building the program by Real Time Workspace (RTW):

In this section conversion of the control model created in the previous section into .exe file by RTW is shown. To achieve this task, the following steps are to be followed.

1. The Simulation Parameters dialog box is opened by choosing *simulation parameters* from the *Simulation* menu.

2. On the dialog box that displays, the type and mode are selected as *Fixed-step* and *Single Tasking* in the "Solver options" field.

3. Then a click on "Real-Time Workshop" tab changes the pane. On the pane that shows up, select "Target configuration" from the "Category" field. Then the "System Target File Browser" window is opened by clicking on the Browse button.

4. On the System Target File Browser dialog, the correct system target file from the list and then OK button is clicked to close the dialog box. Here I-8xx8.tlc is choosen.

5. Now, the "ERT code generation options" (for MATLAB 6.1) or "ERT code generation options(1)" (for MATLAB 6.5) is selected in the Category field. Then the **Terminate function required** and **single output/update function** options are only selected.

6. For MATLAB 6.5, "ERT code generation options(3)" is selected from the Category field. Then the option **Generate an example main program** is cancelled.

7. When the above steps are done, the Build button is clicked to start the build process. After the process ends successfully, the message in the MATLAB command window displays the following message.

Created executable:filename.exe

successful completion of Real-Time Workshop build procedure for model

Note: The name of the model cannot be over 4 characters. (This is due to limitation of Turbo C/C++ Compiler.

4.4.4 Program downloading & data uploading:

Now the .exe so far generated can be downloaded for testing by following the below steps:

1. **I8xx8** control system is turned ON and is set in OS mode.

2. **gui8000** is entered at the MATLAB prompt to start the GUI. Then RS232 communication mode is selected to download the application program.

3. The serial port that we use in our PC(COM 2) is selcted. Then *Baud rate, Parity, Data bits, Stop bit* as '115200, none, 8, 1'.

4. Now the *Connect* button is clicked. If the connection is successful, the message, "Connection is established" appears on the dialog box.

5. Now it's time to download our program. *Download* button is clicked and the selected file is downloaded by pressing OK button and then the download process starts.

6. The *start* button is clicked after the progress of program downloading was completed to run our control program.

7. After the program is executed successfully, *Upload* button is clicked to collect the data from the I8xx8 control system and the data will be saved in a file.

8. Finally close the GUI dialog box.

Hence the Embedded controller is ready to give the generated pulses in MATLAB/Simulink. The six gate signals from DIO module (I-8054) can be given to the six IGBTs' gates.

4.5 CONCLUSION

The implementation of sinusoidal PWM technique is explained in detail. With this technique the gate pulses for the VSI are generated at an frequency of nearly 125 Hz. These pulses are able to trigger the IGBT individually. But if all the six pulses that are being generated by the controller are connected to the six devices at a time, the pulses are being dropped due to loading effect. The pulse output from embedded controller and the voltage across each device (when connected individually) are shown in fifth chapter.

CHAPTER V

RESULTS AND DISCUSSIONS

The performance of VCIMD system is simulated using mathematical equations in MATLAB environment using simulink and Power System Blockset (PSB) toolboxes under different dynamic conditions such as starting, speed reversal and load perturbation i.e load application and load removal. The total system is realized in discrete frame which operates at a sampling interval of 100μsec.

A set of responses consists of reference speed (ω_r^*), rotor speed (ω_r) in electrical rad/sec, three phase reference currents (i_{as}^*,i_{bs}^* and i_{cs}^*), three phase winding currents (i_{as}, i_{bs} and i_{cs}) in Amperes, developed electromagnetic torque (T_e) and the load torque (T_L). The performance of induction motor under different modes of operation is investigated. The simulation results of vector control of induction motor corresponding to 1hp and 30hp with different speed controllers are shown in figs 5.1–5.4 and figs 5.5-5.8 respectively. This section also presents a comparative study of proportional integral (PI), Fuzzy Logic (FL), Fuzzy Pre-compensated Proportional Integral controller (FPPI) and Hybrid (FL and PI) speed controllers for 1hp and 30 hp vector controlled induction motor drive (VCIMD) as presented in tables 5.1 and 5.2 respectively.

The following salient feature are observed for the observed results.

5.1 STARTING DYNAMICS

Three phase squirrel cage induction motor is fed from a controlled voltage and frequency source. Initially the motor is started at low frequency and finally runs at the set reference speed value. In this work the reference speed is set at 250 electrical rad/sec as the base speed is 314 electrical rad/sec. The torque limit is set at twice the rated value and hence the starting current is limited with in twice the rated value when the motor builds up the required starting torque. When the speed error reaches nearly zero rad/sec, the winding current also reduces to no load value and the developed toque equals the load torque as observed in the starting response as shown in figs. 5.1-5.8.

5.2 REVERSAL DYNAMICS

When the reference speed is changed from 250 rad/sec to -250 rad/sec, the motor tends to run in reverse direction. When the controller observes this change, it first reduces the frequency of the stator currents demonstrating the regenerative braking followed by the phase reversal for starting the motor in reverse direction. As the drive is in the same dynamic state (on no load) just before and after the reversal phenomenon, the steady state values of the inverter currents are observed to be same in either directions of the rotation of the motor. However the phase sequence of these currents in two directions will be different.

5.3 LOAD PERTURBATION

The study of the performance of VCIMD under load variations is really important as the speed of the motor should not changed under any load conditions. In this work this study is performed by applying load and removing the load on the motor when it running at a steady speed of 250 rad/sec. sudden application of load on the rotor causes an instantaneous fall in the speed of the motor. In response to this drop in speed value, the output of the controller responds by increasing the reference torque value. Therefore, the developed electromagnetic torque of the motor increases causing the motor speed settle down to the reference speed with the increased winding currents.

Similarily, when the load is removed suddenly from the motor, a small overshoot in the speed of the motor occurs. Because of this small increase in speed, the torque output of the speed controller reduces thereby reducing the speed of the motor. Thus the motor settling at the reference speed value. After the load removal the stator currents also sets to the steady state value. In this manner the controller keeps the motor running at a constant speed under the load variations.

5.4 COMPARATIVE STUDY AMONG DIFFERENT SPEED CONTROLLERS

The dynamics of the motor discussed in the sections 5.1-5.3 are observed using different speed controllers namely PI, FL, Hybrid and FPPI and the responses are shown in figs, 5.1-5.4 for 1hp and figs 5.5-5.8 for 30hp squirrel cage induction motor. Table 5.1 also shows a comparative performance of these different speed controllers. The observations from the tables 5.1-5.2 are discussed below.

The advantages of PI controller are simple in operation and zero steady state error when operating on load. But the disadvantages of this PI controller is the occurrence of overshoot while starting , undershoot while load application and overshoot while load removal. These disadvantages can be eliminated with the help of a FL controller. But the disadvantage of the steady state speed error is observer in case of FL speed controller. Hence to take over the advantages present in both PI and FL controllers, a hybrid controller is used in which both PI and FL controllers are used. In this controller, when the speed error is near to zero, the control is switched to PI thereby eliminating the disadvantage of steady state speed error of FL controller. When the drive speed is away from the reference value, the controller is changed over to FL controller, which provides improved dynamic response.

The control action of PI, FL and hybrid controllers is governed by the magnitude of deviation in the rotor speed from the reference value. Instead of this action, if FL controller is applied to modify the reference speed and the main control action uses PI speed controller then an improvement in the drive performance is observed as seen in table 5.1 for 1hp motor and table 5.2 for 30hp motor. Such a speed controller is known as FPPI controller.

Type of Speed Controller	**Starting Time (msec)**	**Reversal Time (msec)**	**Speed dip on Full Load Application (rad/sec)**	**Speed dip on Full Load Removal (rad/sec)**	**Steady State Speed error on Full load (rad/sec)**
PI	109	200	2.95	3	0
FUZZY	90	170	1.1	0	0.7
HYBRID	100	183	3.1	3.16	0
FPPI	97	175	1.1	0.8	0

Table 5.1 Comparative Performance of Different Speed Controllers for 1hp VCIMD with reference speed of 250 rad/sec, reversal speed of -250 rad/sec and T_L=2.5Nm.

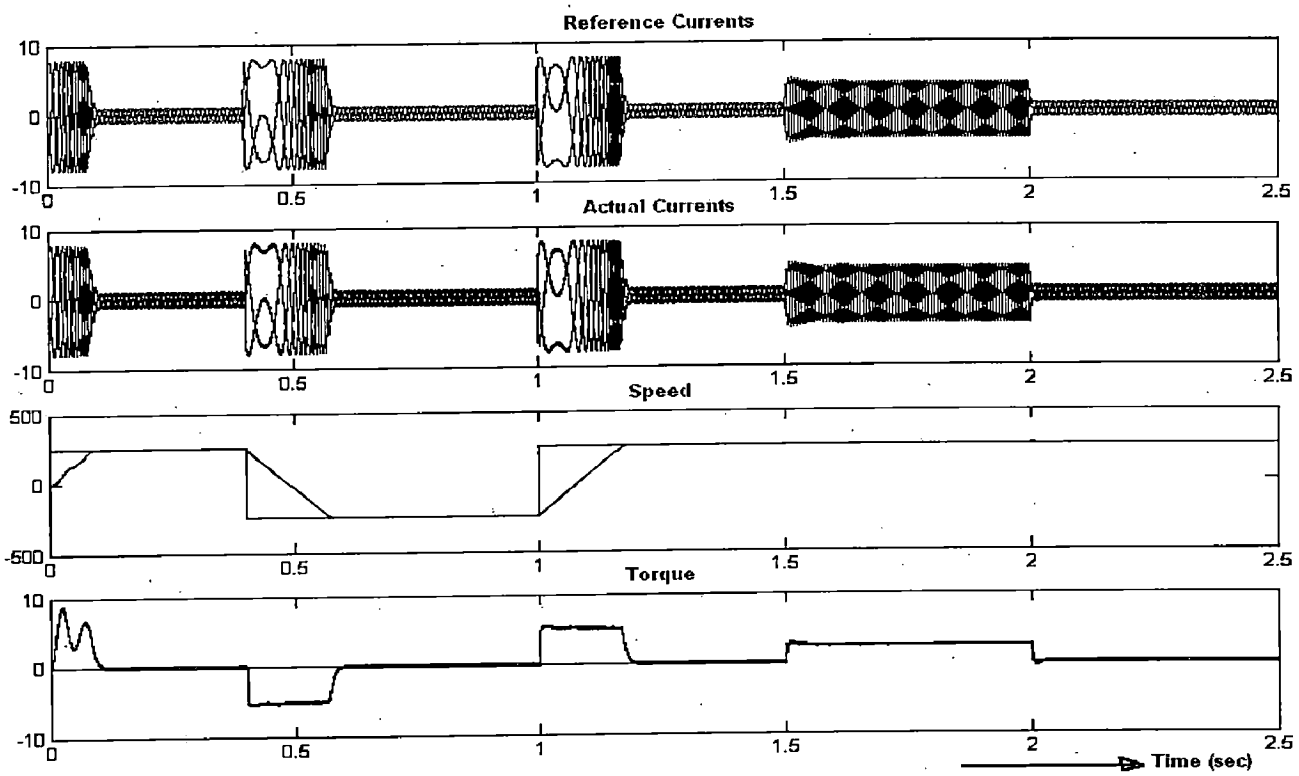

Figure 5.1. Starting, Speed Reversal and Load Perturbation Response of 1hp VCIMD system with Proportional Integral (PI) Speed Controller.

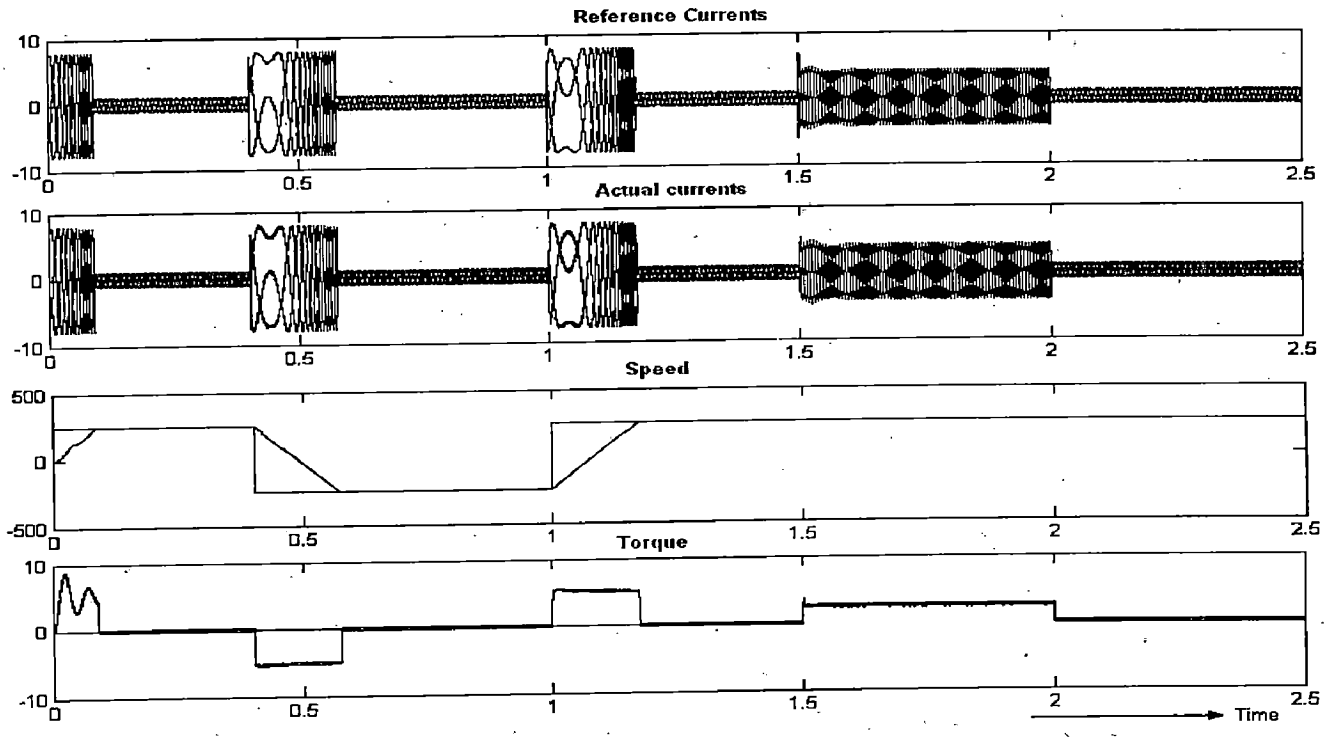

Figure 5.2. Starting, Speed Reversal and Load Perturbation Response of 1hp VCIMD system with Fuzzy Logic (FL) Speed Controller.

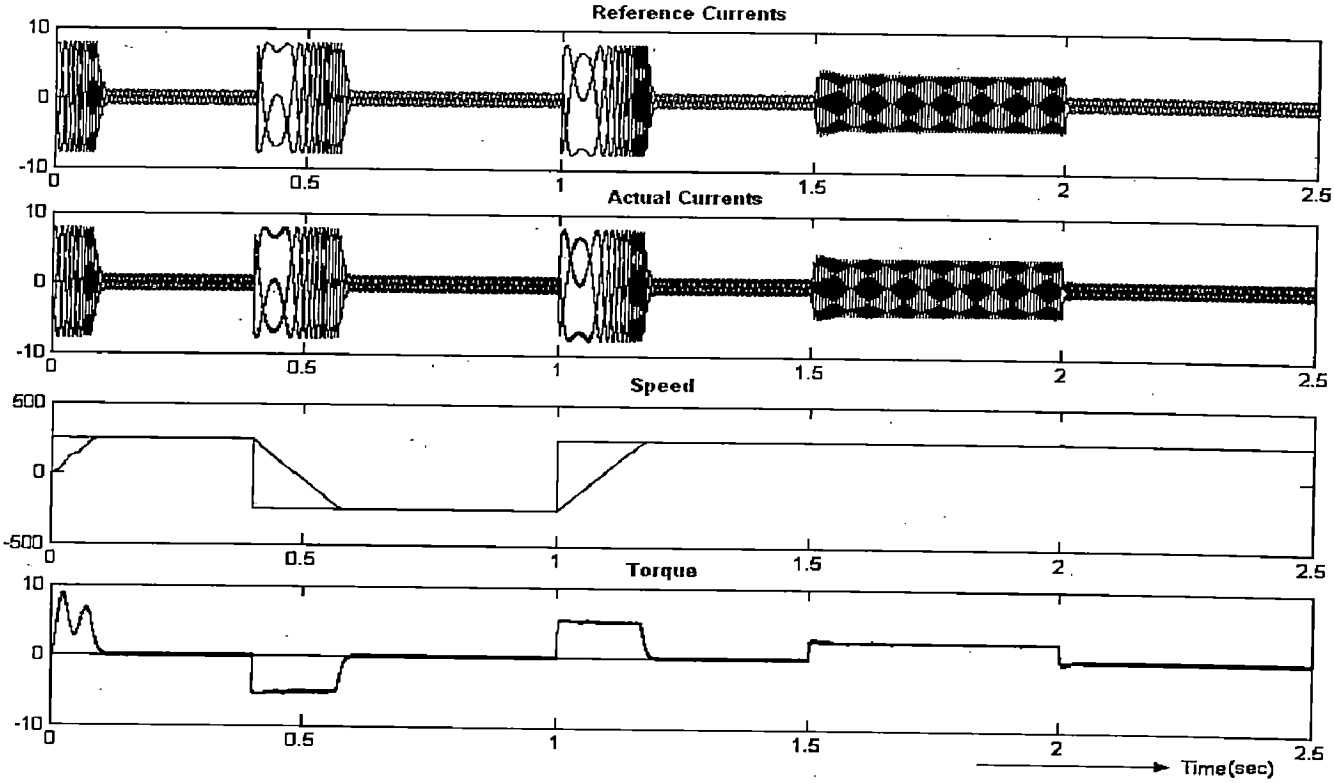

Figure 5.3. Starting, Speed Reversal and Load Perturbation Response of 1hp VCIMD system with Hybrid Speed Controller.

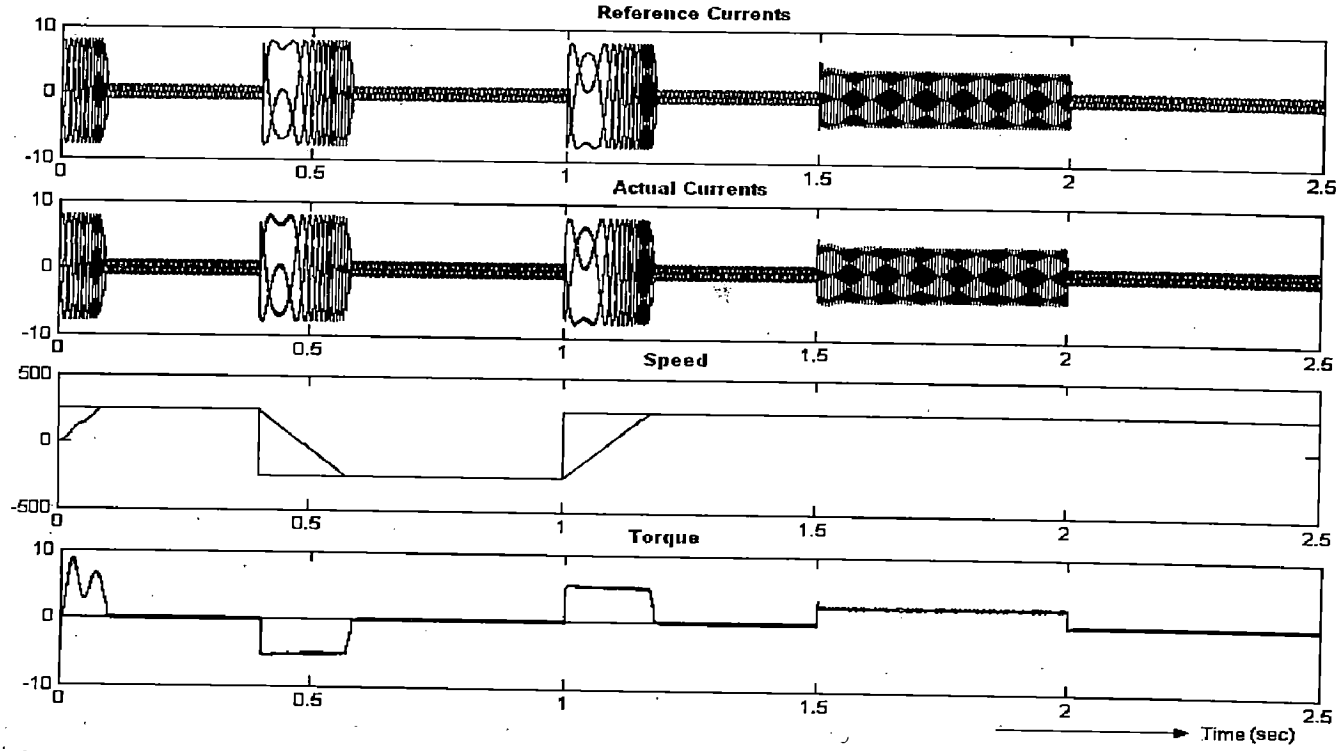

Figure 5.4. Starting, Speed Reversal and Load Perturbation Response of 1hp VCIMD system with Fuzzy Pre-compensated Proportional Integral (FPPI) Speed Controller.

Type of Speed Controller	Starting Time (msec)	Reversal Time (msec)	Speed dip on Full Load Application (rad/sec)	Speed dip on Full Load Removal (rad/sec)	Steady State Speed error on Full load (rad/sec)
PI	298.50	301.75	3.83	3.94	0
FUZZY	210.38	266.30	8.12	0	8.01
HYBRID	230.01	274	4.02	4.12	0
FPPI	169.08	252.04	1.01	0.45	0

Table 5.2 Comparative Performance of Different Speed Controllers for 30hp VCIMD with reference speed of 250 rad/sec, reversal speed of -250 rad/sec and T_L=175Nm.

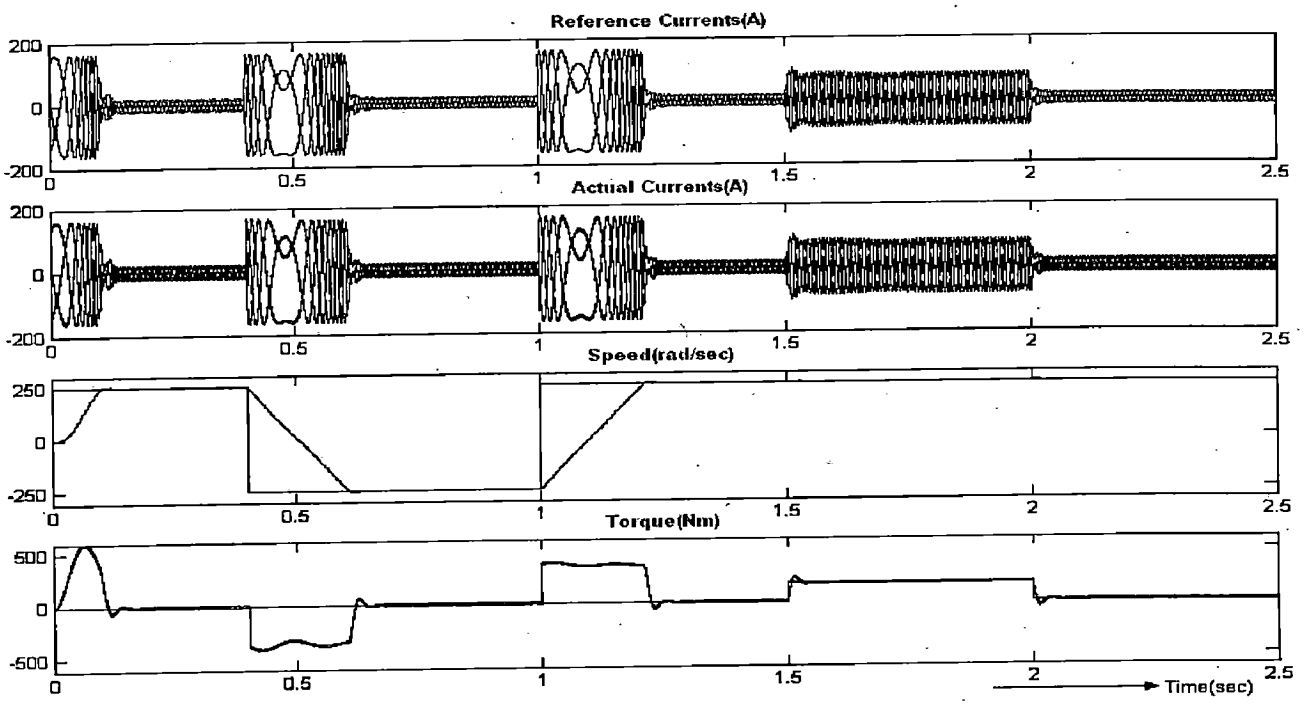

Figure 5.5. Starting, Speed Reversal and Load Perturbation Response of 30hp VCIMD system with Proportional Integral (PI) Speed Controller.

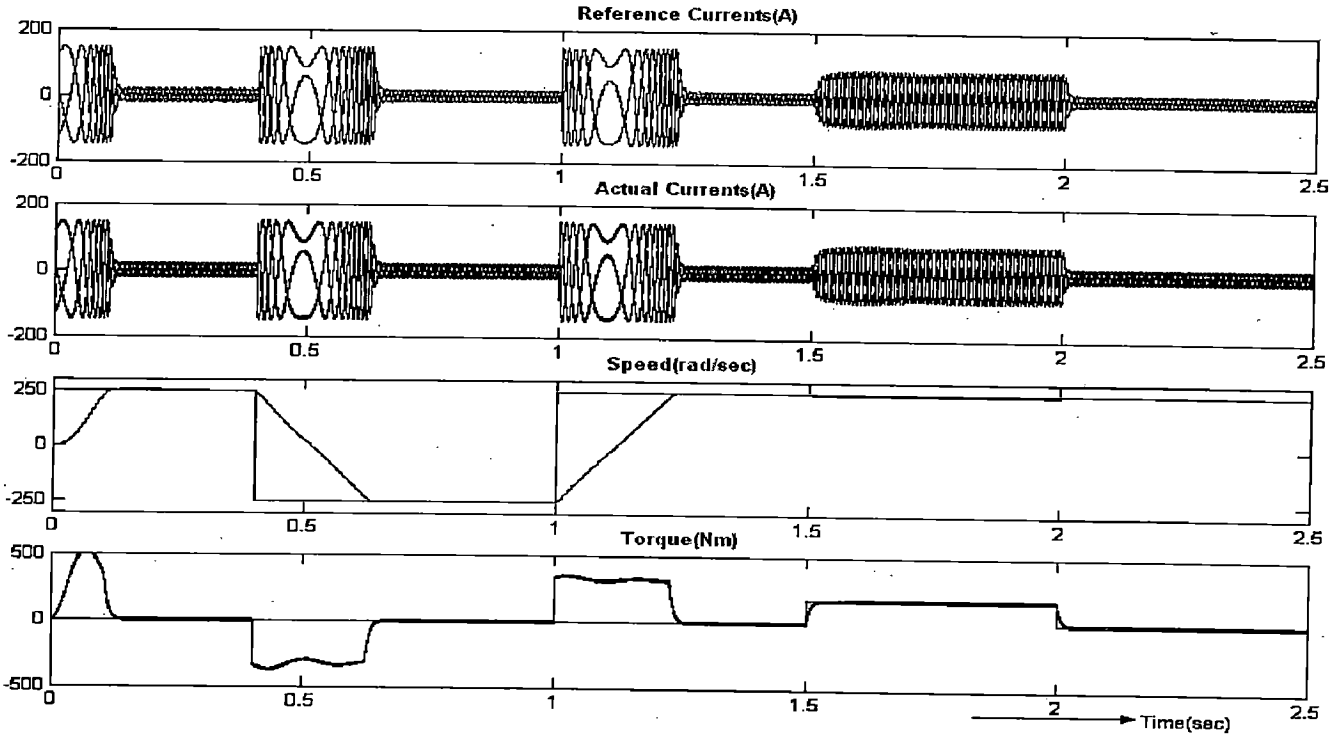

Figure 5.6. Starting, Speed Reversal and Load Perturbation Response of 30hp VCIMD system with Fuzzy Logic (FL) Speed Controller.

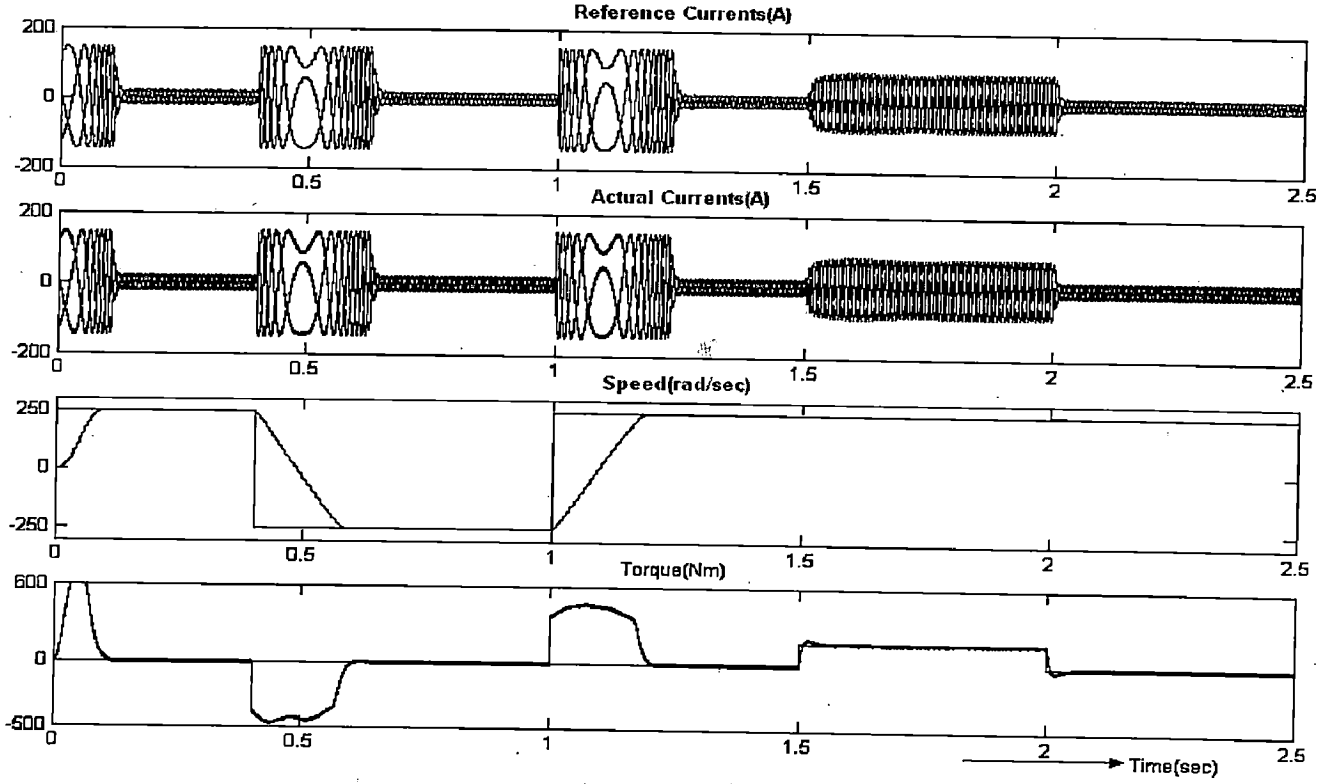

Figure 5.7. Starting, Speed Reversal and Load Perturbation Response of 30hp VCIMD system with Hybrid Speed Controller.

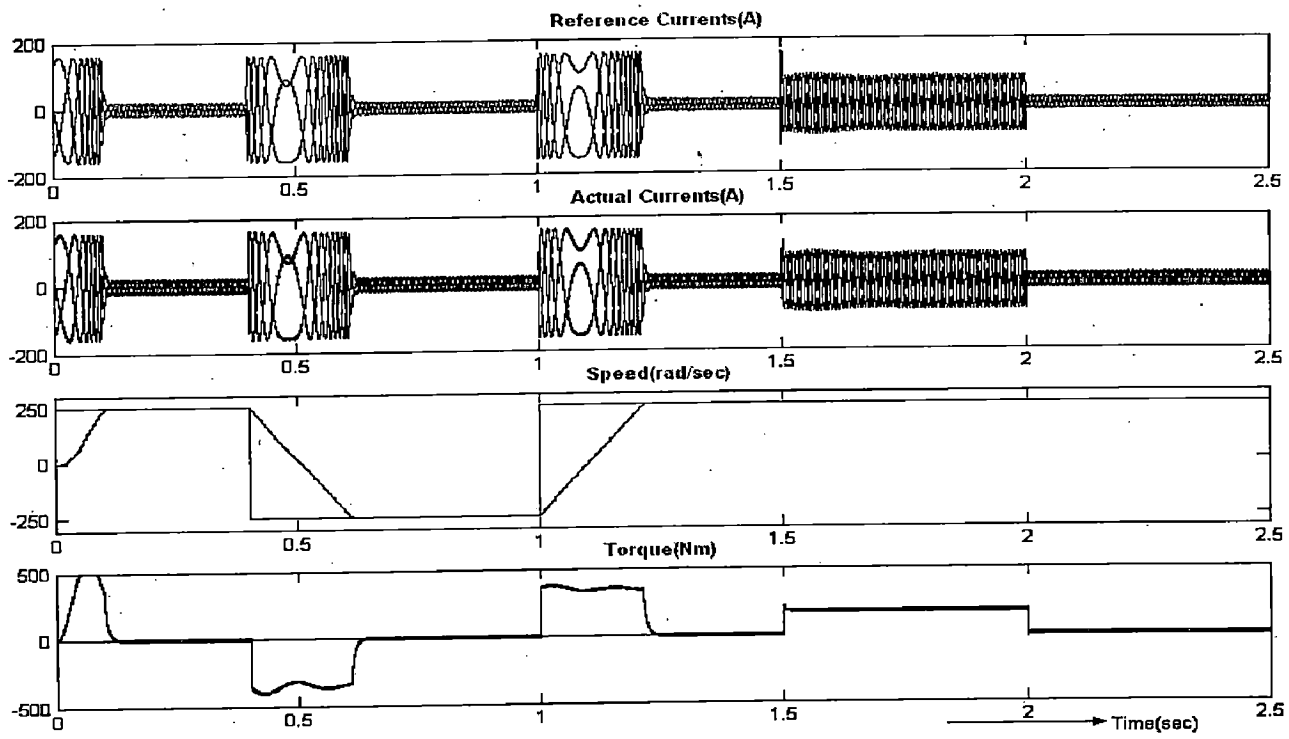

Figure 5.8. Starting, Speed Reversal and Load Perturbation Response of 30hp VCIMD system with Fuzzy Pre-compensated Proportional Integral (FPPI) Speed Controller.

5.5 EXPERIMENTAL RESULTS

The gate pulses for a three phase Voltage Source Inverter (VSI) are generated by using MATLAB Embedded Controller, I-8438. Six gate pulses are generated by the controller by implementing sinusoidal PWM technique. The Embedded controller supports only up to a limited frequency of nearly125 Hz fir sinusoidal PWM. If the pulses are generated by using pulse generator block in MATLAB/simulink library, the a pulse frequencies of 333Hz and 500 Hz can also be obtained as shown in figs. 5.9 and 5.10 respectively. The six pulses generated by sinusoidal PWM technique at about 125Hz are shown in figs. 5.11-5.13 respectively. If these pulses are given to IGBT individually, the devices are being switched on and the corresponding output across each device are shown in figs. 5.14-5.19. But if these six pulses from Embedded controller are all connected to six devices of the inverter, then the pulses are being dropped due to loading effect and the controller is not able to drive the inverter.

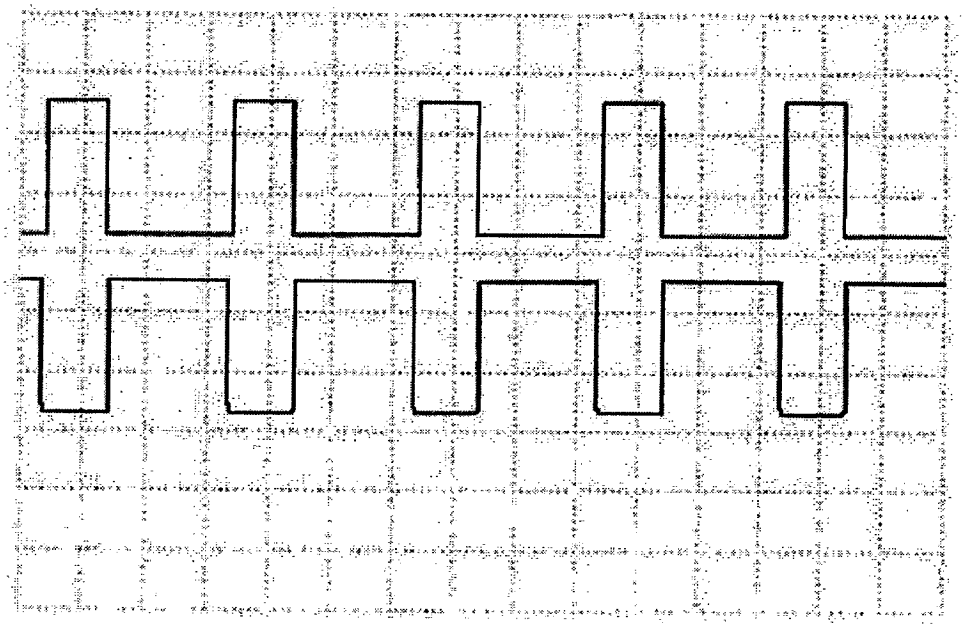

Figure 5.9 Switching pulses generated by Pulse Generator block in MATLAB/simulink library at a freq of 333Hz . Time scale: 1ms/div. Voltage scale: 2V/div

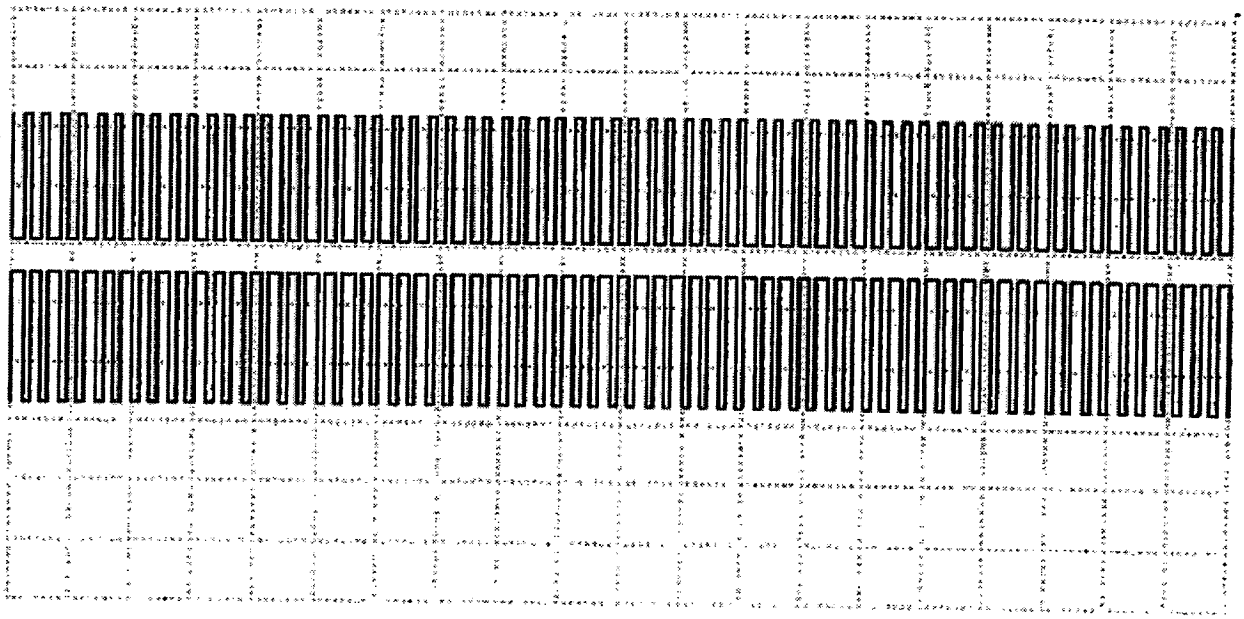

Figure 5.10 Switching pulses generated by Pulse Generator block in MATLAB/simulink library at a freq of 500Hz . Time scale: 10ms/div. Voltage scale: 2V/div

The figures explained below are with respect to the Voltage Source Inverter shown in fig.4.7

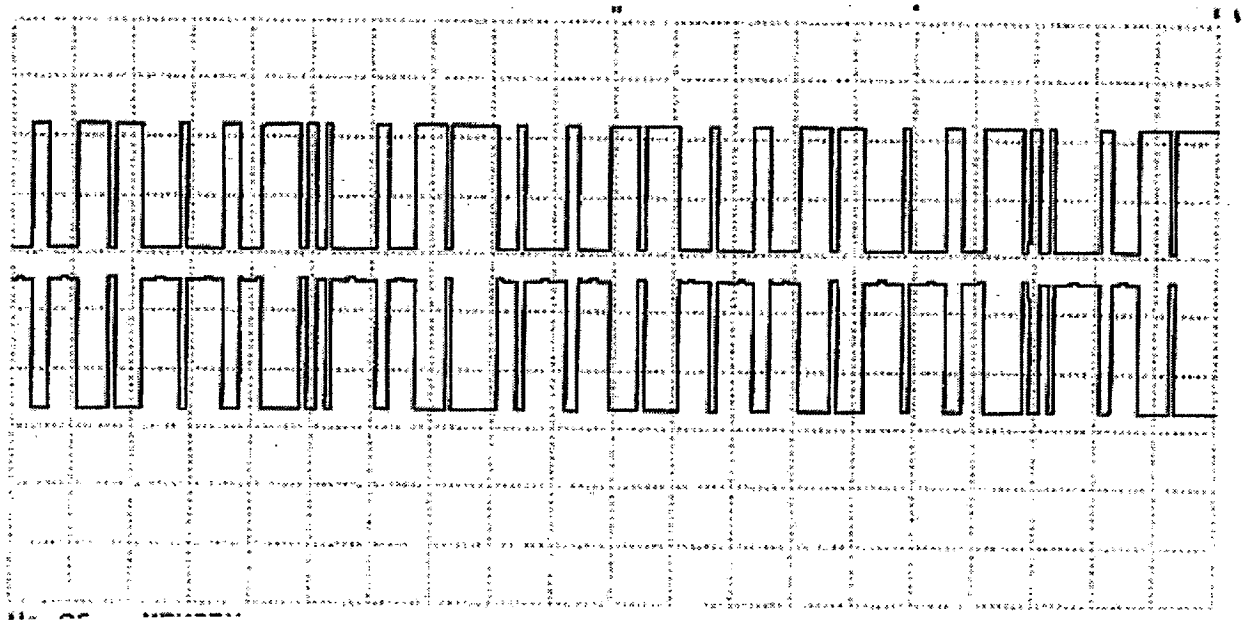

Figure 5.11. Switching pulses for devices S1 and S4 respectively generated by I-8438 controller using sinusoidal PWM technique at a freq of about 125Hz . Time scale: 10ms/div. Voltage scale: 2V/div

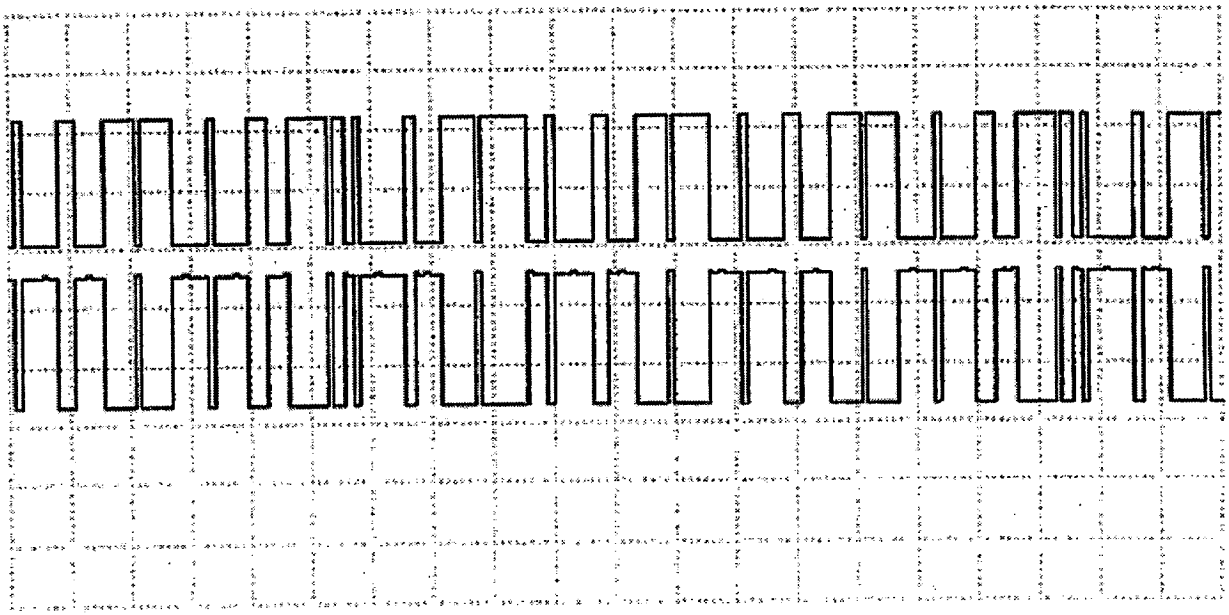

Figure 5.12. Switching pulses for devices S2 and S5 respectively generated by I-8438 controller using sinusoidal PWM technique at a freq of about 125Hz . Time scale: 10ms/div. Voltage scale: 2V/div

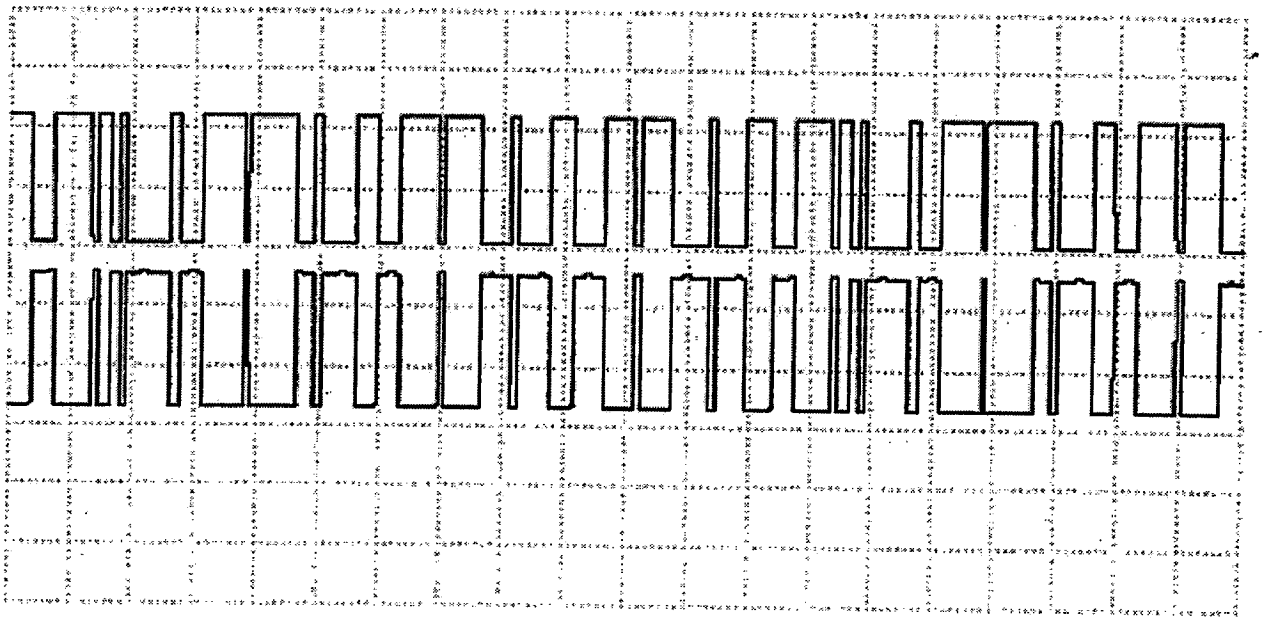

Figure 5.13. Switching pulses for devices S3 and S6 respectively generated by I-8438 controller using sinusoidal PWM technique at a freq of about 125Hz . Time scale: 10ms/div. Voltage scale: 2V/div

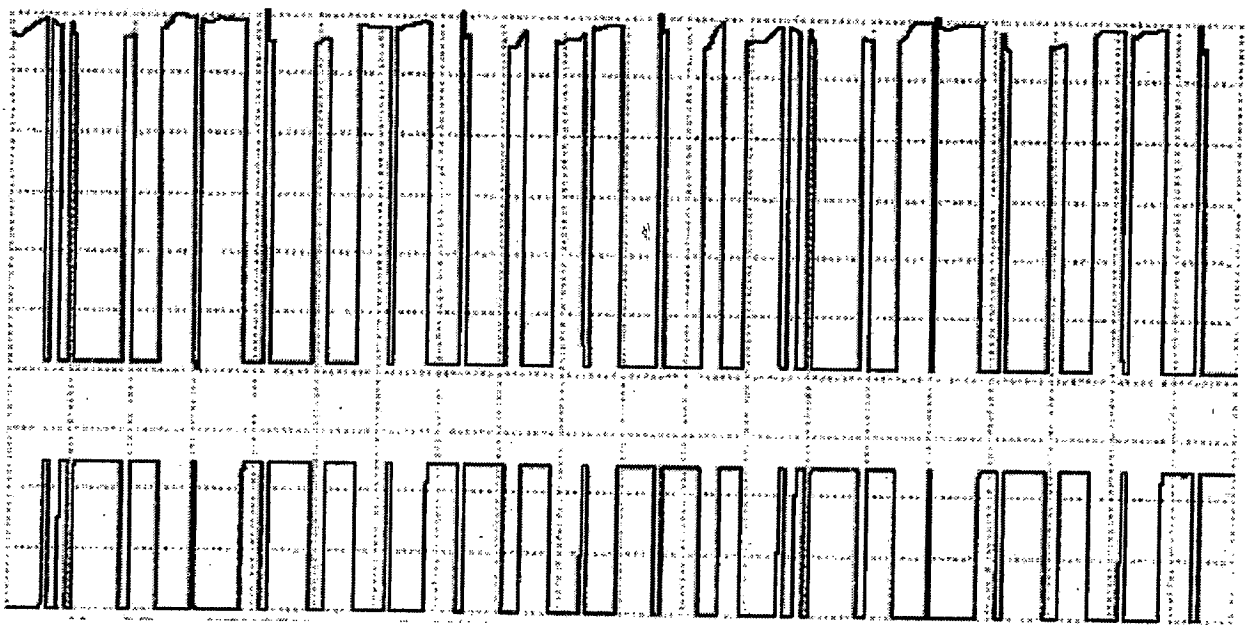

Figure 5.14 The output and input pulses respectively across the switching device S1 with a dc input of 30 V and a load resistance of 50 Ω. Time scale: 10ms/div. Voltage scale: 5V/div.

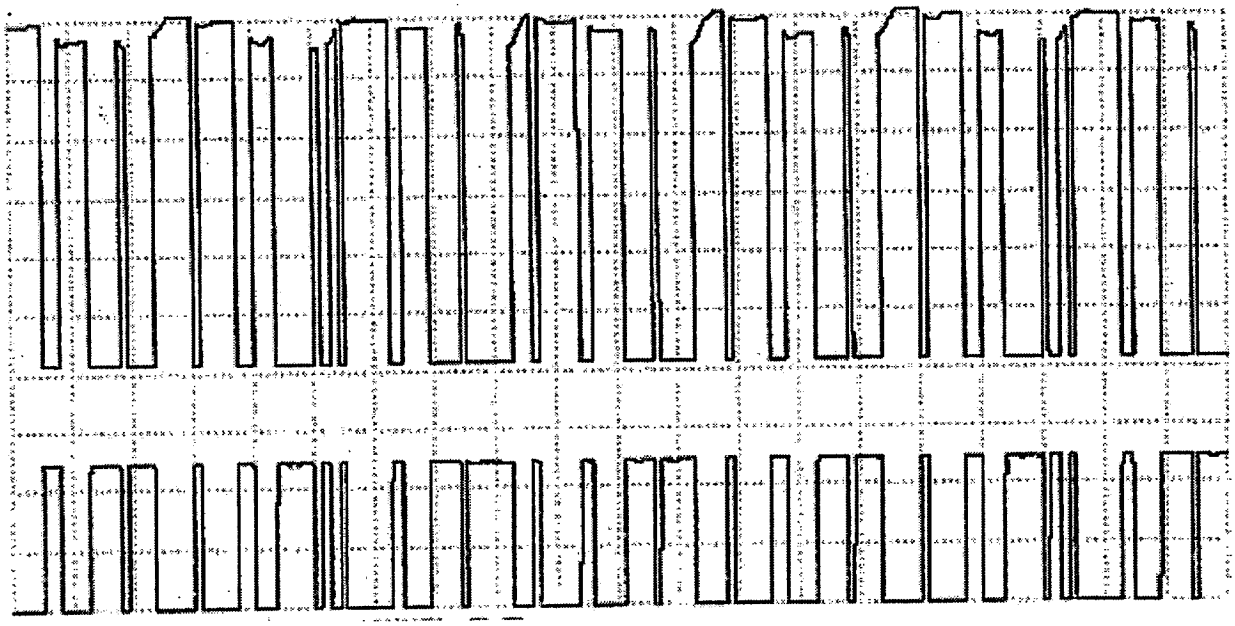

Figure 5.15 The output and input pulses respectively across the switching device S4 with a dc input of 30 V and a load resistance of 50 Ω. Time scale: 10ms/div. Voltage scale: 5V/div.

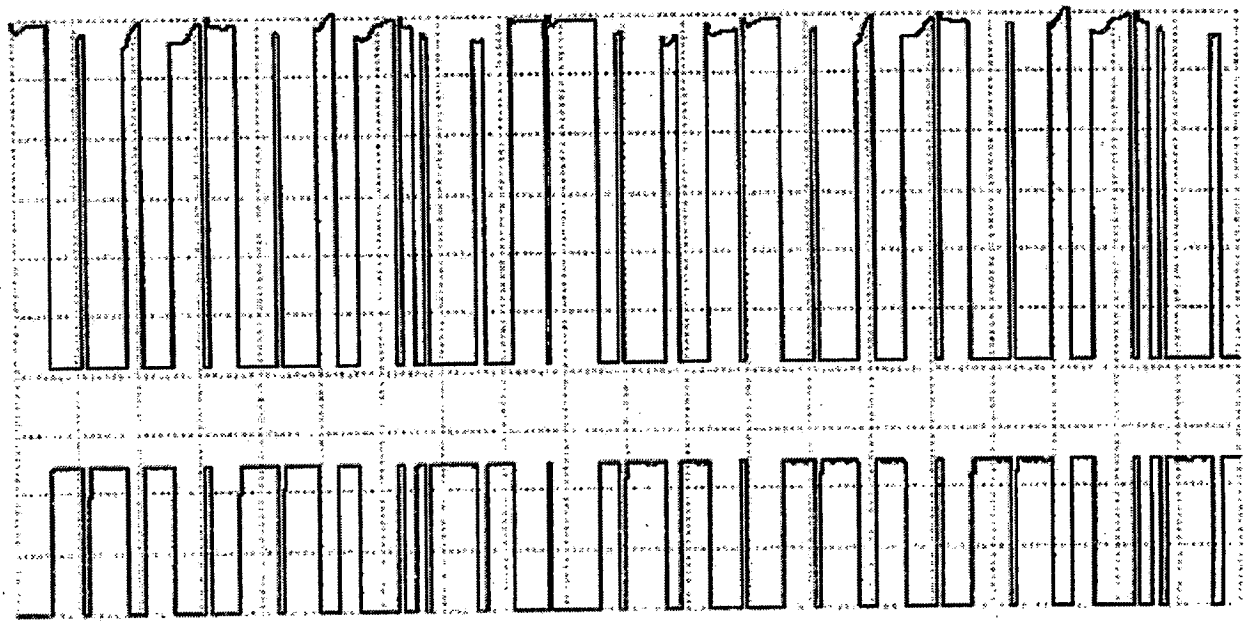

Figure 5.16 The output and input pulses respectively across the switching device S2 with a dc input of 30 V and a load resistance of 50 Ω. Time scale: 10ms/div. Voltage scale: 5V/div.

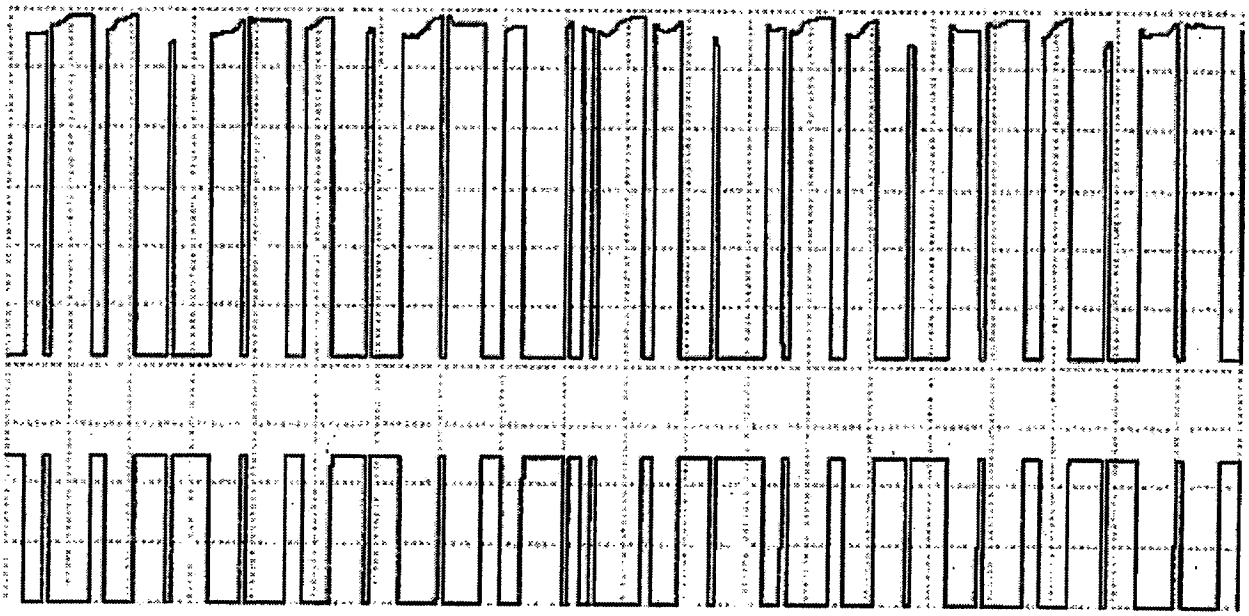

Figure 5.17 The output and input pulses respectively across the switching device S5 with a dc input of 30 V and a load resistance of 50 Ω. Time scale: 10ms/div. Voltage scale: 5V/div.

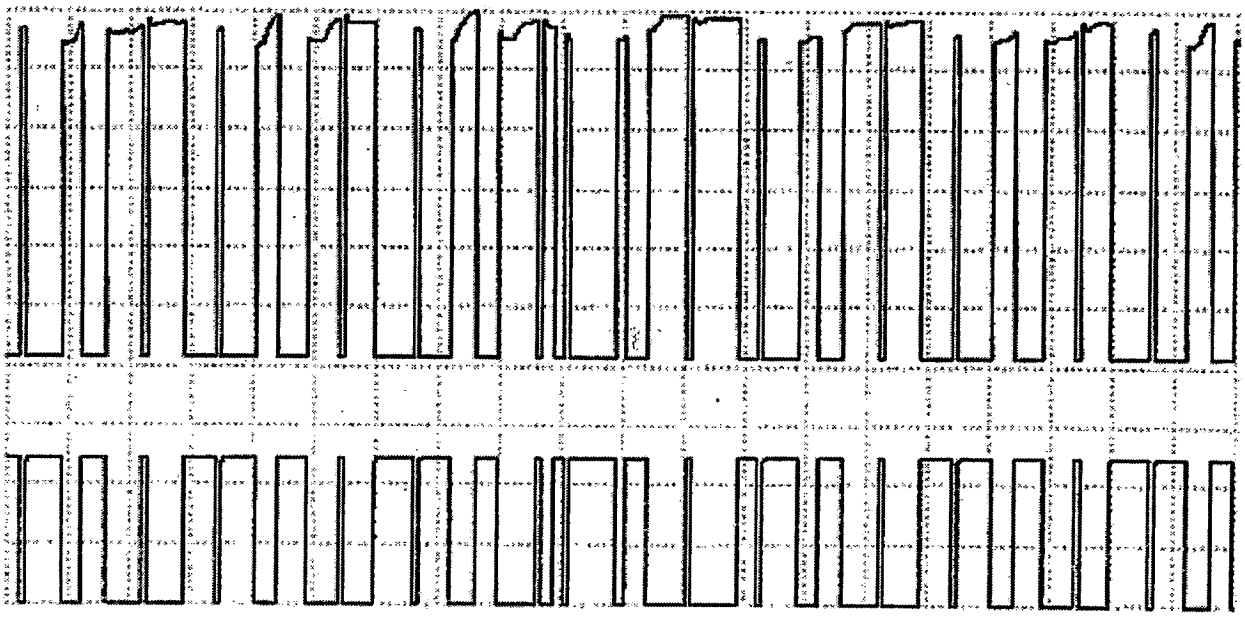

Figure 5.18 The output and input pulses respectively across the switching device S3 with a dc input of 30 V and a load resistance of 50 Ω. Time scale: 10ms/div. Voltage scale: 5V/div.

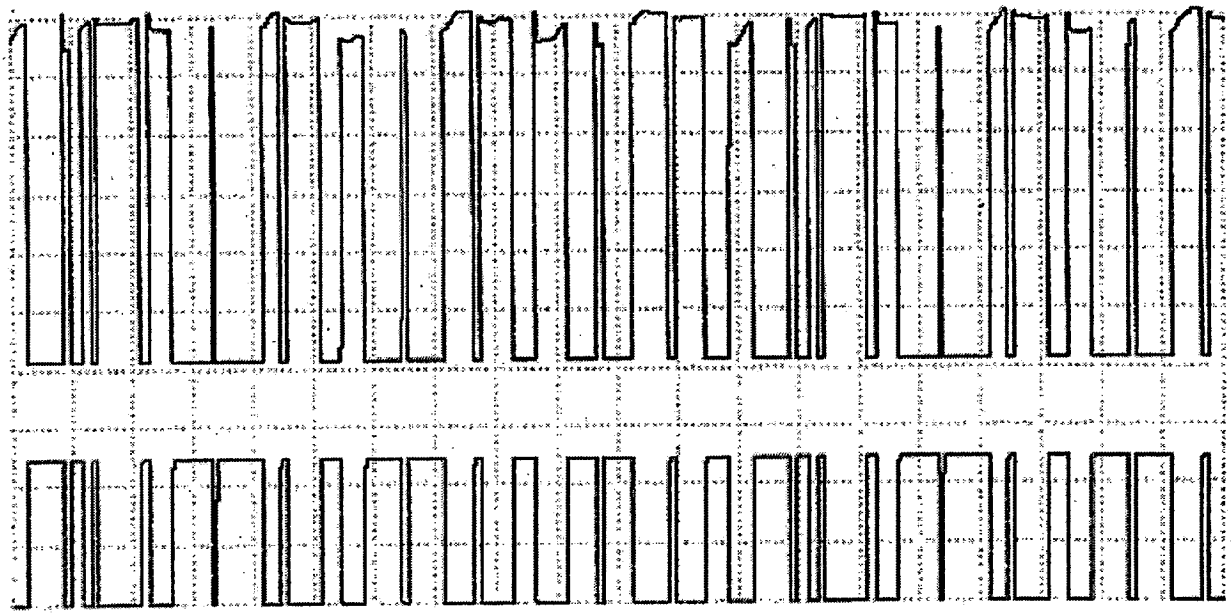

Figure 5.14 The output and input pulses respectively across the switching device S6 with a dc input of 30 V and a load resistance of 50 Ω. Time scale: 10ms/div. Voltage scale: 5V/div.

CHAPTER VI

CONCLUSIONS AND FUTURE WORK

The Vector Controlled Induction Motor Drive (VCIMD) has been mathematically modeled in MATLAB environment using simulink and power system blockset (PSB) toolboxes and the drive response is simulated under different operating conditions such as starting, speed reversal and load perturbation. A comparative study of different speed controllers namely proportional integral (PI) controller, fuzzy logic (FL) controller, hybrid controller and fuzzy pre-compensated proportional integral (FPPI) controller has also been made for the VCIMD system. This comparative study of different speed controllers for variable speed operation has shown their respective merits and demerits of the individual speed controllers. Gate pulses for the voltage source inverter are generated using Sinusoidal pulse width modulation technique.

The comparative study of different speed controllers under various operating conditions of VCIMD system has shown that the individual speed controllers have their own merits and demerits. The choice of the speed controllers depends on the requirement of the application. If the requirement is that of simplicity and ease of application, the PI speed controller is a good choice. But the PI controller suffers with the disadvantage of occurrence of overshoots and undershoots. When intelligence and fast dynamic response without disadvantages such as undershoot and overshoot are required, the FL controller may be better option. The main disadvantage in FL controller is presence of steady state speed error on load application. To eliminate such disadvantages and to maintain a high level of performance, a combination of PI and FL controllers will be a better choice. Such a combination of controllers is referred as the Hybrid controller. To retain simplicity and ease of control and eliminate disadvantages such as overshoot and undershoot, the reference speed signal is pre-compensated using FL controller. This pre-compensated speed signal is used as reference speed signal to the PI controller. Such a combination of controllers is known as FPPI speed controller. Finally it can be concluded that a FPPI speed controller is a much better choice when the requirement is of high-level accuracy and good dynamic VCIMD system.

The gating pulses are generated for a three phase Voltage Source Inverter (VSI) by MATLAB Embedded Controller, I-8438 using sinusoidal PWM technique. Although the pulses are not generated at required frequency, the devices are able to switch on at a freq of about 125 Hz, which is the maximum limit for the controller using Sinusoidal PWM. But the pulses using pulse generator

block can be generated up to a freq of 500 Hz. And also due to loading effect, the pulses are dropping down when given to all the devices at a time and the controller is not able to drive the inverter.

Although, the requirements for a good induction motor drive system can be obtained by vector control and different speed controllers, there are certain factors to be taken in consideration in order to develop a more better VCIMD system. For example the reduction of sensors in VCIMD system can be further investigated and implemented. The reduction in number of sensors without any loss in quality of the signal estimated could lead to a simple controller and the controller can become more robust and can reduce the overall cost of the drive system.

REFERENCES

[1] P. C. Krause, *Electrical Machines*, Prentice Hall, 1985.

[2] J. M. D. Murphy and F. G. Turnbull, *Power Electronic Control of AC Motors,* Oxford Pergamon Press, 1988.

[3] P. Vas, *vector Control of AC Machines*, Oxford University press, 1990.

[4] I. Boldea and S. A. Nasar, *Vector Control of AC Drives,* Florida, CRC press, 1990.

[5] Ned Mohan, Tore M. Underland and William P. Robbins, *Power electronics converters, applications, and design*, John Wiley & Sons, Second edition, 1995.

[6] P. Vas, *Sensorless Vector and Direct Torque Control*", Oxford University Press, New York, 1998.

[7] Bose. B.K, *Modern Power Electronics and AC Drives*, Prentice Hall, 2002.

[8] D. Grahame Holmes and Thomas A. Lipo, *Pulse Width Modulation for Power Converters-Principles and Practice,* IEEE press series on power engineering, 2003.

[9] Muhammad H. Rashid, *Power Electronics circuits, Devices, and applications,*" Pearson education, third edition, 2004.

[10] 8438/8838 User manual, "*8000 series embedded control system*", ver 1.0, 8ms-004-01, Feb 2004.

[11] F. Blaschke, "The Principle of Field Orientation as applied to the New Transvector Closed-loop Control System for Rotating-Field machines," *Siemens Review,* vol.34, no.3, pp. 217-220, May 1972.

[12] Sathi Kumar. S and Vithajathil. Joseph, "Digital Simulation of Field Oriented Control of Induction Motor", *IEEE Transactions on Industrial Electronics,* vol. IE-31, Issue 2, May 1984, pp. 141-148.

[13] H. W. Van Der Broeck, H. C. Skudelny, and G. V. Stanke, "Analysis and realization of a pulse width based on voltage space vectors," *in proc, 1986 IEEE-IAS Annu. Meeting*, pp. 244-251.

[14] C. C. Lee, "Fuzzy Logic on Control Systems-Part I," *IEEE Trans. on systems, Man and Cybernatics,* vol.20, no.2, pp.404-418, Mar/Apr 1990.

[15] C. C. Lee, "Fuzzy Logic on Control Systems-Part II," *IEEE Trans. on systems, Man and Cybernatics,* vol.20, no.2, pp.404-418, Mar/Apr 1990.

[16] P. G. Handley, J. T. Boys, "Space vector modulation: An engineering review," *in proc. July 1990, IEEE, 4th international con. on power electronics and variable-speed drives*, pp. 87-91.

[17] Fodor. O, Katma. Z and Szeszlay. E, "Field Oriented Control of Induction Motors using DSP", *in proc. April 1994 Computing of Control Engineering Journal,* Vol. 5, Issue 2, pp. 61-65.

[18] Kubota. H and Matsure. K, "Speed Sensorless Field-Oriented Control of Induction Motor with Rotor Resistance Adaptation", *IEEE Transactions on Industry Applications,* Vol. 30, Issue 5, September-October 1994, pp. 1219-1224.

[19] Clang. S.C and Yen. S. N, "Current Sensorless Field-Oriented Control of Induction Motor", in *Proc. November 1996 IEEE Electric Power Applications,* Vol. 143, Issue 6, pp. 492-500.

[20] Jian Sun, H. Grotstollen, "Optimised space vector modulation and regular-sampled PWM; a re-examination," *in proc. 6-10 Oct. 1996, 31st IAS Annual Meeting, IEEE,* vol. 2, pp. 956-963.

[21] P. J. P. Perruchoud, P. J. Pinewski, "Power losses for space vector modulation technique," *IEEE Trans. Power electronics*, pp. 167-173, Oct. 1996.

[22] Yen-Shin Lai, S. R. Bowes, "A universal space vector modulation strategy based on regular-sampled pulse-width modulation[inverters]," *in proc. 1996, IEEE IECON 22nd international conf., Industrial Electronics, control and instrumentation.*

[23] R. H. Ahmad, G. G. Kanady, T. D. Blake, P. Pinewski, "Comparison of space vector modulation techniques based on performance indexes and hardware implementation," *in proc. 9-14 Nov. 1997, IEEE IECON 23rd international conf. Industrial electronics, control and instrumentation*, vol. 2, pp. 682-687.

[24] R. Zhang, D. Boroyevich, V. H. Prasad, H. C. Mao, F. C. Lee, S. Dubocsky, "A three phase inverter with a neutral leg with space vector modulation," *in proc., 23-27 Feb. 1997 IEEE 12th Annual Applied Power Electronics conference and Exposition, APEC '97,* vol. 2, pp. 23-27.

[25] S. R. Bowes, Yen-Shin Lai, "The relation between space-vector modulation and regular-sampled PWM," *IEEE Trans. Industrial Electronics,* vol. 44, issue 5, pp. 670-679, Oct. 1997.

[26] Yen-Shin Lai, S. R. Bowes, "A new suboptimal pulse-width modulation technique for per-phase modulation and space vector modulation," *IEEE Trans. Energy conversion*, vol. 12, issue 4, pp. 310-316, Dec. 1997.

[27] Sanjiv Kumar, Bhim Singh and J. K. Chatterjee, " Hybrid Speed Controller for Vector Controlled Cage Induction Motor Drive," *in proc. 1998, International Conf. On Power Electronics Devices and Energy Systems for Industrial growth,* vol.1.1, pp.147-152.

[28] Lofti A. Zadeh, " From Computing with Numbers to Computing with Words-From Manipulation of Measurements to Manipulation of Perceptions," *IEEE Trans. on Circuits and Systems-I: Fundamental Theory and Applications*, vol.45, no.1, pp.105-119 , January 1999.

[29] Jang-Hyoun Youm, Bong-Hwan Kwon, "An effective software implementation of the space-vector modulation," *IEEE Trans. Industrial Electronics*, vol 46, issue 4, pp. 866-868, Aug. 1999.

[30] Tsung-Po Chen, Yen-Shin Lai, Chang-Heran Liu, "A new space vector modulation technique for inverter control," *in proc., 1999, 30th Annual IEEE Power electronics specialists conf.. PESC 99*, vol 2, pp. 777-782.

[31] Bazenella. A.S and Reginalto. R, "Robustness Margins for Indirect Field-Oriented Control of Induction Motor", *IEEE Transactions on Automatic Control*, Vol. 45, Issue 6, June 2000, pp. 1226-1231.

[32] Keliang zhou and Danwei Wang, "Relationship between space-vector modulation and three-phase carrier based PWM: A comprehensive analysis", *IEEE transactions on Industrial Electronics*, vol 49, pp 186-196, February 2002.

[33] H. Pinheiro, F. Botteron, c. Rech, L. Scguch, R. F. Camargo, H. L. Hey, H. A. Grundling, J. R. Pinheiro, "Space vector modulation for voltage source inverters: A unified approach," *in proc., 2002, IEEE 28th IECON conf.* pp.23-29.

[34] M. Nasir Uddin, Tawfik S. Radwan and M. Azizur Rahman, " Performances of Fuzzy-Logic-Based Indirect Vector Control for Induction Motor Drive", *IEEE Transactions on Industry Applications,* vol.38, No.5, pp. 1219-1225, September/October 2002.

[35] Bhim singh and Ghatak choudhuri, "Fuzzy Logic Based Speed Controllers for Vector Controlled Induction Motor Drive," *in proc. November-December 2002, IETE Journal of Research,* vol.48, no.6, pp.441-447.

[36] Texas Instruments, "*AC Induction motor control (three phase)*", system document, digital control system group, 30 April 2003.

[37] Sumit Ghatak Choudhuri, "Analysis and Development of vector Control of Induction Motor Drive," Ph.D Dissertation, Dept. of Electrical Eng., Indian Institute of Technology, Delhi, July 2004.

[38] Rathole. A.K, "Improved Performance of Fuzzy Logic based Direct Field Oriented Controlled Induction Motor", *in proc. 17-22 October 2004, 9th IEE International Conference on Power Electronic Congress*, pp. 152-157.

[39] D. Ratnakumar, J. Lakshmana Pereumal, T. Srinivasan, "A New Software Implementation of Space Vector PWM," *in proc. 2005 IEEE Southeast conf.*, pp. 131-136, 8-10 April 2005.

[40] Bhim Singh and S. Ghatak Choudhuri, " DSP Based Implementation of Vector Controlled Induction Motor Drive using Fuzzy Pre-compensated Proportional Integral Speed Controllers" *in proc.,12-15 Dec 2006, International conference on Power Elcetronics, Drives and Energy Systems (PEDES), New Delhi.* no.2C-01.

[41] Hossain. M.J, Hoque. M.A, Ali. M.A and Rahman. M.A, "Fuzzy-Logic based Control for Induction Motor Drive with the Consideration of Core Loss", *in proc., December 2006, International Conference on Electrical and Computer Engineering*, pp. 333-336.

[42] "Vector Control of Induction Motor using UPWM VSI-Control System for Rotating Field Machines", *in proc., 2007 Seimens Review, The Australian Universities Power Engineering Conf.*, Vol. 39, No.3.

APPENDIX – A

MOTOR PARAMETERS-I

Type : Squirrel cage induction motor

Phase : 3

Power : 1 Hp

Voltage : 420 V

Current : 2 A

Speed : 2820 RPM

Poles : 2

Frequency: 50 Hz

No Load Test parameters: V_{NL}=420 V I_{NL} = 1.38 A W_{NL} = 352 W

Blocked Rotor Test parameters: V_{BR} = 98 V I_{BR} = 2 A W_{BR} = 228 W

Equivalent circuit parameters:

DC Resistance = 9.27 Ω

Stator resistance per phase = 11.124 Ω

Rotor resistance per phase = 8.9838 Ω (referred to stator)

Stator reactance per phase = 10.48 Ω

Rotor reactance per phase = 10.48 Ω (referred to stator)

Magnetizing reactance per phase = 154.08 Ω

Moment of inertia per phase = 0.0018 J (Kg-m^2)

APPENDIX – B

MOTOR PARAMETERS-II

Type : Squirrel cage induction motor

Phase : 3

Power : 30 Hp

Voltage : 420 V

Current : 45 A

Poles : 4

Frequency: 50 Hz

Equivalent circuit parameters:

Stator resistance per phase = 0.2511Ω

Rotor resistance per phase = 0.2489 Ω (referred to stator)

Stator reactance per phase = 0.439 Ω

Rotor reactance per phase = 0.439 Ω (referred to stator)

Magnetizing reactance per phase = 13.085 Ω

Moment of inertia per phase = 0.305 J (Kg-m^2)

APPENDIX – C

HARDWARE SPECIFICATIONS OF I-8438/8838

General environment

Operating temperature: -25° C to +75° C

Storage temperature: -30° C to +85° C

Humidity: 5 ~ 95%

Built-in power protection & network protection circuit

System

CPU: RDC, 80MHz, or compatible

SRAM: 512K bytes

FLASH ROM: 512K bytes

COM ports for the I-8438 & 8838

COM1=RS-232, COM3=RS232/RS485, COM4=RS-232

Ethernet: 10 BaseT

RTC, NVRAM & EEPROM

Programs download from COM1 & Ethernet

Built-in 64-bit hardware unique serial number

Built-in Watchdog Timer

I/O Expansion Slot

4-slot for I-8438

8-slot for I-8838

APPENDIX –D

MATLAB DRIVER BLOCK REFERENCE

This section presents detailed descriptions of used blocks in the MATLAB Driver block library.

➢ SYS_INIT

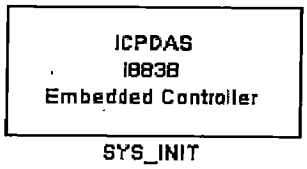

Description: Initialize the I-8xx8 control system.

Library: System

Dialog Box:

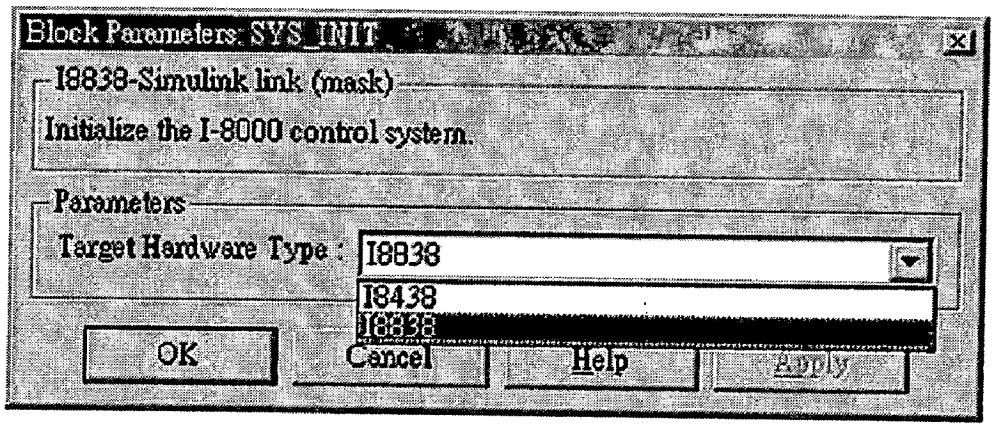

Driver Block Parameters:

Target Hardware Type - The type of the I-8xx8 control system that is used. The setting must match with the actual situation; otherwise, it might cause unexpected problems. The following table presents a list of the types available and the difference between them.

TYPE	Slots Available
I-8438	4
I-8838	8

➢ I-8054

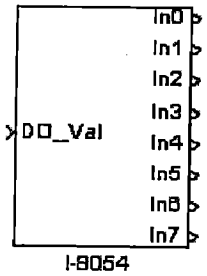

Description:

16-channel Isolated Digital I/O Module.

Library:

DIO

Dialog Box:

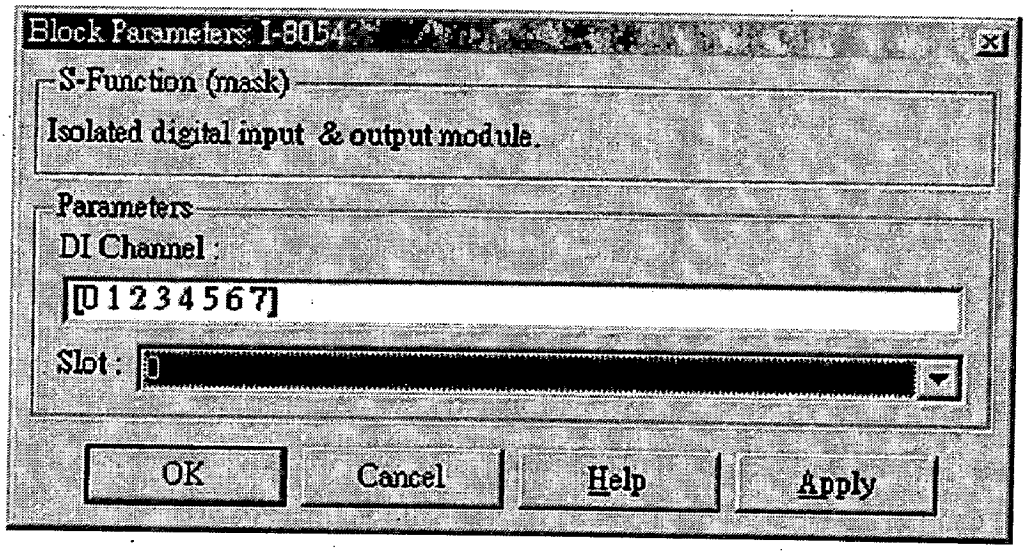

Driver Block Parameters:

DI Channel - Enter numbers between 0 and 7. This block allows the selection of digital input lines in any order. The number of elements defines the number of digital inputs used. For example, to use the first 8 digital inputs, enter [0 1 2 3 4 5 6 7]

Slot - The number of the slot where I-8054 module is located. For example, choose 2 from the popup list if you have mounted an I-8054 module on slot 2.

Scaling Input to Output (digital input):

Hardware Input	Block Output Value
Below 1V	= 0
3.5V ~ 30V	= 1

Scaling Input to Output (digital output):

Block Input Value	Hardware Output
0	All channels are off.
1	Ch0 is on, and the others are off.
2	Ch1 is on, and the others are off.
...	...
255	All channels are on.

APPENDIX –E

HARDWARE CONNECTIONS OF I-8438

Front view of i-8438:

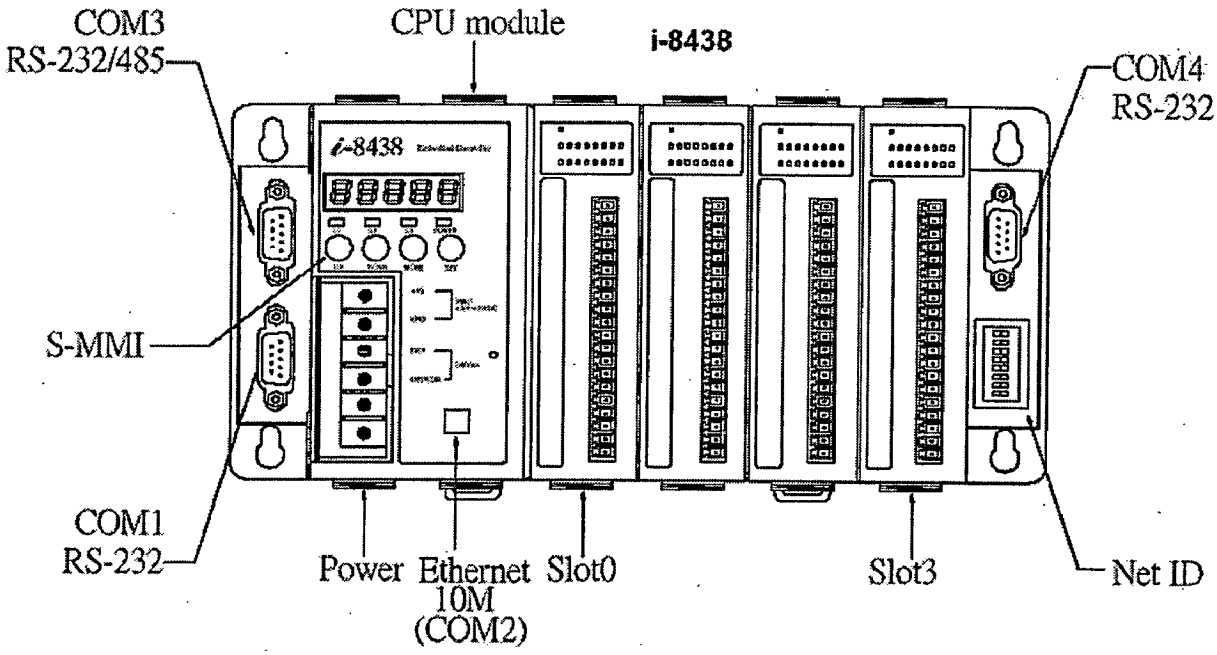

Host PC connect to COM1 of i-8438: